

COMPARISON OF MEAN SITE-SPECIFIC RESPONSE SPECTRA IN TURKEY
WITH THE DESIGN SPECTRA OF AASHTO

A THESIS SUBMITTED TO
THE GRADUATE SCHOOL OF NATURAL AND APPLIED SCIENCES
OF
MIDDLE EAST TECHNICAL UNIVERSITY

BY

GİZEM MESTAV SARICA

IN PARTIAL FULFILLMENT OF THE REQUIREMENTS
FOR
THE DEGREE OF MASTER OF SCIENCE
IN
CIVIL ENGINEERING

DECEMBER 2014

Approval of the thesis:

**COMPARISON OF MEAN SITE-SPECIFIC RESPONSE SPECTRA IN
TURKEY WITH THE DESIGN SPECTRA OF AASHTO**

submitted by **GİZEM MESTAV SARICA** in partial fulfillment of the requirements
for the degree of **Master of Science in Civil Engineering Department, Middle East
Technical University** by,

Prof. Dr. Gülbin Dural Ünver
Dean, Graduate School of **Natural and Applied Sciences**

Prof. Dr. Ahmet Cevdet Yalçiner
Head of Department, **Civil Engineering**

Assoc. Prof. Dr. Ayşegül Askan Gündoğan
Supervisor, **Civil Engineering Dept., METU**

Examining Committee Members:

Prof. Dr. Ahmet Yakut
Civil Engineering Dept., METU

Assoc. Prof. Dr. Ayşegül Askan Gündoğan
Civil Engineering Dept., METU

Assoc. Prof. Dr. Alp Caner
Civil Engineering Dept., METU

Assoc. Prof. Dr. Afşin Sarıtaş
Civil Engineering Dept., METU

Dr. Nazan Kılıç
Disaster and Emergency Management Presidency

Date: 03.12.2014

I hereby declare that all information in this document has been obtained and presented in accordance with academic rules and ethical conduct. I also declare that, as required by these rules and conduct, I have fully cited and referenced all material and results that are not original to this work.

Name, Last Name : Gizem Mestav Sarica

Signature :

ABSTRACT

COMPARISON OF MEAN SITE-SPECIFIC RESPONSE SPECTRA IN TURKEY WITH THE DESIGN SPECTRA OF AASHTO

Mestav Sarıca, Gizem

M.S., Department of Civil Engineering

Supervisor: Assoc. Prof. Dr. Ayşegül Askan Gündoğan

December 2014, 129 pages

Seismic design of bridges is a significant problem for all seismically-active countries including Turkey which has gone through recent destructive earthquakes. Bridges are important elements of transportation and their robustness is important in the aftermath of major earthquakes. Turkish engineers currently employ a modified version of AASHTO (American Association of State Highway and Transportation Officials) LFD Design Specifications for bridge design. Within the scope of a national project (TÜBİTAK 110G093) a new bridge design code for Turkey is being prepared by a large team of civil and earthquake engineers. In this code, proposal of a new design spectrum is also planned. The main objective of this study is to compare the mean site-specific response spectra in Turkey based on data from past earthquakes with the design spectra in AASHTO (2007) and AASHTO (2010) by focusing on the descending part (long period range). The site-specific response

spectra for different soil conditions and magnitude ranges are obtained from strong ground motion data gathered on the Turkish National Strong-Motion Observation Network. To observe the effects of these site-specific spectra on the bridge response, response spectrum analyses are performed with these empirical spectra and the results are compared with those from AASHTO (2007 and 2010). The case studies are applied on three different models of bridges that are located in Bursa (a large city located in Northwest Turkey) which are namely Balikli, Panayir and Demirtas bridges. Finally, linear time history analyses are performed with ground motions that match the site-specific and AASHTO LRFD spectra; the results are compared with each other. LARSA 4D Structural and Earthquake Engineering Integrated Analysis and Design Software is used for the response spectrum and linear time history analyses on these bridges.

Keywords: Ground motion characteristics, site-specific hazard spectra, response spectrum analysis, linear time history analysis, seismic analysis of bridges

ÖZ

TÜRKİYE'DEKİ ZEMİNE ÖZGÜ ORTALAMA TEPKİ SPEKTURUMLARININ AASHTO İLE KARŞILAŞTIRILMASI

Mestav Sarıca, Gizem

Yüksek Lisans, İnşaat Mühendisliği Bölümü

Tez Yöneticisi: Doç. Dr. Ayşegül Askan Gündoğan

Aralık 2014, 129 sayfa

Köprülerin sismik tasarımı son dönemlerde yıkıcı depremler geçirmiş olan Türkiye de dahil olmak üzere sismik olarak aktif olan bütün ülkelerde büyük bir problemdir. Köprüler ulaşımın önemli elemanlarıdır ve büyük depremler sonrasındaki dayanımları çok önemlidir. Günümüzde Türk mühendisleri köprü tasarımı için AASHTO (American Association of State Highway and Transportation Officials) LFD Köprü Tasarım Şartnamesi'nin değiştirilmiş bir versiyonunu kullanmaktadırlar. Yetkin bir inşaat ve deprem mühendisi topluluğu tarafından ulusal bir proje (TÜBİTAK KAMAG 110G093) kapsamında yeni bir köprü tasarım kodu hazırlanmaktadır. Bu kod dahilinde yeni bir tasarım spektrumu önerisi de planlanmıştır. Bu çalışmanın asıl amacı AASHTO LRFD Köprü Tasarım Şartnamesi'nin iki farklı versiyonu (2007 ve 2010) ile Türkiye'deki geçmiş

depremlere dayanılarak elde edilen zemine özgü ortalama tepki spektrumlarını, spektrumların uzun periyotlarda azalma gösteren kısmına odaklanarak karşılaştırmaktır. Farklı zemin tipleri ve deprem büyüklükleri için Türkiye Ulusal Kuvvetli Yer Hareketi Gözlem Ağı'ndan toplanan veriler ile zemine özgü tepki spektrumları elde edilmiştir. Daha sonra Bursa'da bulunan Balikli, Panayir ve Demirtas köprüleri modelleri üzerinde vaka çalışmaları yapılmıştır. Elde edilen spektrumların köprü tepkisi üzerindeki etkilerini görmek üzere tepki spektrumu analizleri yapılmış ve sonuçlar AASSHTO (2007 ve 2010)'dan elde edilen sonuçlar ile karşılaştırılmıştır. Son olarak, bahsedilen spektrumlara uyumlu yer hareketleri ile lineer zaman tanım alanı analizleri yapılmış ve AASHTO LRFD spektrumları ile uyumlu kayıtlardan elde edilen sonuçlar karşılaştırılmıştır. Bahsedilen köprüler üzerindeki tepki spektrumu ve lineer zaman tanım alanı analizleri için LARSA 4D yapısal analiz ve tasarım yazılımı kullanılmıştır.

Anahtar Kelimeler: Yer hareketi karakteristiği, zemine özgü tehlike spektrumu, tepki spektrumu analizi, lineer zaman tanım alanı, köprülerin sismik analizi

To my beloved grandfathers Mehmet Kaymakçı and M. Rasim Mestav

ACKNOWLEDGEMENTS

I would like to thank my supervisor Assoc.Prof.Dr. Ayşegül Askan Gündoğan for her valuable encouragement, support, guidance and especially friendship throughout this study. I am grateful to her especially for the last period which is a tough but very special time of her life.

I would like to express my deep gratitude to Assoc.Prof.Dr. Alp Caner, Prof.Dr. Ahmet Yakut, Dr. Nazan Kılıç, Assoc.Prof.Dr. Afşin Sarıtaş and Prof.Dr. M. Semih Yücemem for their encouraging comments, suggestions and background they shared with me. Also I would like to thank Asst.Prof.Dr. Onur Pekcan for his help and support. I owe my sincere gratitude to Dr. Erhan and Dr. Engin Karaesmen for everything. Seeing their smiling faces any moment always motivated me.

Müge Özgenoğlu and Arzu İpek Yılmaz, my beyond lovely thesis-sisters, made everything easier and possible for me. It was a pleasure to study with them in any place and any time. Besides academic support, their existence was just enough for me to be inspired.

Very special thanks go to dear Kadir Korçak for his help on this thesis and also for making me smile under any circumstance. I am sure we will do greater things together in the future.

I would like to thank my precious colleagues Dr. Zeynep Çekinmez, Dr. Ahmet Kuşyılmaz, Alper Aldemir, Ozan Demirel, Erhan Budak and Fatma Nurten Şişman for their support, motivation and patience in this period.

Finally, my deepest thanks belong to my dearest father Mehmet Mestav, my warmhearted mother Fatma Mestav, my genius brother Kürşat Rasim Mestav and my pure love Serhad Sarıca for enlightening and sweetening my life.

TABLE OF CONTENTS

ABSTRACT	v
ÖZ	vii
ACKNOWLEDGEMENTS	xi
TABLE OF CONTENTS	xiii
LIST OF TABLES	xv
LIST OF FIGURES	xvii
LIST OF SYMBOLS AND ABBREVIATIONS.....	xxi
CHAPTERS	
1.INTRODUCTION.....	1
1.1 General.....	1
1.2 Literature Review	4
1.3 Aim and Scope.....	6
2.SEISMIC DESIGN SPECTRA IN AASHTO (2007 AND 2010)	9
2.1 Design Spectra of AASHTO LRFD (2007)	9
2.2 Design spectra of AASHTO LRFD (2010)	15
3.MEAN SITE-SPECIFIC RESPONSE SPECTRA IN TURKEY	23
3.1 Compilation and Classification of Strong Ground Motion Data	23
3.2 Normalized Mean Site-Specific Response Spectra	25
4.COMPARISON OF THE MEAN SITE-SPECIFIC SPECTRA AND AASHTO DESIGN SPECTRUM IN TERMS OF RSA	41
4.1 Information on the Selected Bridges	41

4.1.1 Panayir Bridge.....	44
4.1.2 Balikli Bridge	51
4.1.3 Demirtas Bridge	58
4.2 Computer Modelling	64
4.3 Dynamic Analysis of Bridges	70
4.4 Response Spectrum Analysis (RSA) on LARSA 4D Software	73
4.5 Results of Response Spectrum Analyses	76
5.FURTHER APPLICATIONS: LINEAR TIME HISTORY ANALYSES (LTHA) ON A SELECTED BRIDGE	81
5.1 Definition and Procedure	81
5.2 Results of Time History Analyses.....	85
6.CONCLUSIONS AND FUTURE WORK.....	91
REFERENCES	95
APPENDICES	
A.SELECTED STATIONS WITH MEAN SHEAR VELOCITY VALUES	101
B.AASHTO (2010) SITE CLASSIFICATION FOR SELECTED STATIONS	109
C.EZ-FRISK ANALYSES	115

LIST OF TABLES

Table 2.1 Site Coefficients in AASHTO (2007).....	11
Table 2.2 Soil Profile Classification in AASHTO (2007)	12
Table 2.3 Site Class Definitions in AASHTO (2010).....	16
Table 2.4 Fpga Values Corresponding to Different PGA (Zero-Period Range) Values in (AASHTO 2010)	18
Table 2.5 Fa Values Corresponding to Short Period Range Values in (AASHTO 2010).....	18
Table 2.6 Fv Values Corresponding to Long Period Range Values in (AASHTO 2010).....	19
Table 2.7 PGA, Ss and S1 Values for Selected Sites for 1000 Years.....	19
Table 3.1 Site Classification of the Selected Stations (According to AASHTO (2010) Site Class Definitions).....	24
Table 3.2 P and R2 Values for Different Groups.....	33
Table 4.1 Information about the Bridges	64
Table 4.2 Seismic Zones in AASHTO 2010.....	71
Table 4.3 Regular Bridge Requirements.....	72
Table 4.4 Minimum Analysis Requirements for Seismic Effects.....	73
Table 4.5 Maximum Column Moment Values for Different RSA Cases for Demirtas Bridge	78
Table 4.6 Maximum Column Moment Values for Different RSA Cases for Balikli Bridge	78
Table 4.7 Maximum Column Moment Values for Different RSA Cases for Panayir Bridge	79
Table 4.8 Maximum Column Tip Displacement Values for Different RSA Cases for Demirtas Bridge.....	79

Table 4.9 Maximum Column Tip Displacement Values for Different RSA Cases for Balikli Bridge	80
Table 4.10 Maximum Column Tip Displacement Values for Different RSA Cases for Panayir Bridge	80
Table 5.1 Information on the Records Used in Spectral Matching	83
Table 5.2 Maximum Column Moment Values for Different Linear Time History Analyses Cases for the Bridges Selected	86
Table 5.3 Maximum Column Tip Displacement Values for Different Linear Time History Analyses Cases for the Bridges Selected	88
Table A.1 V_{S30} Values for Selected Stations and Corresponding Site Classes for Different Building Codes (Sandikkaya, 2008).....	101
Table B.1 Site Classification of the Selected Sites According to AASHTO (2010).	109

LIST OF FIGURES

Figure 1.1 Example of a Typical Design Spectrum	3
Figure 1.2 Potential Plastic Hinge Regions on Columns (a) in Longitudinal Direction (b) in Transverse Direction (Adopted from Yılmaz, 2008).....	7
Figure 2.1 Design Spectra Trend for AASHTO (2007).....	13
Figure 2.2 AASHTO (2007) Design Spectra for Site Class C and Site Class D	14
Figure 2.3 Design Spectra Trend for AASHTO (2010).....	20
Figure 2.4 AASHTO (2010) Design Spectra for Site Class C and Site Class D	20
Figure 3.1 Normalized Mean and Mean + Std (Mean-Plus-One-Standard-Deviation) Response Spectrum Curves for Site Classes C and D for Different M_w Intervals (Site Classes are Shown in Parenthesis)	27
Figure 3.2 Comparison of Mean (Continuous Lines) and Mean-Plus-One-Standard- Deviation (Dashed Lines) Normalized Acceleration Spectra for Records of NEHRP Site Classes C and D for Magnitude Ranges (a) $3.5 < M_w < 4.5$, (b) $4.5 < M_w < 5.5$, (c) $5.5 < M_w < 6.5$, (d) $6.5 < M_w < 7.5$. The Number in Parenthesis Gives the Number of Records Used for Calculation of Mean Spectrum (Sandikkaya et al., 2010)	28
Figure 3.3 Formulae and Corresponding R^2 Values of the Fits on Long-Period Portions of Normalized Mean Response Spectra for Site Classes C and D and for Different M_w Intervals.....	32
Figure 3.4 Comparison of Normalized Mean Site-Specific Spectra With Design Spectra For Different Cases.....	37
Figure 3.5 Combined Mean Site-Specific Spectra.....	38
Figure 3.6 Fits and Corresponding P and R^2 Values for the Combined Spectra for Different Site Classes	39

Figure 4.1 Distribution of Bridges in Turkey According to Skew Angle (Adopted from Sevgili, 2007)	42
Figure 4.2 Distribution of Bridges in Turkey According to Maximum Span Length (Adopted from Sevgili, 2007)	43
Figure 4.3 Distribution of Bridges in Turkey According to Number of Spans (Adopted from Sevgili, 2007)	43
Figure 4.4 Plan View (Panayir Bridge) (in cm)	44
Figure 4.5 Scheme of Design Level (Panayir Bridge) (elevations in m, lengths in cm)	44
Figure 4.6 Elevation View of Panayir Bridge	45
Figure 4.7 Cross Section of the Beam (Panayir Bridge) (in cm).....	46
Figure 4.8 Vertical Cross Section of Superstructure (Panayir Bridge) (in cm).....	47
Figure 4.9 Detail of the Shear Key (Panayir Bridge) (in cm).....	48
Figure 4.10 Superstructure Details on Abutment (Panayir Bridge) (in cm).....	48
Figure 4.11 Superstructure Details on Pier (Panayir Bridge) (in cm)	49
Figure 4.12 Pier Detail (Panayir Bridge) (in cm)	49
Figure 4.13 Cross Section of the Column (Panayir Bridge) (in cm)	50
Figure 4.14 Plan View (Balikli Bridge) (in cm).....	51
Figure 4.15 Scheme of Design Level (Balikli Bridge) (elevations in m, lengths in cm)	51
Figure 4.16 Elevation View (Balikli Bridge)	52
Figure 4.17 Beam Cross Section (Balikli Bridge) (in cm)	52
Figure 4.18 Vertical Cross Section of Superstructure (Balikli Bridge).....	54
Figure 4.19 Detail of the Shear Key (Balikli Bridge) (in cm).....	55
Figure 4.20 Superstructure Details on Abutment (Balikli Bridge) (in cm)	55
Figure 4.21 Superstructure Details on Pier (Balikli Bridge) (in cm)	56
Figure 4.22 Pier Detail (Balikli Bridge)	56
Figure 4.23 Cross Section of the Column (Balikli Bridge) (in cm)	57
Figure 4.24 Elevation View (a) Start, (b) Middle and (c) End (Demirtas Bridge).....	60

Figure 4.25 Vertical Cross Section of the Superstructure (Demirtas Bridge).....	60
Figure 4.26 Cross Section of the Beam (Demirtas Bridge) (in cm).....	61
Figure 4.27 Detail of the Shear Key (Demirtas Bridge) (in cm).....	61
Figure 4.28 Superstructure Details on Abutment (Demirtas Bridge) (in cm).....	62
Figure 4.29 Superstructure Details on Pier (Demirtas Bridge) (in cm)	62
Figure 4.30 Pier Detail (Demirtas Bridge).....	63
Figure 4.31 Cross Section of the Column (Demirtas Bridge) (in cm)	63
Figure 4.32 A Typical Bridge Model (Adopted from Sevgili, 2007)	65
Figure 4.33 Model of Demirtas Bridge on LARSA 4D	66
Figure 4.34 Modelling of Superstructure and Supports at Piers (Demirtas Bridge)...	66
Figure 4.35 Representation of Balikli Bridge on LARSA 4D	67
Figure 4.36 Modelling of Superstructure and Supports at Piers (Balikli Bridge).....	68
Figure 4.37 Representation of Panayir Bridge on LARSA 4D.....	69
Figure 4.38 Modelling of Superstructure and Supports at Piers (Panayir Bridge)	70
Figure 4.39 Definitions of Global Axes for Bridge Models (X-Axis in Longitudinal and Y-Axis in Transverse Direction).....	75
Figure 5.1 Ground Motion Records Used in Spectral Matching (a) A-TIN000, (b) DZC-DZC 1058e and (c) H-SUP135	84
Figure C.1 Spectral Matching for AASHTO 2010 Using A-TIN000.....	115
Figure C.2 Spectral Matching for AASHTO 2010 Using DZC-DZC 1058E.....	115
Figure C.3 Spectral Matching for AASHTO 2010 Using HSUP-135	116
Figure C.4 Spectral Matching for AASHTO 2007 Using A-TIN000.....	116
Figure C.5 Spectral Matching for AASHTO 2007 Using DZC-DZC 1058E.....	117
Figure C.6 Spectral Matching for AASHTO 2007 Using HSUP-135	117
Figure C.7 Spectral Matching for $3.5 < M_w < 4.5$ Using A-TIN000 (mean).....	118
Figure C.8 Spectral Matching for $3.5 < M_w < 4.5$ Using DZC-DZC 1058E (mean)....	118
Figure C.9 Spectral Matching for $3.5 < M_w < 4.5$ Using HSUP-135 (mean)	119
Figure C.10 Spectral Matching for $4.5 < M_w < 5.5$ Using A-TIN000 (mean).....	119
Figure C.11 Spectral Matching for $4.5 < M_w < 5.5$ Using DZC-DZC 1058E (mean) ..	120

Figure C.12 Spectral Matching for $4.5 < M_w < 5.5$ Using HSUP-135 (mean)	120
Figure C.13 Spectral Matching for $5.5 < M_w < 6.5$ Using A-TIN000 (mean)	121
Figure C.14 Spectral Matching for $5.5 < M_w < 6.5$ Using DZC-DZC 1058E (mean) ..	121
Figure C.15 Spectral Matching for $5.5 < M_w < 6.5$ Using HSUP-135 (mean)	122
Figure C.16 Spectral Matching for $6.5 < M_w < 7.5$ Using A-TIN000 (mean)	122
Figure C.17 Spectral Matching for $6.5 < M_w < 7.5$ Using DZC-DZC 1058E (mean) ..	123
Figure C.18 Spectral Matching for $6.5 < M_w < 7.5$ Using HSUP-135 (mean)	123
Figure C.19 Spectral Matching for $3.5 < M_w < 4.5$ Using A-TIN000 (mean+std)	124
Figure C.20 Spectral Matching for $3.5 < M_w < 4.5$ Using DZC-DZC 1058E (mean+std)	124
Figure C.21 Spectral Matching for $3.5 < M_w < 4.5$ Using HSUP-135 (mean+std).....	125
Figure C.22 Spectral Matching for $4.5 < M_w < 5.5$ Using A-TIN000 (mean+std)	125
Figure C.23 Spectral Matching for $4.5 < M_w < 5.5$ Using DZC-DZC 1058E (mean+std)	126
Figure C.24 Spectral Matching for $4.5 < M_w < 5.5$ Using HSUP-135 (mean+std).....	126
Figure C.25 Spectral Matching for $5.5 < M_w < 6.5$ Using A-TIN000 (mean+std)	127
Figure C.26 Spectral Matching for $5.5 < M_w < 6.5$ Using DZC-DZC 1058E (mean+std)	127
Figure C.27 Spectral Matching for $5.5 < M_w < 6.5$ Using HSUP-135 (mean+std).....	128
Figure C.28 Spectral Matching for $6.5 < M_w < 7.5$ Using A-TIN000 (mean+std)	128
Figure C.29 Spectral Matching for $6.5 < M_w < 7.5$ Using DZC-DZC 1058E (mean+std)	129
Figure C.30 Spectral Matching for $6.5 < M_w < 7.5$ Using HSUP-135 (mean+std).....	129

LIST OF SYMBOLS AND ABBREVIATIONS

AASHTO	American Association of State Highway and Transportation Officials
ASCE	American Society of Civil Engineers
ABSSUM	Absolute Sum
CALTRANS	California Department of Transportation
C_{sm}	Elastic Seismic Response Coefficient
CQC	Complete Quadratic Combination
EQ	Earthquake
GDH	General Directorate of Highways
GMPE	Ground Motion Prediction Equation
KGM	Karayolları Genel Müdürlüğü
KAMAG	Support Program for Research and Development Projects of Public Institutions (in Turkish)
LFD	Load Factor Design
LRFD	Load and Resistance Factor Design
LTHA	Linear Time History Analysis
METU	Middle East Technical University
MM	Multimode Elastic Method
M_w	Moment Magnitude
\bar{N}	Average Standard Penetration Test (SPT) Blow Count
NLTHA	Nonlinear Time History Analysis
NEHRP	National Earthquake Hazards Reduction Program
TÜBİTAK	Scientific and Technological Research Council of Turkey (in Turkish)
P	Power of T (period) in long period range
PGA	Peak Ground Acceleration
PI	Plasticity Index

R^2	Coefficient of Determination
R_{epi}	Epicentral Distance
RSA	Response Spectrum Analysis
RSM	Response Spectrum Method
S_a	Spectral Acceleration
S_{D1}	Acceleration Coefficient
SEAOC	Structural Engineers Association of California
SM	Single-Mode Elastic Method
SPT	Standard Penetration Test
SRSS	Square Root of Sum of Squared
\bar{s}_u	Average Undrained Shear Strength
T	Period of Vibration
TH	Time History Method
UL	Uniform Load Elastic Method
USGS	United States Geological Survey
\bar{v}_s	Average Shear Wave Velocity
V_{S30}	Average Shear Wave Velocity of the Upper 30 m of Soil Layers
w	Moisture Content

CHAPTER 1

INTRODUCTION

1.1 General

Seismic design of bridges is a significant problem for seismically active countries including Turkey. After recent devastating earthquakes, seismic design became more of an issue for the bridge designers with the experience gained after significant damage and failure of bridges. Engineers utilize earthquake codes for seismic design, thus the revision of earthquake codes according to the recent studies plays an important role in keeping the design strategies updated.

Currently an adapted version of American Association of State Highway and Transportation Officials Standard Specifications for Highway Bridges (AASHTO LFD) is being used by Republic of Turkey General Directorate of Highways (GDH in English and KGM in Turkish, from here after will be named as KGM). Although there are other supplementary tools (prepared by KGM in previous years) to follow in the design of bridges, the main specification in regulation is AASHTO LFD. Thus, focusing on the revisions made in AASHTO recently would be beneficial for presenting effective solutions to current design problems.

Civil Engineering Department of the Middle East Technical University (METU) and KGM have collaborated to conduct a research project, Development of Design and Construction Technologies for Bridge Engineering in Turkey, funded by the Scientific and Technological Research Council of Turkey (TÜBİTAK), to update the current practice in Turkey. The results of this thesis are planned to be included in the

“Loads” section under the topic of “Earthquake Spectrum Coefficient Analysis” in the final project report.

Several methods are used for dynamic analysis of bridges which may be summarized as the uniform load elastic method, single-mode elastic method, multimode elastic method and time history method according to AASHTO (2010). One of the most commonly methods is the Response Spectrum Analysis (RSA) which is described in single-mode and multimode spectral analyses sections. According to several researchers (Hudson, 1956; Tehranizadeh and Safi, 2004; Chopra, 2011), this method is simple and practical. As a result, RSA is employed as the main method of analysis in this thesis. Design spectra are generally affected by the revisions aforementioned; as a result, examining the revisions is also substantial. Furthermore, as the local ground conditions affect the seismic activity and the design spectra accordingly, site-specific consideration of response spectra at several locations in a region of interest is important. (Doğangün, and Livaoğlu, 2006)

Before going into details, it would be appropriate to define response spectra curves briefly. Response spectra curves are graphs representing the maximum response in terms of displacement, velocity or acceleration of a single degree-of-freedom system which is exposed to a specified excitation. The solution of single degree-of-freedom systems with a sequence of natural frequency and damping ratio values is required to construct these plots. For each solution, one point on the response spectrum is obtained. For all interested frequencies the same task is applied repeatedly. After obtaining these curves for specified seismic excitation, natural frequencies and mode shapes of the structure are utilized for response spectrum analyses.

Although design spectra tend to be smooth curves, response spectra obtained at a site of interest generally show fluctuations with sharp spikes and vales. Methods for obtaining a smooth design spectrum are used in order to get rid of the sharp points and shape variations in the actual response spectra obtained from the time history records at a site. There are several ways to obtain design response spectrum which

represents an average spectrum by incorporating the spectra of several earthquakes. Mostly, the design response spectra statistically depend on the mean, median, mean-plus-one-standard-deviation or median-plus-one-standard-deviation of the selected variables of the ground motion records (Tehranizadeh and Safi, 2004). Detailed information about the construction of a current design spectrum is given in the literature survey section of this thesis. A typical example of design spectrum is demonstrated in Figure 1.1. In the ordinate of the curve, spectral acceleration values (S_a) are specified while in the abscissa period values (T) are presented. It should be noted that the values in the abscissa and ordinate of response spectrum curve must be positive or zero. The ordinates may be the original values or they may be normalized according to a specified value, e.g. Peak Ground Acceleration (PGA).

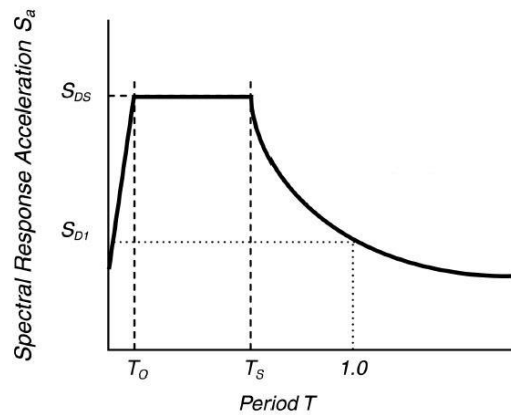


Figure 1.1 Example of a Typical Design Spectrum

In July 2007, major changes were made by AASHTO on the seismic design of highway bridge specifications. Through these changes, the methodology used for response spectrum construction has also changed with the contribution of new values of spectral acceleration. As a result, the response of bridges has been exposed to changes with this “improved seismic response spectrum” (Manceaux, 2008). The

consequences of these modifications on typical bridge responses will also be studied in this study.

1.2 Literature Review

Biot and Housner (1941) introduced the response spectrum concept for the first time with Response Spectrum Method (RSM). Later, strong motion records of El Centro (1934, 1940), Olympia (1949) and Kern County (1952) earthquakes with various damping values were used by Housner (1959) to develop average acceleration spectra. Improved developments were then made on the studies about the response spectra of nuclear reactor facilities by Mohraz et al. (1972), Blume et al. (1972) and Hall et al. (1975). With the increasing number of ground motion records, additional investigations are performed on these topics. Hayashi et al. (1971) divided the spectra into three groups after the studies on various ground motion records on different site conditions. Stiff soil, loose soil and intermediate soil are the classes assigned as the main soil types. With the studies of Mohraz et al. (1972), Hall et al. (1975), Hayashi et al. (1971) and Seed et al. (1976), it is pointed that the response spectra obtained on soils are different from the ones obtained on rock. After observing that the shape of the spectra is affected by soil conditions, alternative spectra for different geological conditions were proposed by Shannola and Wilson (1974). Lack of strong motion data on different soil conditions led the combination of data from different regions and geological conditions all over the world for the studies of Mohraz (1976), Seed and Idriss (1979), Singh (1985), Atkinson and Boore (1990), Crouse and McGuire (1996) and Sabetta and Pugliese (1996). As the number and quality of strong motion instruments increased all over the world, increasingly more strong motion data were made ready to use. Later large destructive earthquakes in Turkey, Japan, Taiwan and California provided some near-source ground motion records. Especially Northridge (1994, $M_w=6.7$) and Chi-Chi (1999, $M_w=7.6$) earthquakes yielded over a thousand time history records. Influence of magnitude, local site effects and wave propagation

effects on response spectra utilizing the ground motion data from large earthquakes in Turkey, Taiwan and US were studied by Su et al. (2006) recently.

Until the early 1970s, the RSM was not accepted as an engineering tool but it stayed in the academic sphere mostly. The main reasons behind this are the difficulties confronted during the computation of response of structures in that era to different ground motions and lack of number of records. Before the late 1960s and early 1970s, digital computation and the digitization of analog accelerograph records were time consuming and the results were unreliable. However, this situation started to change in 1970s with the advances in the computers. In 1971, the modern era for RSM started with San Fernando, California earthquake. 241 accelerographs were recorded by this earthquake and it was possible to perform the empirical scaling analyses of response spectra for the first time with this earthquake (Trifunac, 2012).

The necessity of handling response spectra and dynamic analyses (as they are regulated in modern building codes) required the use and understanding by design engineers (Sigmund, 2007). The basis of the development of current seismic building codes was started by a joint committee of the Structural Engineers Association of Northern California and San Francisco section of American Society of Civil Engineers (ASCE) (Anderson et al., 1952). A “modal lateral force provision” was prepared by this committee proposing the design curve $C=K/T$ where it descends in proportion to $1/T$ after the corner period. Then, the concept of response spectra was introduced in the building codes of United States by Structural Engineers Association of California (SEAOC) through the coefficient C with the lateral force equation $V=KCW$ in where V is equal to the total lateral force, K is equal to structural systems coefficient and W is the total dead load of structure. This new recommended curve had a descending proportion of $1/T^{1/3}$ resulting in a larger load factor for the structures with high natural period values (Sigmund, 2007). Although several revisions were later applied on the coefficients and variables, two codes mentioned may be called as the pioneer regulations about design spectrum shapes.

When more recent methods of developing design spectra are examined, it would be appropriate to have a look at the California Department of Transportation (CALTRANS, 2013) seismic design criteria which is used worldwide and explained the process in detail at the end of the regulations. According to these criteria, the design response spectrum can be constructed with the help of the envelope of a deterministic and probabilistic spectrum. In the deterministic approach, arithmetic average of median response spectra is calculated by the ground motion prediction equations (GMPE's) of Campbell-Bozorgnia and Chiou-Youngs (2008) to account for deterministic spectrum. These equations are employed to the faults which are considered to be active in the last 700,000 years in or near California and can produce earthquakes with a moment magnitude of 6.0 or greater. On the other hand, for probabilistic criteria, design spectrum is obtained from the United States Geological Survey (USGS) Seismic Hazard Map for 975 year return period with several adjustment factors (Peterson et al., 2008).

Comparisons between design spectra of different codes and the response of reinforced concrete buildings to these codes were studied in previous studies (e.g. Doğangün and Livaoglu, 2006). However, applications of design spectrum analysis on bridges and comparison of the results are not extensively investigated. Moreover, as investigated in other studies for different structures (Chai et al., 2004), mean site-specific response spectra should be taken into consideration for purposes of structural response comparison against the design spectra. This thesis aims to fill such a gap in the literature.

1.3 Aim and Scope

The main objective of this study is to compare the mean site-specific response spectra in Turkey with the design spectra in AASHTO (2007) and AASHTO (2010) by focusing on the descending part (long period range). Selection of the stations used for

constructing mean response spectra, is made according to a recent study in Turkey (Akkar et al., 2010). Strong motion data recorded at stations that constitute Turkish National Strong-Motion Observation Network is used in this thesis as the primary database.

After comparing the mean site-specific spectra with the corresponding design spectra in the form of PGA-normalized curves, the differences in bridge response due to these different spectra is studied. For this purpose, three bridges in Bursa region (Demirtas, Panayir and Balikli bridges) are compared in terms of the maximum moment values on the columns. According to Yılmaz (2008), damage is allowed to occur at the plastic hinge zones of columns in seismic design of multi-span bridges (Figure 1.2). Thus, maximum column moments are selected for response comparison purposes.

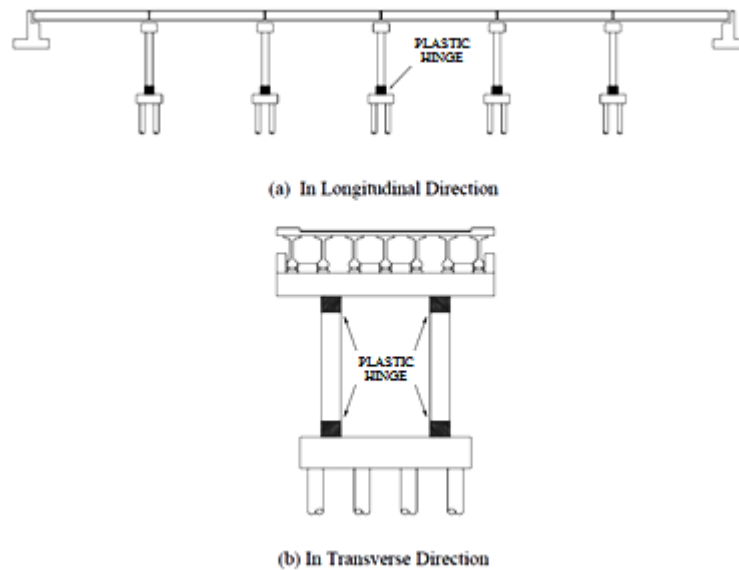


Figure 1.2 Potential Plastic Hinge Regions on Columns (a) in Longitudinal Direction
(b) in Transverse Direction (Adopted from Yılmaz, 2008)

In this thesis, initially regular response spectrum analyses are performed on the selected bridges. Then as a further application, linear time history analyses are presented using records that match the spectra of interest. These particular bridges are selected in coordination with the other work packages in TÜBİTAK 110G093 Project (2014), as they supply necessary (seismic hazard and site conditions-related) information as input to the analyses on bridges.

In Chapter 2, seismic design spectra in AASHTO (2007 and 2010) are investigated in detail. Site classification criteria and the evaluation of necessary seismic coefficients are mentioned as they compose the main steps to construct the design spectra.

In Chapter 3, after the classification and compilation of Turkish strong ground motion data; mean site-specific response spectra are presented. Different site class and Moment Magnitude (M_w) values are used to classify the response spectra. Then, comparisons are made between mean site-specific response spectra and AASHTO (2007 and 2010) design spectra.

In Chapter 4, detailed information is given about the three bridges used in the analyses. Then, computer modelling is presented and response spectrum analysis is described. Next, maximum column moment values obtained from RSA are discussed in detail and compared with each other.

In Chapter 5, linear time history analysis is introduced along with the spectral matching procedure applied to the selected ground motions. Results obtained from LTHA on bridges are discussed and compared with each other for all cases. They are also compared with the results from RSA.

Finally, summary, conclusions and future work are presented in Chapter 6.

CHAPTER 2

SEISMIC DESIGN SPECTRA IN AASHTO (2007 AND 2010)

2.1 Design Spectra of AASHTO LRFD (2007)

Design spectrum for bridges is addressed under the chapter named Earthquake Effects in AASHTO LRFD Bridge Design Specifications (2007) in detail. Elastic response coefficient, C_{sm} , and equivalent weight of the superstructure are multiplied to get earthquake loads in horizontal direction while response modification factor, R , is used for the adjustment subsequently. The equivalent weight is calculated with the help of the actual weight and the configuration of the structure where for single-mode and multimode analyses it is automatically included.

The provisions of these specifications offers that the bridges designed and detailed accordingly may suffer damage, but should not collapse due to ground shaking which is seismically induced.

According to the specifications, the provisions in that chapter shall be used for total multiple span lengths not exceeding 1.5 km on conventional slab, beam girder, box girder bridges, and truss superstructure constructions. For other construction types and bridges with spans larger than 1.5 km, the owner shall indicate provisions that are appropriate to use.

Design and detailing provisions are established in these specifications to minimize the susceptibility of bridges against earthquake damages. In addition, a flow chart that summarizes the design provisions for earthquakes is supplied in the Appendix of Loads and Load Factors section of AASHTO (2007).

Development of these specifications is made according to the following principles:

- Bridges should resist to the small to moderate earthquakes within the elastic ranges of their structural components.
- Forces and seismic ground motion intensities used in the design procedures should be realistic.
- All or part of the bridge should not fail exposing to shaking from large earthquakes. Damage that has a possibility of occurrence should be both detectable and accessible to be inspected and repaired.

Bridges are categorized according to their importance level as critical bridges, essential bridges and other bridges. Essential bridges, as a minimum, should satisfy security/defense requirements and be open to emergency vehicles after the design earthquake which has a 475-year return period. On the other hand, after the design earthquake, some bridges which are regarded as critical structures must be open to all traffic, satisfy security/defense requirements and be usable by emergency vehicles after a destructive earthquake that has a 2500-year return period.

The elastic seismic response coefficient, C_{sm} , for the m^{th} mode of vibration can be calculated with the help of the following formula:

$$C_{sm} = \frac{1.2AS}{T_m^{2/3}} \leq 2.5A \quad (2-1)$$

where T_m is the period of vibration of the m^{th} mode (sec.), A is the acceleration coefficient and S is the site coefficient.

This value shall be computed for each relevant mode in a bridge as an earthquake can excite different modes of vibration. However, there are several exceptions to the general formula of C_{sm} stated below. C_{sm} should not exceed $2.0A$ for the bridges in areas where A is not less than 0.30 and on soil profiles III or IV. For modes that have period values less than $0.3s$ except the fundamental mode and for soil profile III and IV, C_{sm} shall be calculated as;

$$C_{sm} = A(0.8 + 4.0T_m) \quad (2-2)$$

For the modes that the period of vibration exceeds 4.0s, C_{sm} shall be calculated as;

$$C_{sm} = \frac{3AS}{T_m^{4/3}} \quad (2-3)$$

Necessary detailed explanations related to the variables used during calculations can be found in the subchapter named site effects in AASHTO (2007). The acceleration coefficient, A, basically depends on seismic zones. On the other hand, site coefficient, S, depends on site classes and reflects the effect of site classes on the elastic seismic response coefficient. In Table 2.1 relation between S and different soil profile types is provided. If there is not sufficient detail about the soil properties to define site classes or the soil does not fit to the four classes supplied, Soil Profile Type II should be used to determine the site coefficient.

Table 2.1 Site Coefficients in AASHTO (2007)

Site Coefficient	Soil Profile Type			
	I	II	III	IV
<i>S</i>	1.0	1.2	1.5	2.0

Also several contour maps reflecting seismic zones for the selection of acceleration coefficient, A, can be found and used for United States, while for other regions in world they are not provided in AASHTO LRFD Bridge Design Specifications. Special studies by professionals are suggested for the determination of site -and structure- specific acceleration coefficients if one of the cases below occurs;

- The location of site is close to an active fault,
- In the region, earthquakes of long-duration are expected,

- Importance of bridge is so high that a longer return period should be used.

The site classification in AASHTO (2007) is tabulated and presented in Table 2.2. To classify soil profiles of different subsurface conditions, the results of a statistical study of spectral shapes (obtained with the help of past earthquakes from the soils which are close to seismic sources) are used.

Table 2.2 Soil Profile Classification in AASHTO (2007)

Soil Profile Type	Description
I*	<ul style="list-style-type: none"> ● Rock of any description, either shale-like or crystalline in nature, or ● Stiff soils where the soil depth is less than 60 000 mm, and the soil types overlying the rock are stable deposits of sands, gravels or stiff clays.
II	A profile with stiff cohesive or deep cohesionless soils where the soil depth exceeds 60 000 mm and the soil types overlying the rock are stable deposits of sands, gravels, or stiff clays
III	A profile with soft to medium-stiff clays and sands, characterized by 9000 mm or more of soft to medium-stiff clays with or without intervening layers of sand or other cohesionless soils
IV**	A profile with soft clays or silts greater than 12 000 mm in depth
* may be characterized by a shear wave velocity greater than 765 m/sec ** may be characterized by a shear wave velocity greater than 152 m/sec and might include natural deposits or manmade, nonengineered fill	

For the calculations in this study, AASHTO (2010) site classification is employed. It is different from the one in AASHTO (2007), thus the corresponding site classes for site class C (Soil Profile Type II in AASHTO 2007) and site class D (Soil Profile Type III in AASHTO 2007) are used in response spectra calculations. General trend of the normalized (with respect to A) response spectrum curves based on five percent damping for different soil profiles in AASHTO (2007) is shown in Figure 2.1. On the other hand, corresponding normalized response spectrum curves that will be used in analyses for site classes C and D are presented in Figure 2.2.

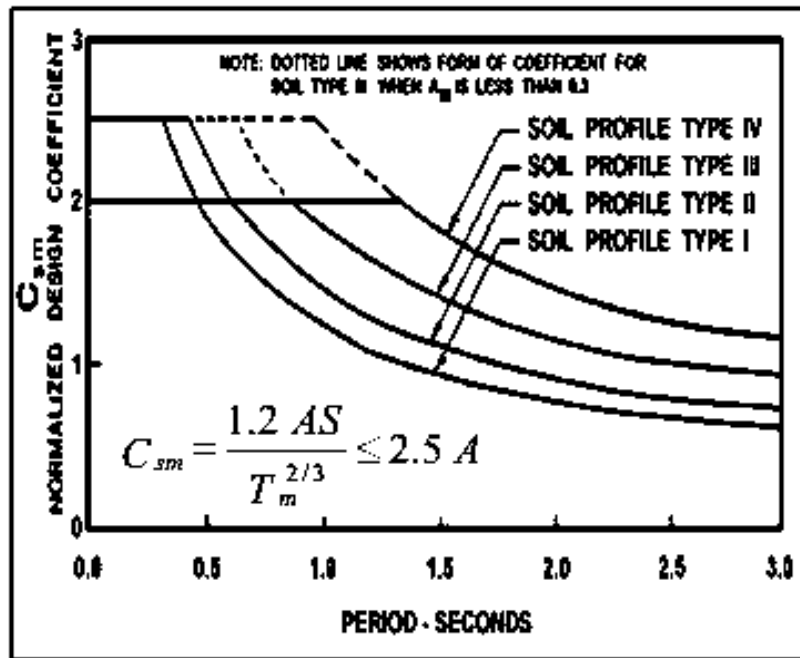


Figure 2.1 Design Spectra Trend for AASHTO (2007)

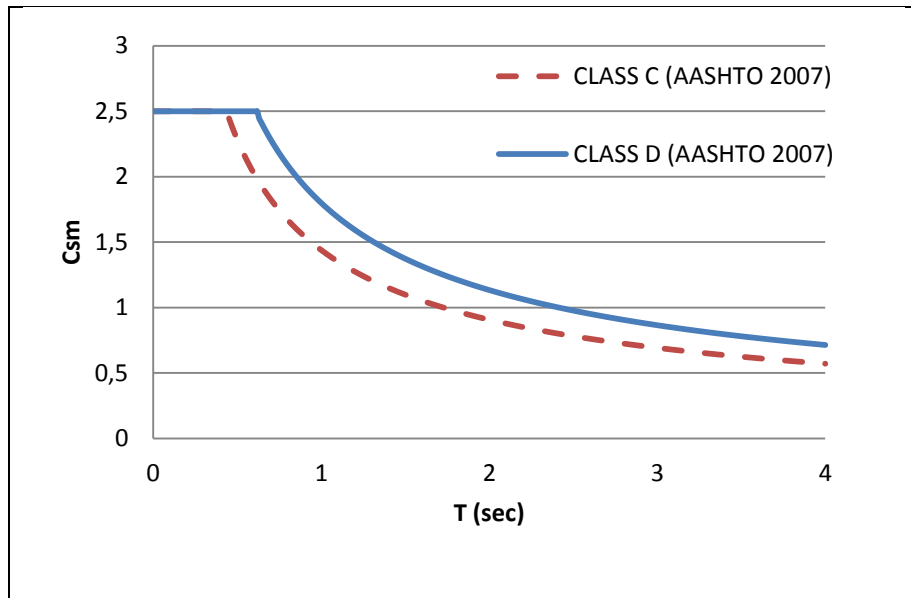


Figure 2.2 AASHTO (2007) Design Spectra for Site Class C and Site Class D

Combining the elastic seismic force effects on principal axes in two perpendicular directions, two load cases are formed as follows:

- A combination is formed using the absolute value of the force effects in one of the perpendicular directions in 100 percent with the absolute value of the force effects in the second perpendicular direction in 30 percent, and
- A combination is formed using the absolute value of the force effects in the second perpendicular direction in 100 percent with the absolute value of the force effects in the first perpendicular direction in 30 percent.

For the cases where plastic hinging of the columns are used to determine foundation or column forces, the combinations provided should not be considered. Necessary further information about handling those cases can be found in the chapter named Calculation of Design Forces in AASHTO (2007).

2.2 Design spectra of AASHTO LRFD (2010)

Several revisions were applied to AASHTO (2007) Earthquake Effects chapter for the newer version AASHTO (2010) some of which are also taken into account in this study. Basic changes and explanations involved and related to this study are summarized next.

Design of bridges should be performed according to the potential damage levels that would result from earthquake ground motions which have a 7 percent probability of exceedance in 75 years (return period of about 1000 years). Complete or partial replacement may be necessary and higher performance levels can be used with bridge owner's mandate whenever required.

Bridges with single- or multi-column piers, wall-type piers, pile bent substructures and slab, beam, box girder, or truss superstructures are called conventional bridges. On the other hand, arch bridges, cable-stayed/cable-suspended bridges and bridges with truss towers or hollow pier substructures are called nonconventional bridges.

Two kinds of measures are considered mostly in the specifications which are namely force-based and displacement-based procedures. AASHTO (2010) specifications are regarded as "force-based" because bridges designed according to them must have adequate strength, which can be called capacity, to resist earthquake forces, in other words, demands. Displacement capacity of bridges that are designed with the help of these specifications should be confirmed also using a displacement-based procedure. AASHTO (2009) specifications for LRFD seismic design are displacement-based in which the limit states resulting in collapse after damage are identified and bridges are designed to have a sufficient displacement capacity.

A subchapter called Seismic Hazard was added to Earthquake Effects chapter in AASHTO (2010). Detailed information about determining coefficients PGA , S_S and S_1 can be found in this subchapter where similar to AASHTO (2007) maps of United States can be utilized. Furthermore, it is noted that instead of using national ground

motion maps, state ground motion maps conforming several conditions mentioned in this chapter can be used to derive the coefficients. For obtaining a uniform-hazard acceleration spectrum, detailed explanations are also involved in another subchapter about site-specific probabilistic ground-motion analysis.

In the chapter named Site Effects in AASHTO (2010), Site Class Definitions are defined. They are listed in Table 2.3. This classification is selected for use in the calculations and comparisons included in the next chapters since it is up to date and comprehensive.

Table 2.3 Site Class Definitions in AASHTO (2010)

Site Class	Soil Type and Profile
A	Hard rock with measured shear wave velocity, $\bar{v}_s > 5000$ ft/s (1525 m/s)
B	Rock with 2500 ft/sec (762.5 m/s) $< \bar{v}_s < 5000$ ft/s (1525 m/s)
C	Very dense soil and soil rock with 1200 ft/sec (366 m/s) $< \bar{v}_s < 2500$ ft/s (762.5 m/s), or with either $\bar{N} > 50$ blows/ft (164 blows/m), or $\bar{s}_u > 2.0$ ksf (0.096 MPa)
D	Stiff soil with 600 ft/s (183 m/s) $< \bar{v}_s < 1200$ ft/s (366 m/s), or with either $15 < \bar{N} < 50$ blows/ft ($50 < \bar{N} < 164$ blows/m), or $1.0 < \bar{s}_u < 2.0$ ksf (0.048 MPa $< \bar{s}_u < 0.096$ MPa)
E	Soil profile with $\bar{v}_s < 600$ ft/s (183 m/s) or with either $\bar{N} < 15$ blows/ft (50 blows/m) or $\bar{s}_u < 1.0$ ksf (0.048 MPa), or any profile with more than 10 ft of soft clay defined as soil with $PI > 20$, $w > 40$ percent and $\bar{s}_u < 0.5$ ksf (0.024 MPa)

Site Class	Soil Type and Profile
F	Soils requiring site-specific evaluations, such as: <ul style="list-style-type: none"> ● Peats or highly organic clays ($H > 10$ ft (3.05 m) of peat or highly organic clay where H = thickness of soil) ● Very high plasticity clays ($H > 25$ft (7.625 m) with $PI > 75$) ● Very thick soft/medium stiff clays ($H > 120$ ft (36.6 m))

Explanations on Table 2.3:

Exceptions: At sites where the soil properties are not known in sufficient detail to determine the site class, a site investigation shall be undertaken for defining the site class. Site classes E or F should not be assumed unless the authority having jurisdiction determines that site classes E or F could be present at the site or in the event that site classes E or F are established by geotechnical data.

where:

\bar{v}_s = average shear wave velocity for the upper 100 ft (30.5m) of the soil profile

\bar{N} = average Standard Penetration Test (SPT) blow count (blows/ft) for the upper 100 ft of the soil profile

\bar{s}_u = average undrained shear strength in ksf for the upper 100 ft of the soil profile

PI = plasticity index

w = moisture content

F_{pga} , F_a and F_v are the site factors that are used in the design response spectrum calculations. Site classes can be used to determine these factors from the tables provided in Site Factors chapter of AASHTO (2010). Information related to these coefficients is provided below in Table 2.4, Table 2.5 and Table 2.6 for F_{pga} , F_a and F_v respectively.

Table 2.4 F_{pga} Values Corresponding to Different PGA (Zero-Period Range) Values in (AASHTO 2010)

Site Class	Peak Ground Acceleration Coefficient (PGA) ¹				
	$PGA < 0.10$	$PGA = 0.20$	$PGA = 0.30$	$PGA = 0.40$	$PGA > 0.50$
A	0.8	0.8	0.8	0.8	0.8
B	1.0	1.0	1.0	1.0	1.0
C	1.2	1.2	1.1	1.0	1.0
D	1.6	1.4	1.2	1.1	1.0
E	2.5	1.7	1.2	0.9	0.9
F ²	*	*	*	*	*

Notes:

¹Use straight-line interpolation for intermediate values of PGA .

²Site-specific geotechnical investigation and dynamic site response analysis should be performed for all sites in Site Class F.

Table 2.5 F_a Values Corresponding to Short Period Range Values in (AASHTO 2010)

Site Class	Spectral Acceleration Coefficient at Period 0.2 sec (S_s) ¹				
	$S_s < 0.25$	$S_s = 0.50$	$S_s = 0.75$	$S_s = 1.00$	$S_s > 1.25$
A	0.8	0.8	0.8	0.8	0.8
B	1.0	1.0	1.0	1.0	1.0
C	1.2	1.2	1.1	1.0	1.0
D	1.6	1.4	1.2	1.1	1.0
E	2.5	1.7	1.2	0.9	0.9
F ²	*	*	*	*	*

Notes:

¹Use straight-line interpolation for intermediate values of S_s .

²Site-specific geotechnical investigation and dynamic site response analysis should be performed for all sites in Site Class F.

Table 2.6 F_v Values Corresponding to Long Period Range Values in (AASHTO 2010)

Site Class	Spectral Acceleration Coefficient at Period 1.0 sec (S_1) ¹				
	$S_1 < 0.1$	$S_1 = 0.2$	$S_1 = 0.3$	$S_1 = 0.4$	$S_1 > 0.5$
A	0.8	0.8	0.8	0.8	0.8
B	1.0	1.0	1.0	1.0	1.0
C	1.7	1.6	1.5	1.4	1.3
D	2.4	2.0	1.8	1.6	1.5
E	3.5	3.2	2.8	2.4	2.4
F ²	*	*	*	*	*

Notes:
¹Use straight-line interpolation for intermediate values of S_1 .
²Site-specific geotechnical investigation and dynamic site response analysis should be performed for all sites in Site Class F.

General trend for five-percent-damped-design response spectrum curves in AASHTO (2010) is presented in Figure 2.3. Since for the regions except United States, site factors S_s , S_1 and PGA are not provided in AASHTO (2010), they are obtained for the sites of interest herein within the TÜBİTAK 110G093 project as summarized in Table 2.7. In Figure 2.4, the design response spectrum curves that are obtained for the selected sites and used in analyses are presented.

Table 2.7 PGA, S_s and S_1 Values for Selected Sites for 1000 Years

Name of the Bridge	Latitude (o)	Longitude (o)	PGA (g)	S_s (g)	S_1 (g)
Demirtas	40.28 N	29.10 E	0.601	1.441	0.792
Panayir	40.24 N	29.06 E	0.553	1.333	0.727
Balikli	40.22 N	29.06 E	0.527	1.275	0.702

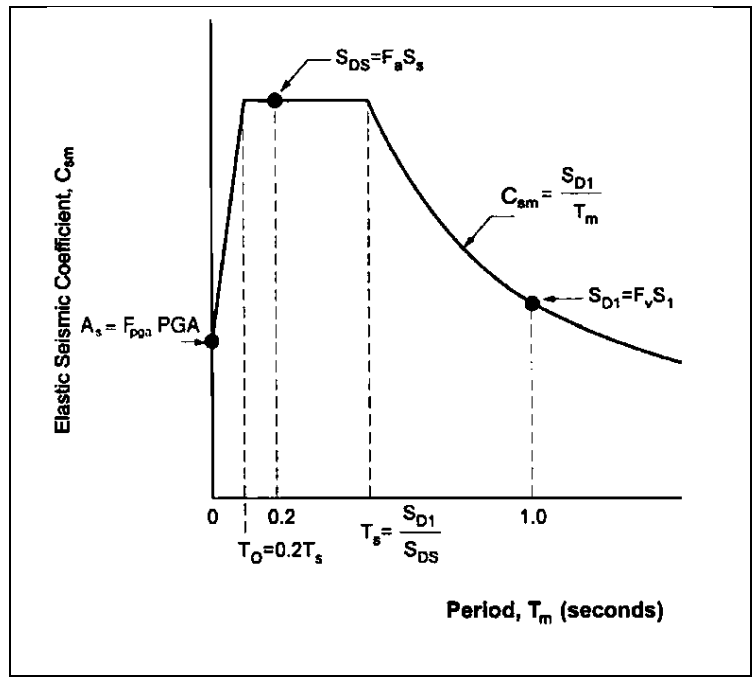


Figure 2.3 Design Spectra Trend for AASHTO (2010)

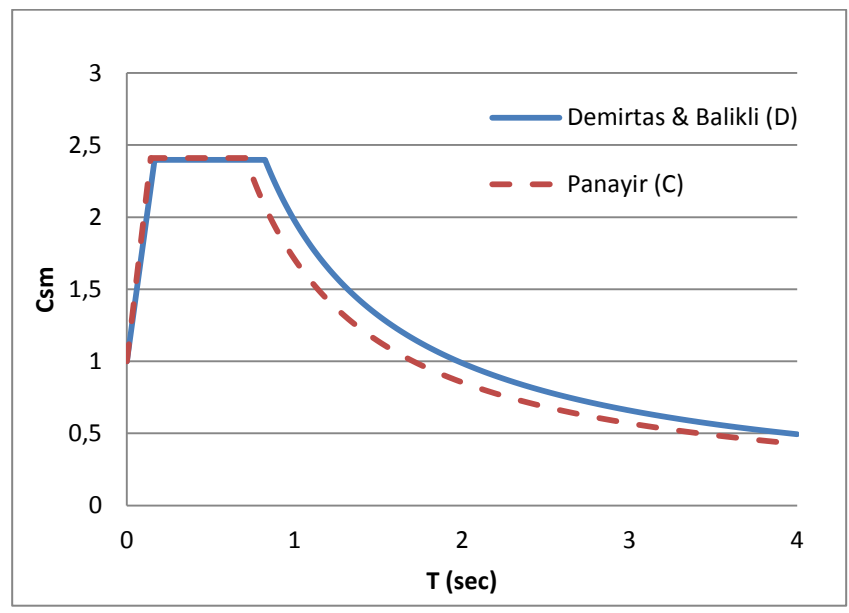


Figure 2.4 AASHTO (2010) Design Spectra for Site Class C and Site Class D

For periods less than or equal to T_0 , C_{sm} shall be calculated as:

$$C_{sm} = A_S + (S_{DS} - A_S) (T_m/T_0) \quad (2-4)$$

in which:

$$A_S = F_{pga} \text{PGA} \quad (2-5)$$

$$S_{DS} = F_a S_S \quad (2-6)$$

where PGA is the peak ground acceleration coefficient on rock (Site Class B), S_S is the horizontal response spectral acceleration coefficient at 0.2-sec period on rock (Site Class B), T_m is the period of vibration of the m th mode (s), T_0 is the period used to define spectral shape ($0.2 T_S$) and T_S is the corner period at which spectrum changes from being independent of period to being inversely proportional to period (S_{D1}/S_{DS}).

For periods greater than or equal to T_0 and less than or equal to T_S , C_{sm} shall be calculated as:

$$C_{sm} = S_{DS} \quad (2-7)$$

For periods greater than T_S , C_{sm} shall be calculated as:

$$C_{sm} = S_{D1}/T_m \quad (2-8)$$

where:

$$S_{D1} = F_v S_1 \quad (2-9)$$

AASHTO LRFD Bridge Design Specifications (2012) Design Spectra: For the Earthquake Effects Chapter in AASHTO (2012) there are only slight changes, however, they will not be mentioned herein since they do not affect the results of this thesis.

CHAPTER 3

MEAN SITE-SPECIFIC RESPONSE SPECTRA IN TURKEY

3.1 Compilation and Classification of Strong Ground Motion Data

The strong motion data used in mean site-specific response spectra calculations is obtained from the Turkish National Strong-Motion Observation Network. This network is constructed and maintained by the Earthquake Department of Republic of Turkey Prime Ministry, Disaster and Emergency Management Presidency (AFAD in Turkish) after setting up several accelerographs on Anatolian Peninsula near seismic sources since 1973 to monitor destructive earthquakes (Sandikkaya et al., 2010). In this database, raw records of the events that occurred since 1976 can be found. Currently, there are 12,594 records available for public use. For each record, necessary reliable information on the source parameters of the earthquake is also available in the mentioned network.

The selection of the stations is made according to the results of a previous study held within the scope of a national project called Compilation of National Strong Ground Motion Database in Accordance with International Standards (Sandikkaya, 2008). Obtaining the average shear wave velocity values of the upper 30 m of soil layers (V_{S30}) from the mentioned study, 153 stations which had available geophysical and geotechnical information are selected among a total of 479 stations within the Turkish National Strong-Motion Observation Network. The data recorded at these 153 stations are used in deriving the mean site-specific response spectra. It must be noted that for consistency in terms of tectonic settings, majority of the earthquake records are obtained from events with strike-slip source mechanisms.

For the classification of stations according to the site class definitions, AASHTO LRFD Bridge Design Specifications (2010) is used. Seven different site classes (from class A to class F) given in AASHTO (2010) are described in Chapter 2 in Table 2.3. These classes are mainly defined according to V_{S30} values. However, Standard Penetration Test (SPT), undrained shear strength of the soil sample from soil borings and blow counts can also be used for classification.

In Table 3.1, the site classification of the selected stations is shown. Since the number of records in class B is very limited (only 3 stations), this class is omitted in the classification. For deriving the site-specific mean response spectra, 62 stations with class C and 88 stations with class D are chosen to be used consequently.

After the compilation of strong motion data and classification of sites, records are further grouped according to M_w values of the earthquakes. A total of 4 groups are obtained for $3.5 < M_w < 4.5$, $4.5 < M_w < 5.5$, $5.5 < M_w < 6.5$ and $6.5 < M_w < 7.5$ bins. Then, records with epicentral distance (R_{epi}) values smaller than 15 km are eliminated to remove potential near-field effects. In addition, records with PGA values smaller than $0,981 \text{ cm/s}^2$ (0,001g) and records obtained at epicentral distances greater than 100 km are also eliminated to account for mostly moderate to large seismic sources and intermediate-field effects.

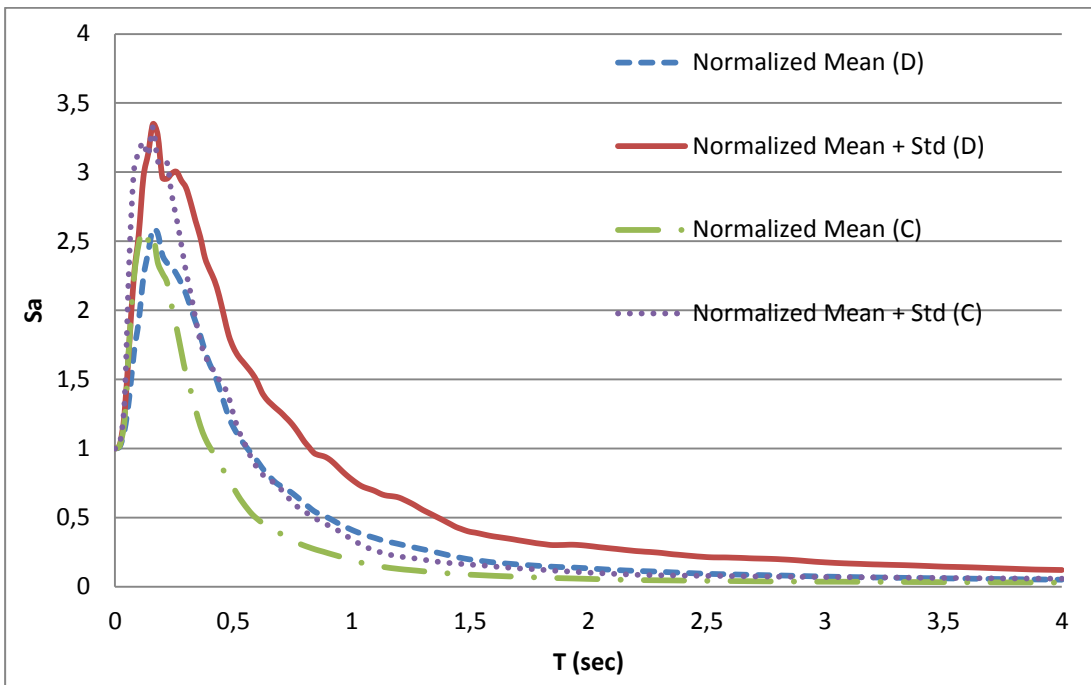
Furthermore, an outlier analysis is performed to remove records that remain significantly outside the main trend.

Table 3.1 Site Classification of the Selected Stations (According to AASHTO (2010) Site Class Definitions)

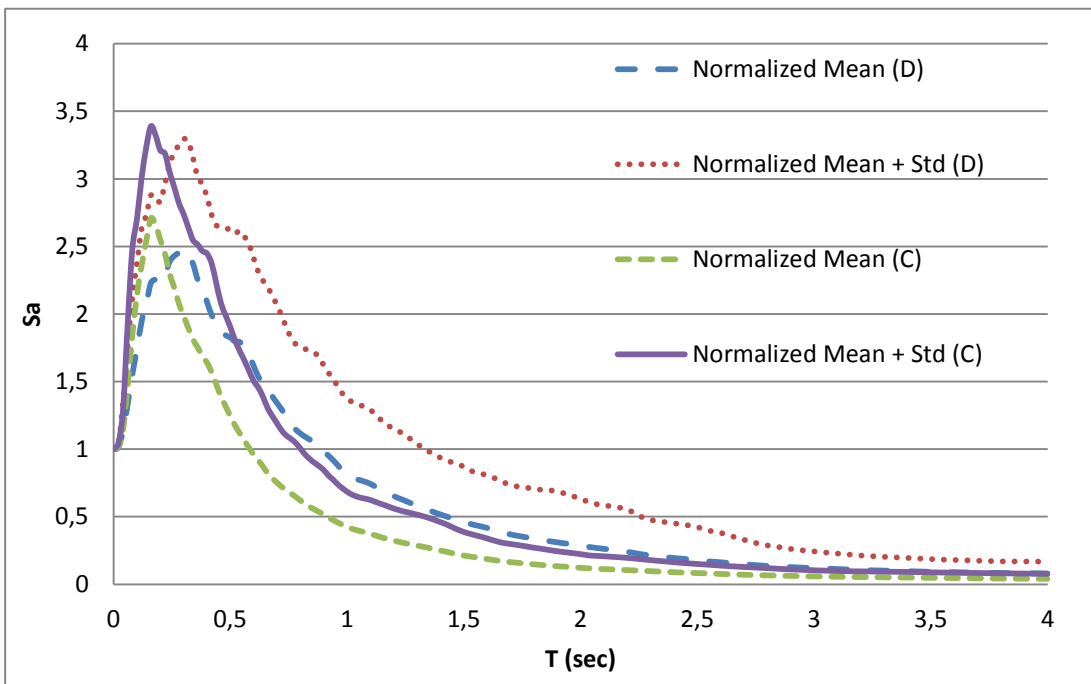
Class	# of stations selected
B	3
C	62
D	88
Total	153

3.2 Normalized Mean Site-Specific Response Spectra

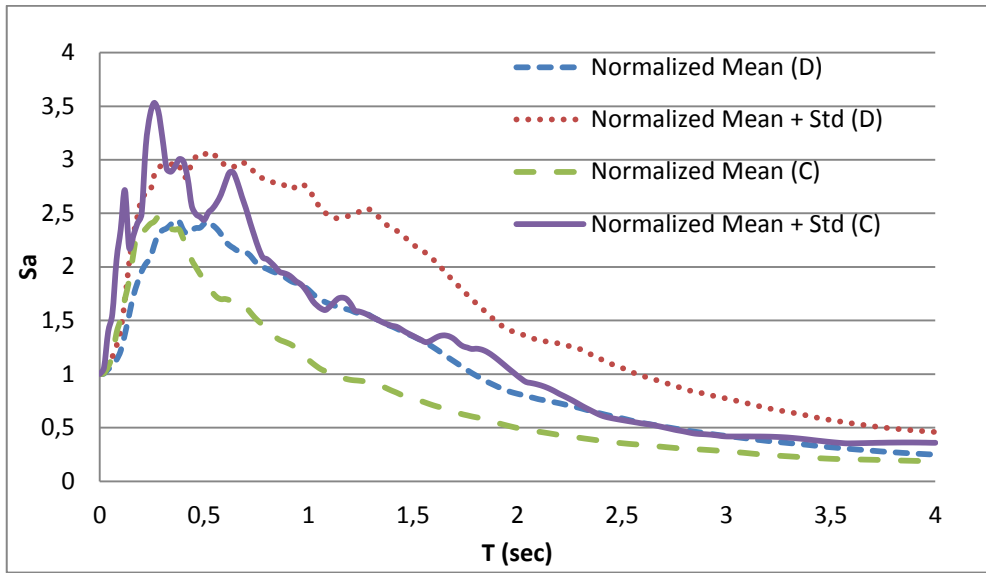
Response spectrum curves are obtained for each record using SeismoSignal software (version 5.0.0) after arranging the earthquake record data sets for Site classes C and D and different M_w intervals. Raw data is baseline-corrected and filtered with 4th order Butterworth filters between 0.1 and 25 Hz. Matching time step values are chosen accordingly to get elastic response spectra with 5% damping for the records. E-W and N-S components of each record are used to obtain the geometric mean of these components. Normalized mean response spectra are obtained for different site classes and magnitude ranges after normalizing the amplitudes of each response spectrum according to its own PGA value and calculating the average of all normalized spectra for each group. Calculating standard deviation values, normalized mean-plus-one-standard-deviation (mean + std) response spectra are also derived. Normalized mean response spectrum curves as well as normalized mean-plus-one-standard-deviation response spectrum curves for site class C and site class D and for different M_w intervals are presented in Figure 3.1. As expected, the curves for Class D lies above the curves for Class C in the long-period range, while in the short period range the curves for Class D lies below the curves for Class C. This difference between different site classes gets more significant as the M_w values increase. In addition, for the largest magnitude range, the area under the response spectra increases indicating enriched longer period (low frequency) content of the large earthquakes.



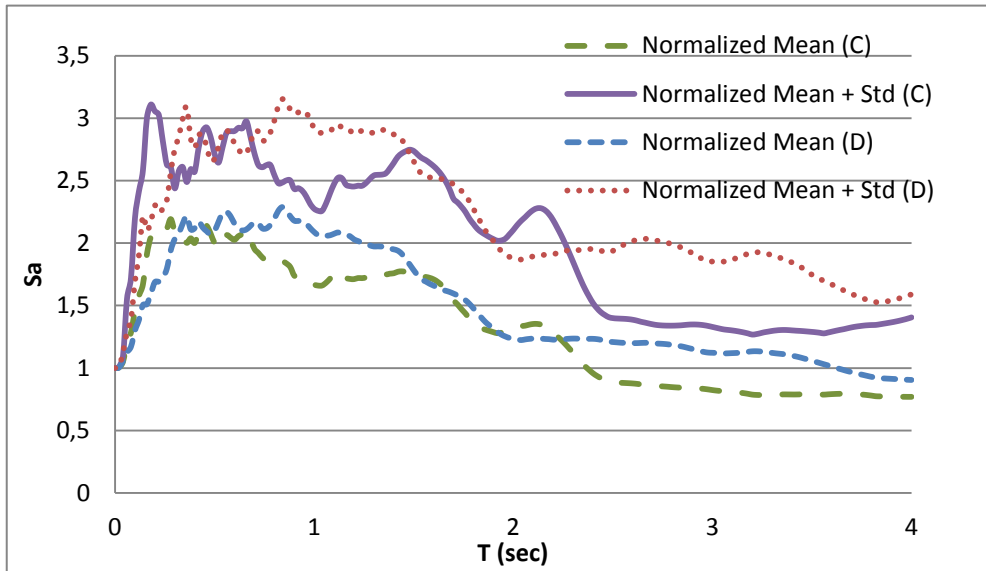
(a) $3.5 < M_w < 4.5$



(b) $4.5 < M_w < 5.5$



(c) $5.5 < M_w < 6.5$



(d) $6.5 < M_w < 7.5$

Figure 3.1 Normalized Mean and Mean + Std (Mean-Plus-One-Standard-Deviation) Response Spectrum Curves for Site Classes C and D for Different M_w Intervals (Site Classes are Shown in Parenthesis)

A similar study (Sandikkaya et al., 2010) was conducted previously at Middle East Technical University that utilized the same 153 stations used in this study to get normalized mean site spectra for Turkey. However, the total number of records was limited compared to the number of records used in this study. The aim of the mentioned study was to investigate the dependency of spectrum shape on site classes and M_w . The site classification was made according to the National Earthquake Hazards Reduction Program (NEHRP) provisions. When the normalized mean response spectrum curves in that study for two site classes and four M_w intervals in Figure 3.2 are considered, it is observed that they are consistent with the curves obtained in this thesis as shown in Figure 3.1.

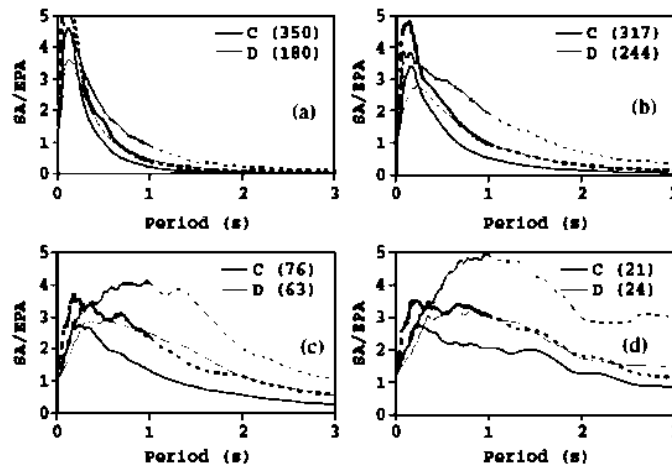
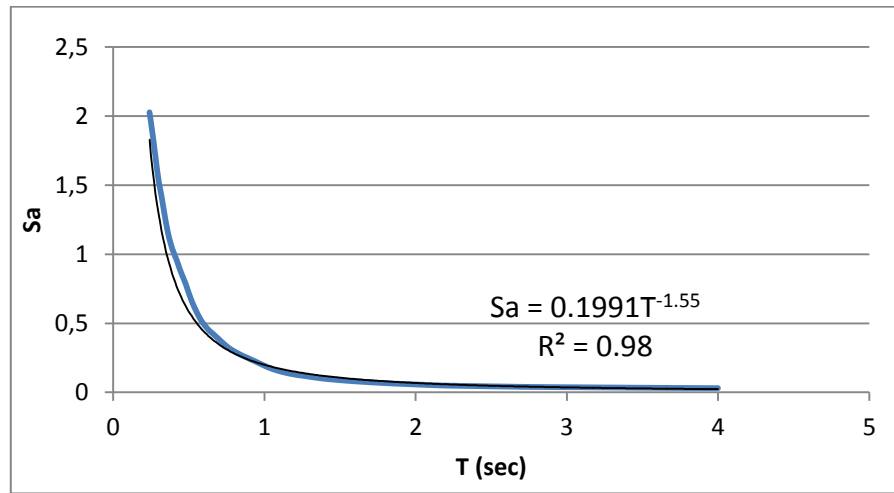
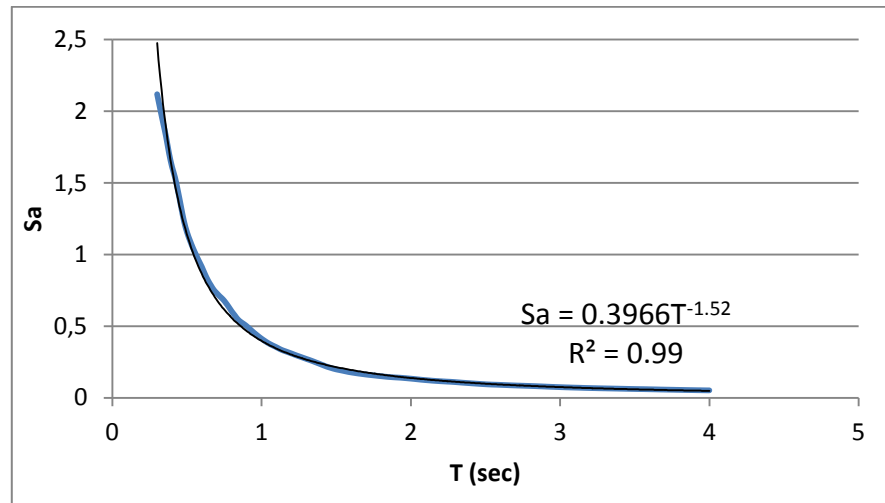


Figure 3.2 Comparison of Mean (Continuous Lines) and Mean-Plus-One-Standard-Deviation (Dashed Lines) Normalized Acceleration Spectra for Records of NEHRP Site Classes C and D for Magnitude Ranges (a) $3.5 < M_w < 4.5$, (b) $4.5 < M_w < 5.5$, (c) $5.5 < M_w < 6.5$, (d) $6.5 < M_w < 7.5$. The Number in Parenthesis Gives the Number of Records Used for Calculation of Mean Spectrum (Sandikkaya et al., 2010)

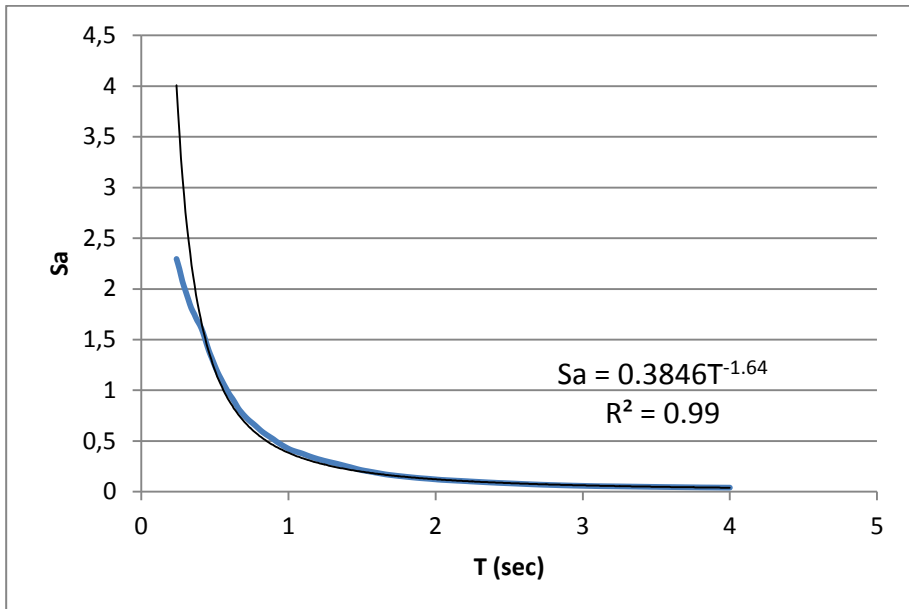
Through standard curve fitting to the normalized mean spectrum curves in Fig.3.1, formulae for amplitude decay at the long-period band and corresponding R^2 (coefficient of determination) values of the fits are obtained as shown on graphs in Figure 3.3. The long period power of T (P value where the spectral amplitude decay is modelled as T^P) computed for each group and corresponding R^2 values are summarized in Table 3.2.



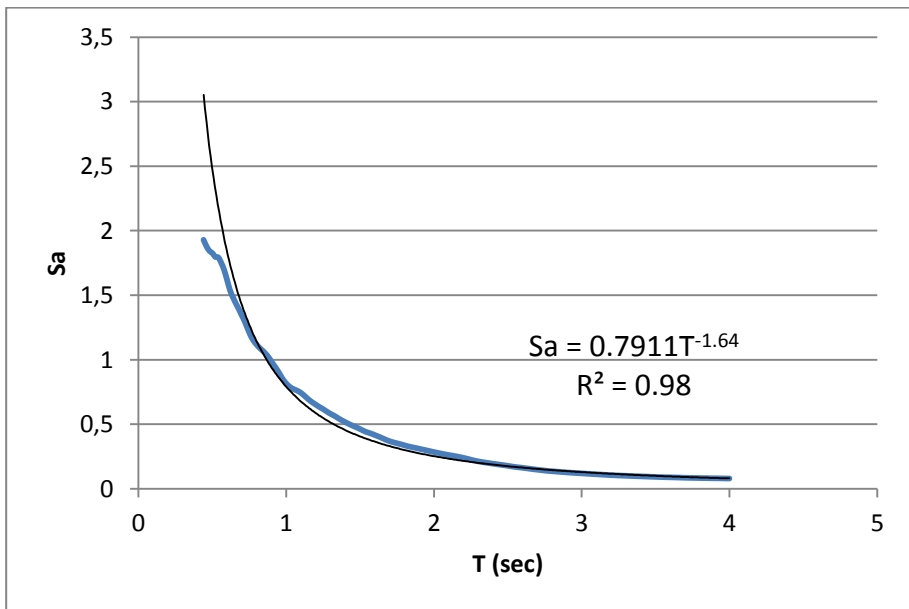
(a) Site Class C, $3.5 < M_w < 4.5$



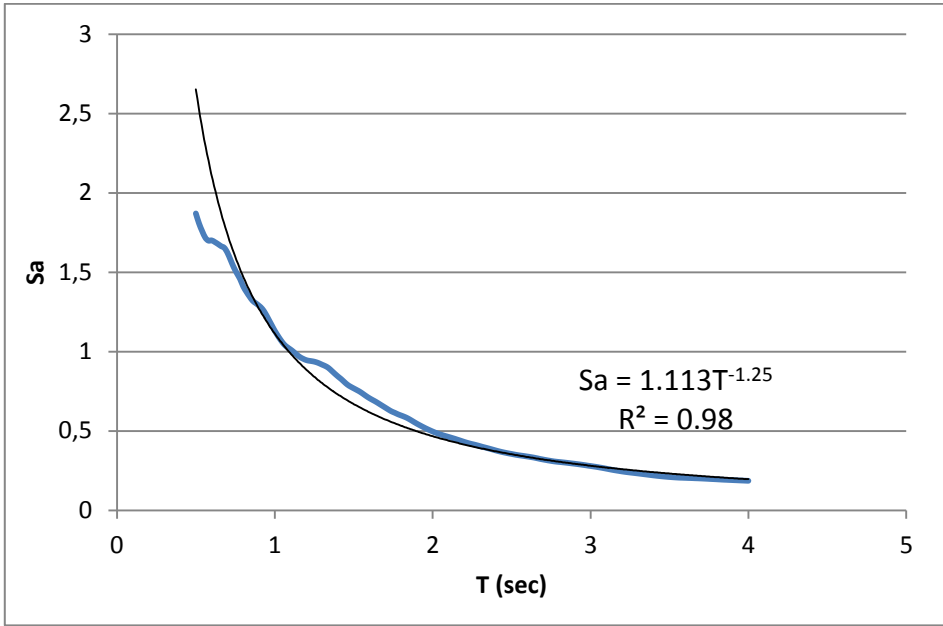
(b) Site Class D, $3.5 < M_w < 4.5$



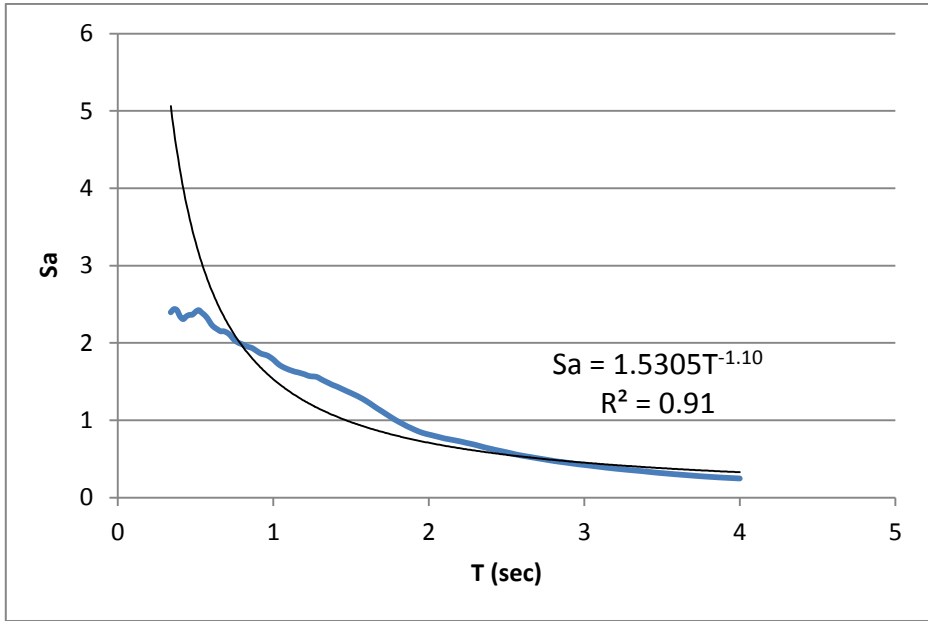
(c) Site Class C, $4.5 < M_w < 5.5$



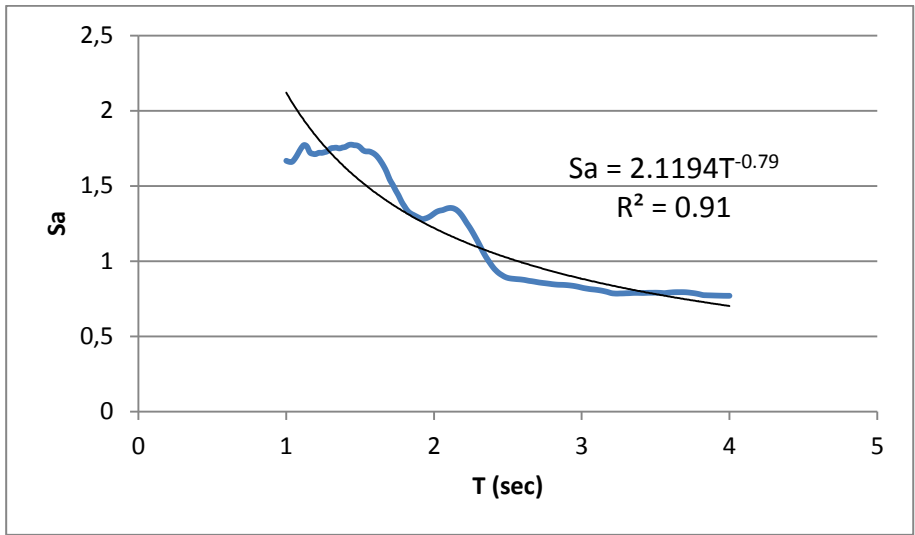
(d) Site Class D, $4.5 < M_w < 5.5$



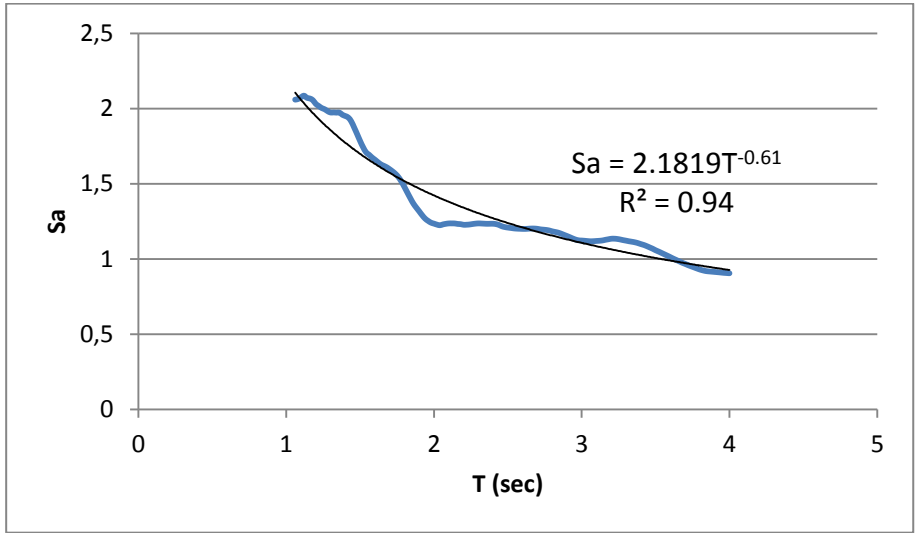
(e) Site Class C, $5.5 < M_w < 6.5$



(f) Site Class D, $5.5 < M_w < 6.5$



(g) Site Class C, $6.5 < M_w < 7.5$



(h) Site Class D, $6.5 < M_w < 7.5$

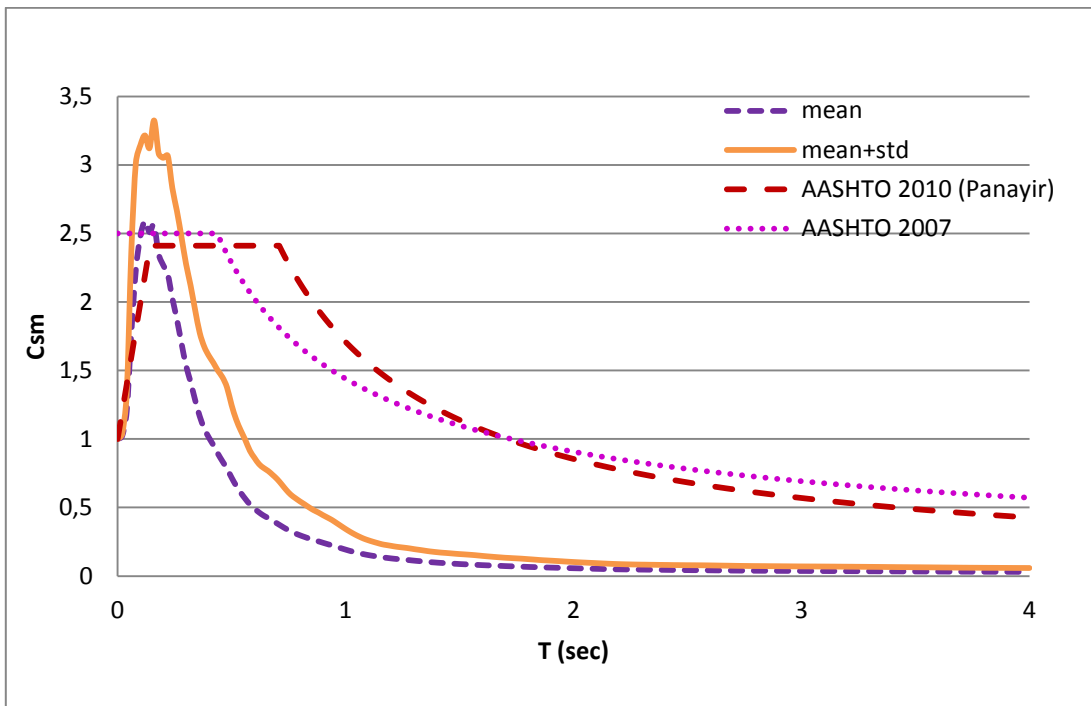
Figure 3.3 Formulae and Corresponding R^2 Values of the Fits on Long-Period Portions of Normalized Mean Response Spectra for Site Classes C and D and for Different M_w Intervals

Table 3.2 P and R² Values for Different Groups

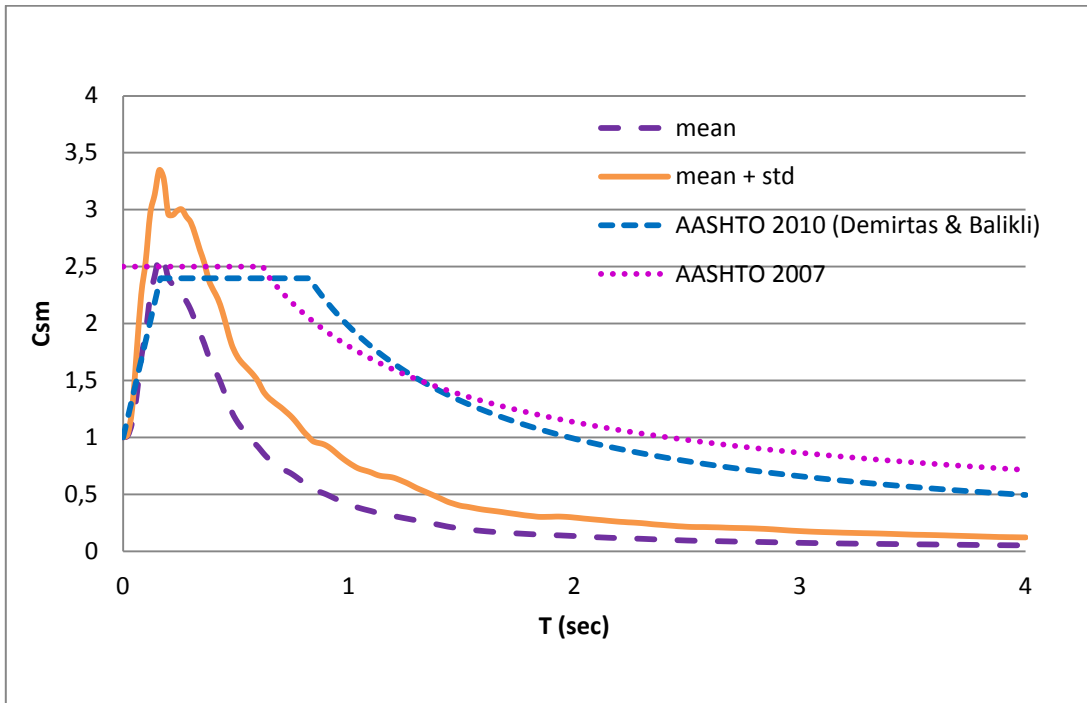
	Site class C		Site class D	
	P*	R ²	P*	R ²
3.5<M _w <4.5	-1.55	0.98	-1.52	0.99
4.5<M _w <5.5	-1.64	0.98	-1.64	0.98
5.5<M _w <6.5	-1.25	0.98	-1.10	0.91
6.5<M _w <7.5	-0.79	0.91	-0.61	0.94

(*: P values represent the decay rate of long period spectral amplitudes in the form of T^P)

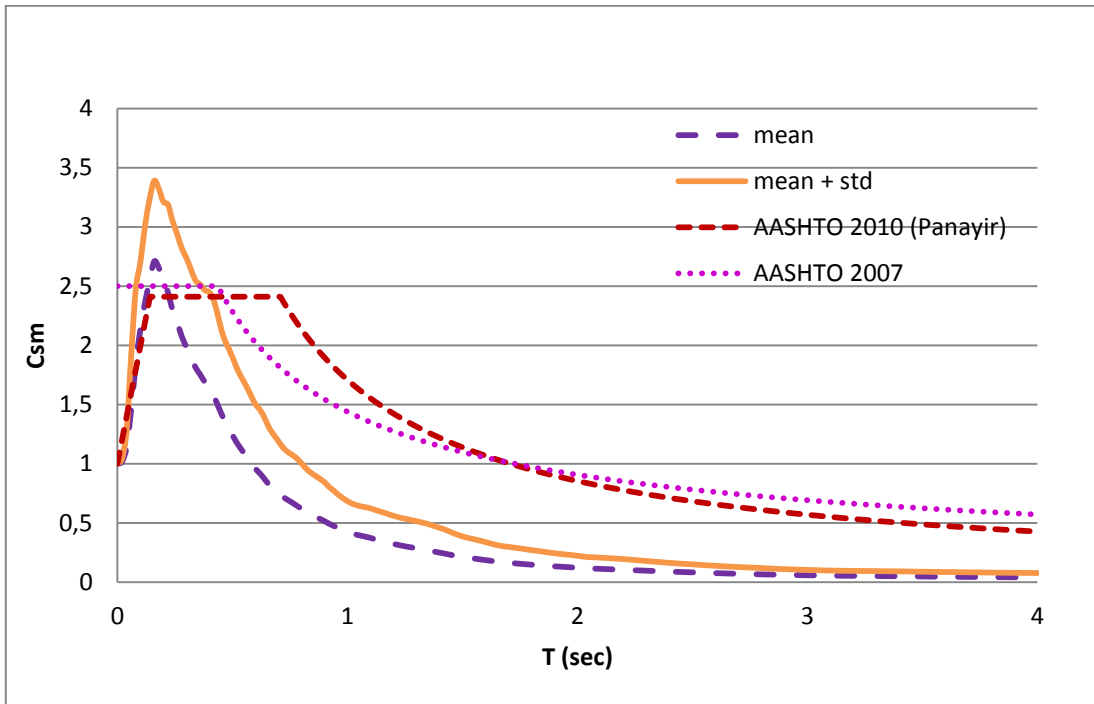
According to the R² values which are close to a hundred percent for most of the groups, the proposed relationships are observed to be promising. Next, the normalized response spectra obtained from mean site-specific load case and two different AASHTO load cases (2007 and 2010) are compared in Figure 3.4. It is observed that for both site classes in the magnitude bins of 3.5<M_w<4.5 and 4.5<M_w<5.5, the long period decay is observed to be faster than those defined in AASHTO (2007 and 2010) for the corresponding site classes. This observation is consistent with several discussions by researchers that mention the overdesign due to the slower decays of long periods as given in seismic codes (Chopra and Choudhury, 2011; Bommer, 2000). For smaller periods however, the mean site-specific spectra and the design spectra are relatively closer to each other for these magnitude bins. On the other hand, mean site-specific spectra is observed to match closely the spectral amplitudes obtained from AASHTO specifications especially for Class D curves for the interval of 5.5<M_w<6.5 (Figure 3.4 (e) and 3.4 (f)). Finally, it can be observed from Figure 3.4 (g) and Figure 3.4 (h) that the mean site-specific response spectra for magnitude interval 6.5<M_w<7.5 yield slightly higher spectral amplitudes than those of design spectra. This point is indeed interesting since it states that the design spectra can actually underestimate the spectral amplitudes of the longer period range for large earthquakes. It can also mean that the number of records from large events is naturally smaller than those from other magnitude ranges which could also have caused some bias.



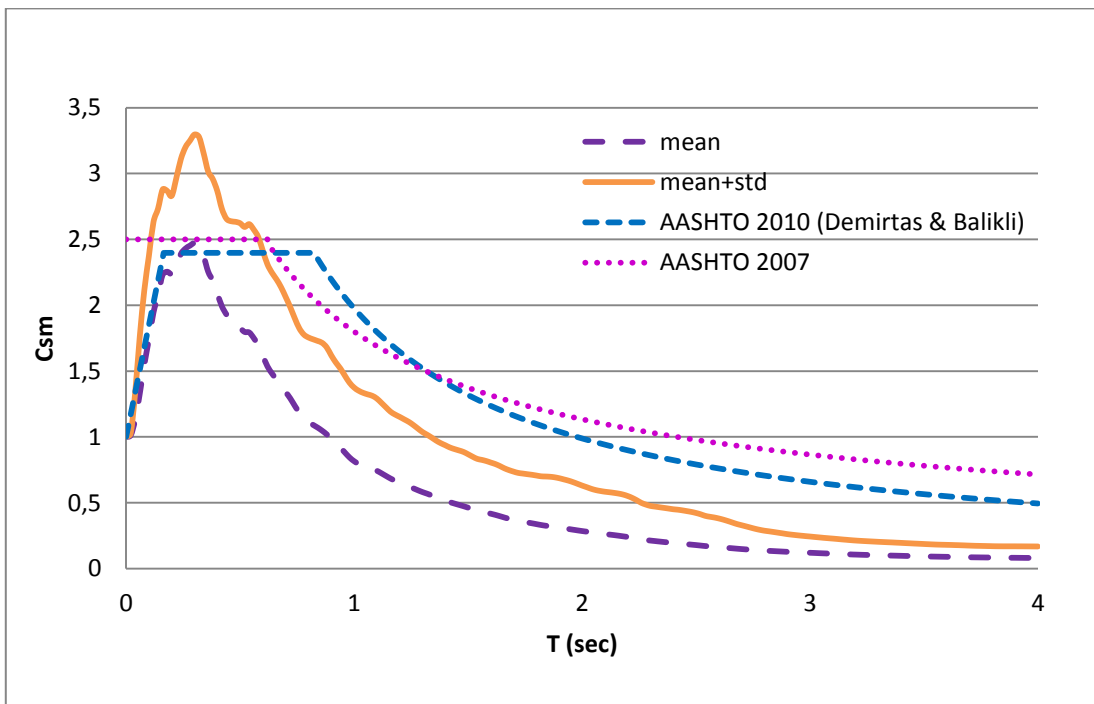
(a) Site Class C, $3.5 < M_w < 4.5$



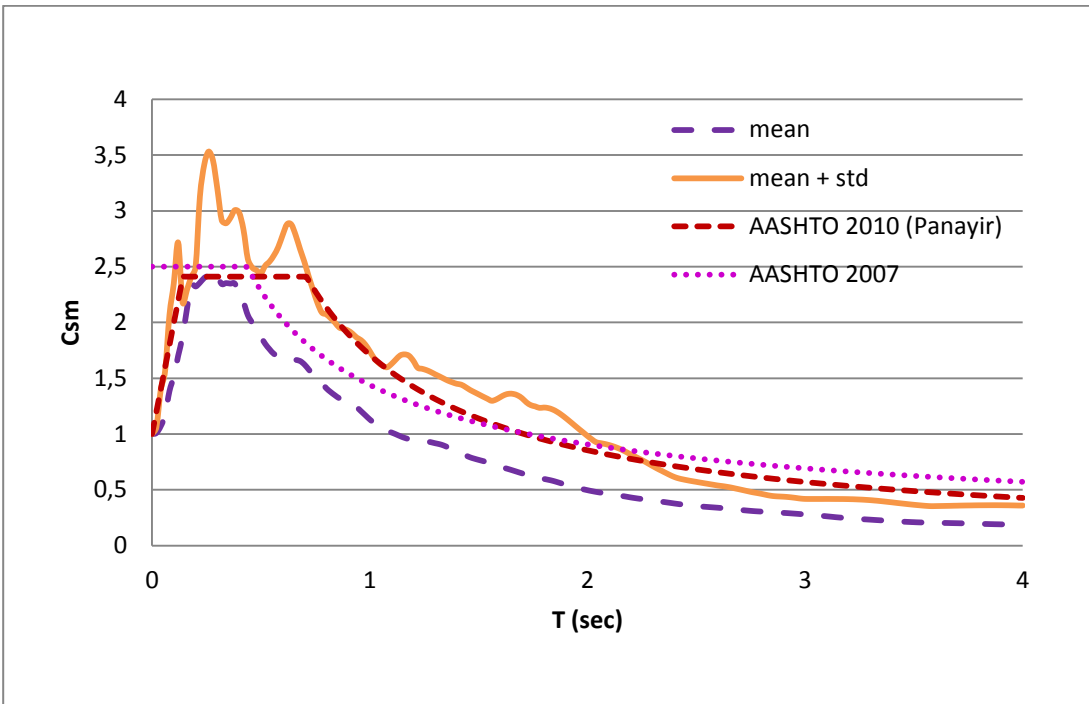
(b) Site Class D, $3.5 < M_w < 4.5$



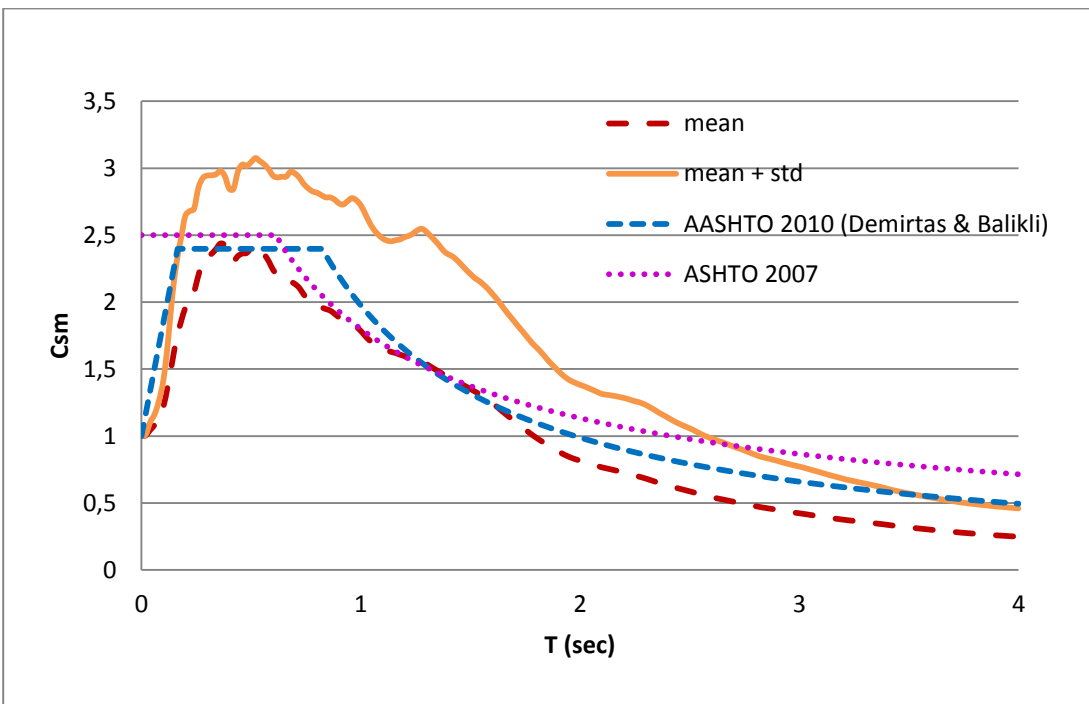
(c) Site Class C, $4.5 < M_w < 5.5$



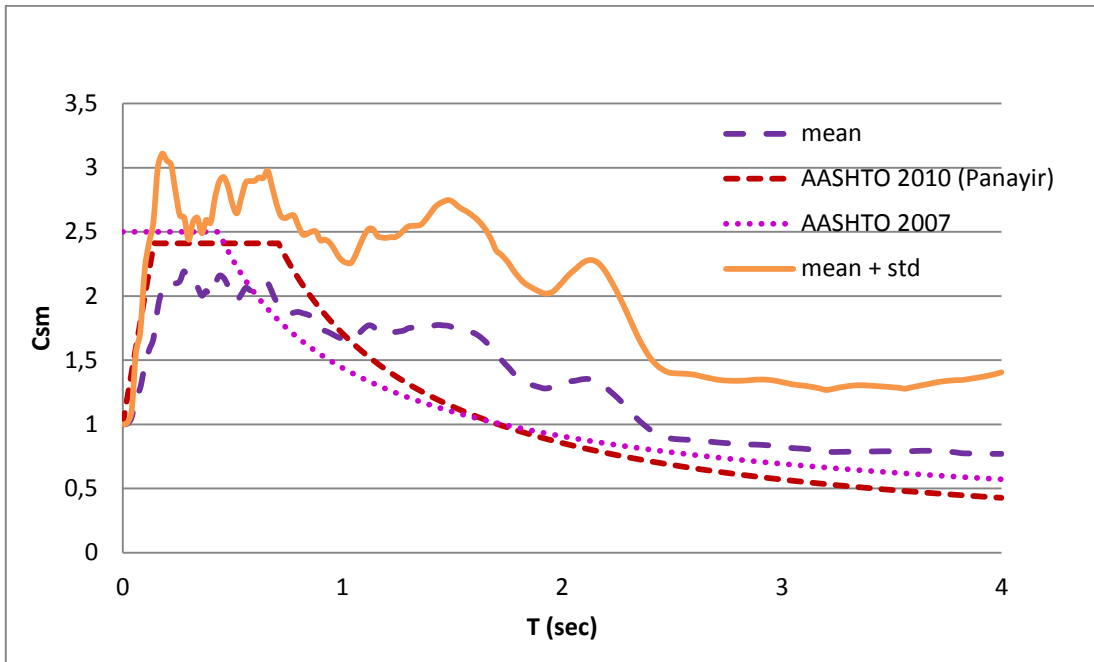
(d) Site Class D, $4.5 < M_w < 5.5$



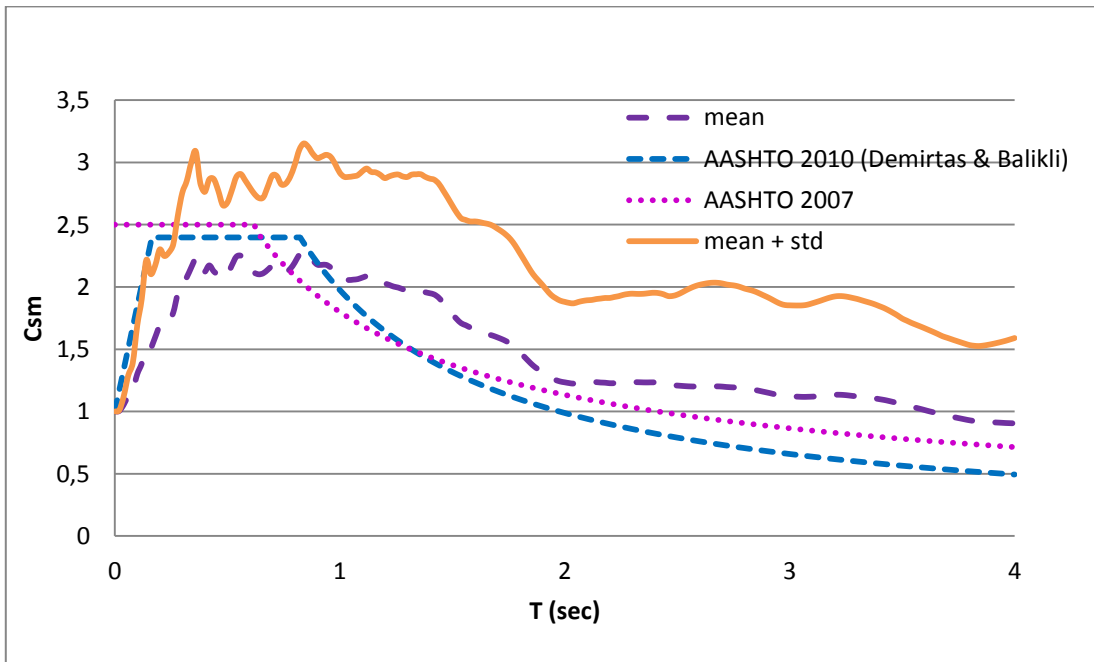
(e) Site Class C, $5.5 < M_w < 6.5$



(f) Site Class D, $5.5 < M_w < 6.5$



(g) Site Class C, $6.5 < M_w < 7.5$



(h) Site Class D, $6.5 < M_w < 7.5$

Figure 3.4 Comparison of Normalized Mean Site-Specific Spectra With Design Spectra For Different Cases

Finally, since AASHTO does not directly provide design spectra as a function of moment magnitudes, a combined mean site-specific spectra independent of earthquake magnitude is provided in Figure 3.5 with the corresponding fits in Figure 3.6. It is once again observed that the decay of longer periods is faster with a larger power than those defined in AASHTO.

Next, in order to see the differences in the seismic response of bridges due to different spectra obtained in this chapter, response spectrum analyses are presented in Chapter 4 following the description of the modelled bridges.

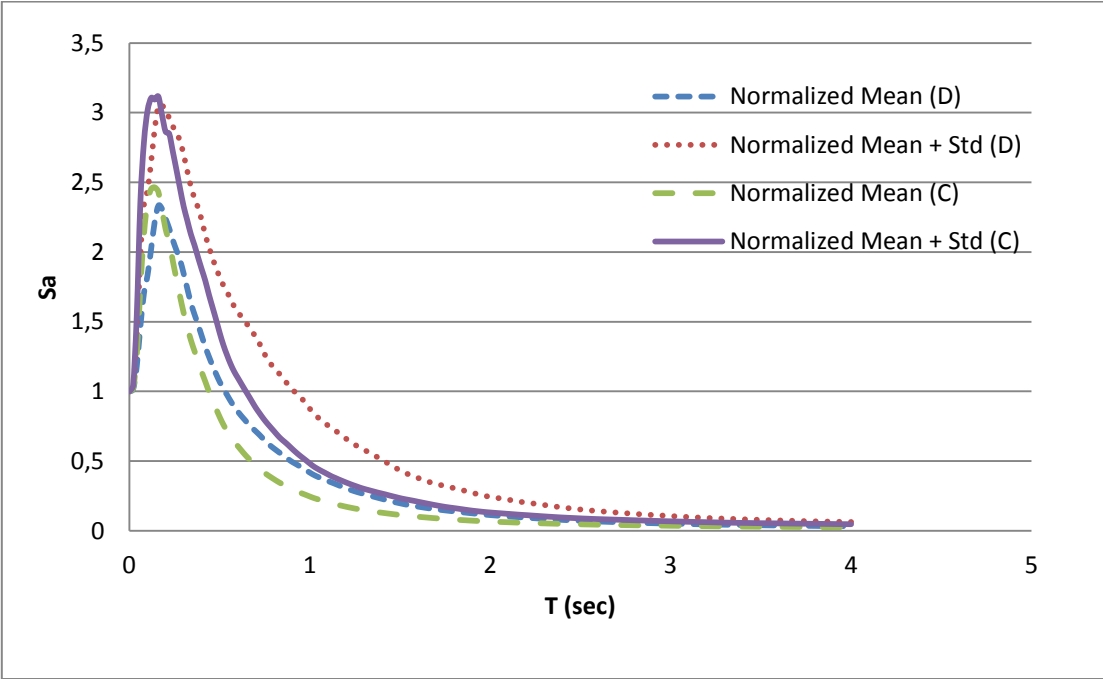
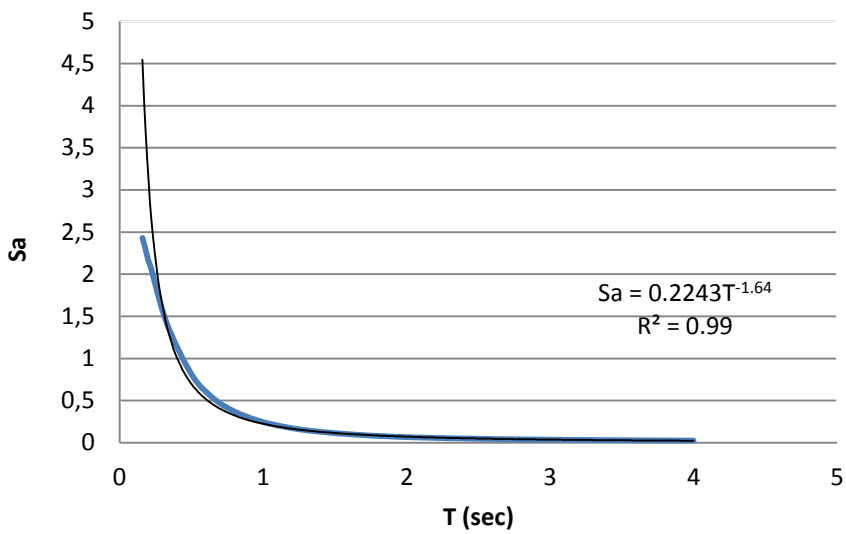
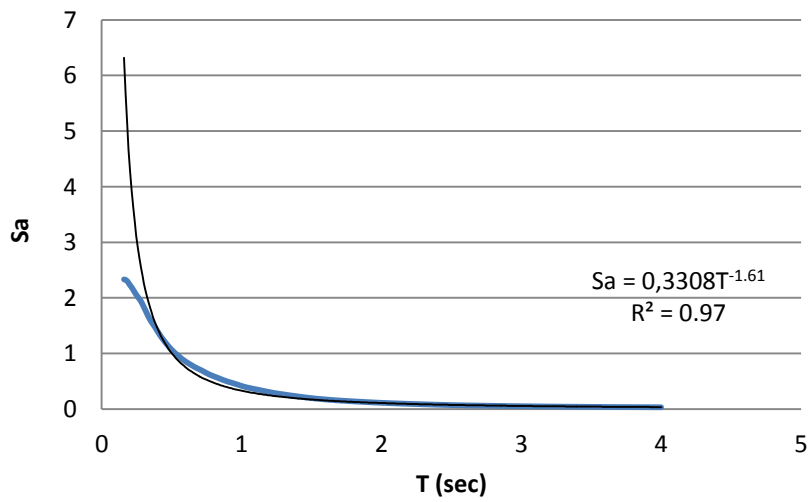


Figure 3.5 Combined Mean Site-Specific Spectra



(a) Site Class C



(b) Site Class D

Figure 3.6 Fits and Corresponding P and R^2 Values for the Combined Spectra for Different Site Classes

CHAPTER 4

COMPARISON OF THE MEAN SITE-SPECIFIC SPECTRA AND AASHTO DESIGN SPECTRUM IN TERMS OF RSA

4.1 Information on the Selected Bridges

Three bridges, which are namely Demirtas, Panayir and Balikli bridges are selected in Bursa for response spectrum analyses to see the structural response of different spectrum curves. Bursa is especially preferred for this study because of several reasons. Firstly, it is a populated city with industrial facilities that includes many small and large scaled bridges. Secondly, it is an earthquake prone city, in the first earthquake zone and close to North Anatolian Fault with several measurements available considering soil and earthquake characteristics. Finally, in the scope of the project mentioned before (TÜBİTAK, 2014) a couple of bridge models are ready to use and necessary seismic coefficients (S_s , S_1 etc.), peak ground acceleration (PGA) and shear velocity values (V_{S30}) which are used during site classification and response spectrum analysis are provided by other researchers(given in Table 2.7).

According to a recent study (Sevgili, 2007), for short span bridges I-girder is the girder type which is used mostly. As span lengths of Balikli and Panayir bridges are smaller than 30m, they can be called as short span bridges. As a result, it can be stated that they reflect the common short span bridge girder type in Turkey well. On the other hand, Demirtas bridge is a long span I-girder prestressed bridge which reflects the common long span bridges in Turkey well since prestressing against their own weight and post tensioning against additional weight are used commonly.

When a statistical study about the bridges in Turkey is considered (Sevgili, 2007) several statements can be made about the selected bridges. Firstly, according to Figure 4.1 it can be seen that most of the bridges in Turkey are not skewed, where Demirtas bridge is in this class. Skew angles of Balikli and Panayir bridges are 15° and 20° respectively, they are in the second most common group which has a frequency of occurrence of 20%.

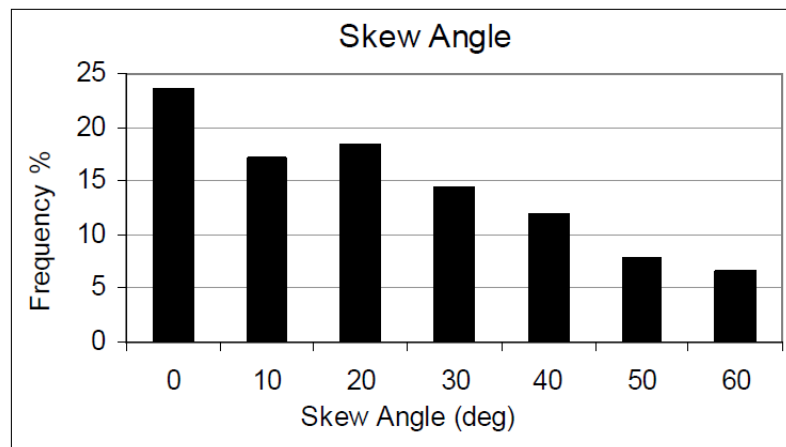


Figure 4.1 Distribution of Bridges in Turkey According to Skew Angle (Adopted from Sevgili, 2007)

Secondly, maximum span lengths can be considered for comparison purposes. Demirtas, Balikli and Panayir bridges have 39, 23 and 28.25 meters maximum span lengths, respectively. According to these values, frequency of occurrence of maximum span length for Demirtas bridge is below 10% which is an exception for Turkey (Figure 4.2). On the other hand, Balikli bridge is in the most common group with a 30% frequency of occurrence where Panayir bridge has a frequency value of nearly 15%.

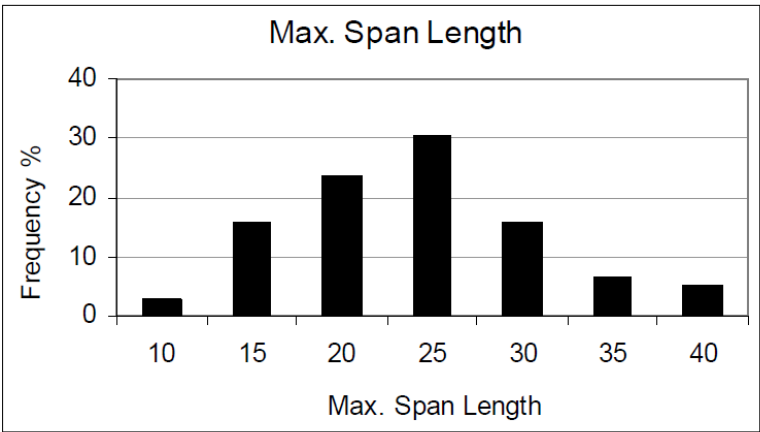


Figure 4.2 Distribution of Bridges in Turkey According to Maximum Span Length (Adopted from Sevgili, 2007)

Finally when number of spans is taken into account, it is seen that Demirtas -with 28 spans- is uncommon in Turkey (Figure 4.3). However, Balikli and Panayir bridges with 2 and 3 spans are in the first and second most frequently encountered span number groups.

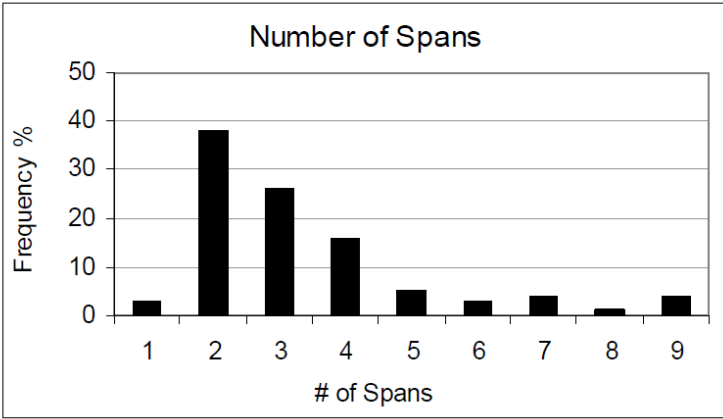


Figure 4.3 Distribution of Bridges in Turkey According to Number of Spans (Adopted from Sevgili, 2007)

4.1.1 Panayir Bridge

Panayir Bridge is located on the Bursa – Yalova State Highway between Km: 4+743.78 and Km: 4+829.35. Plan view of the bridge is given in Figure 4.4.

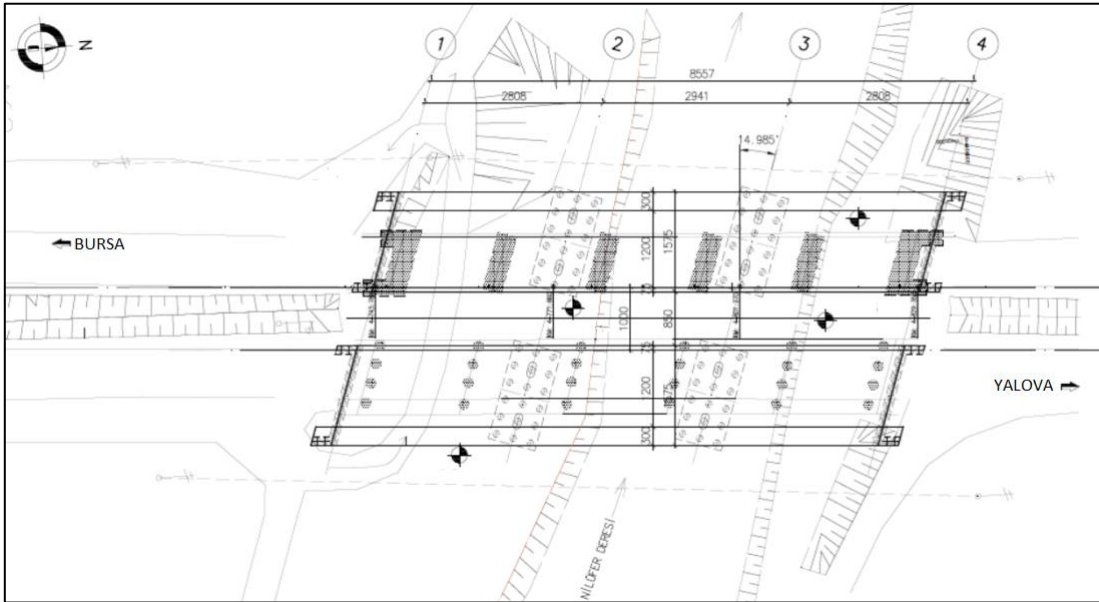


Figure 4.4 Plan View (Panayir Bridge) (in cm)

It is designed as a three-span bridge where spans have 27.50, 28.25 and 27.50 m lengths, respectively. Total length of the bridge is 85.57 meters and the platform width is 12.00 meters. The angle of skew is given as 14.985° . In Figure 4.5 design level scheme is given where in Figure 4.6 elevation view is presented.

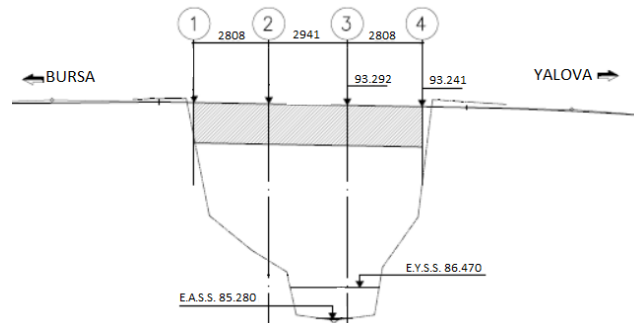


Figure 4.5 Scheme of Design Level (Panayir Bridge) (elevations in m, lengths in cm)

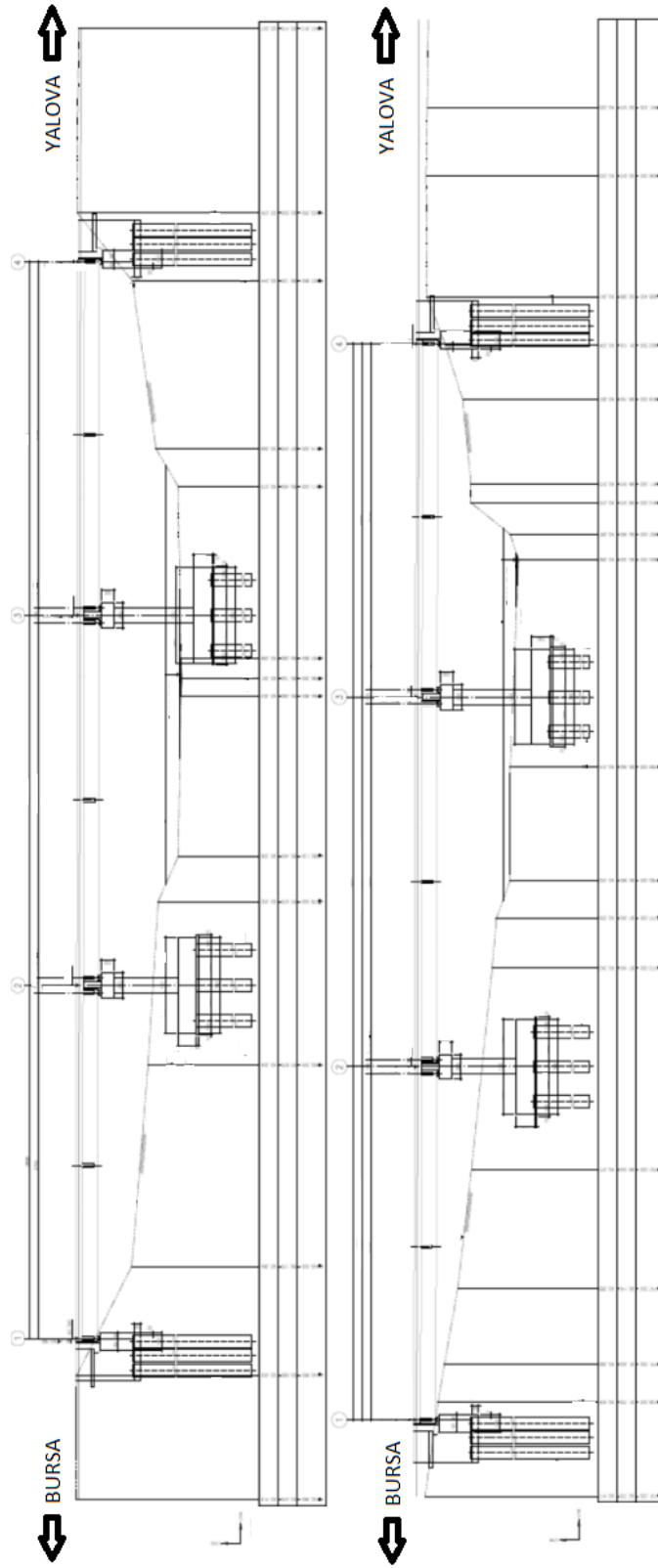


Figure 4.6 Elevation View of Panayir Bridge

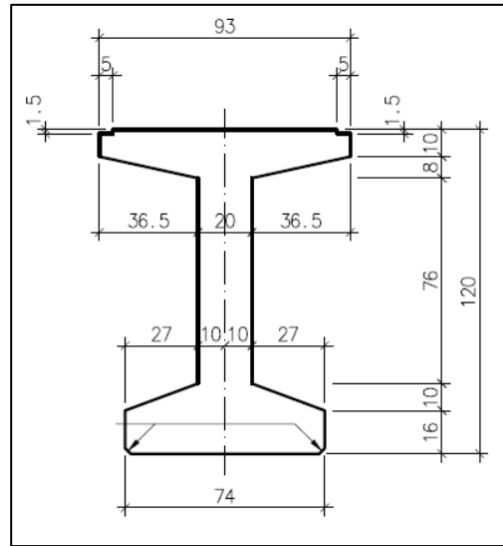


Figure 4.7 Cross Section of the Beam (Panayir Bridge) (in cm)

There are 13 pre-stressed pre-tensioned I girders with a height of 120 cm (Figure 4.7), supporting a 25 cm thick slab. Spacing between two adjacent girders is designed to be 1.22 meters. In Figure 4.8, vertical cross section of the girders is shown.

Totally, there are 9 diaphragm walls -3 for each span- to consider live load distribution properly. Expansion joints leaving a gap of 6.9 cm are used in abutments for movements in longitudinal axes caused by earthquake, shrinkage and thermal effects to satisfy slab level continuity. Also shear keys are used to prevent collision between two adjacent girders.

Detail of the shear key is shown in Figure 4.9 where details of diaphragm walls and expansion joints are demonstrated in Figure 4.10 and Figure 4.11.

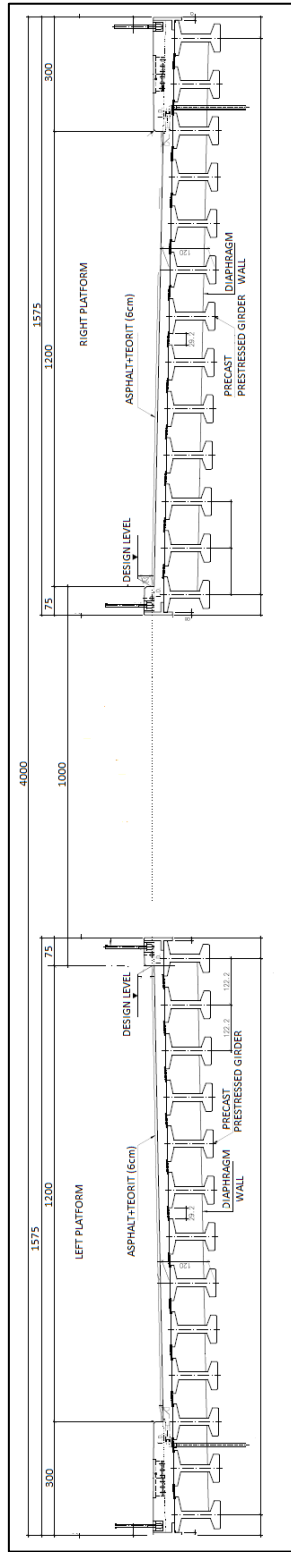


Figure 4.8 Vertical Cross Section of Superstructure (Panayir Bridge) (in cm)

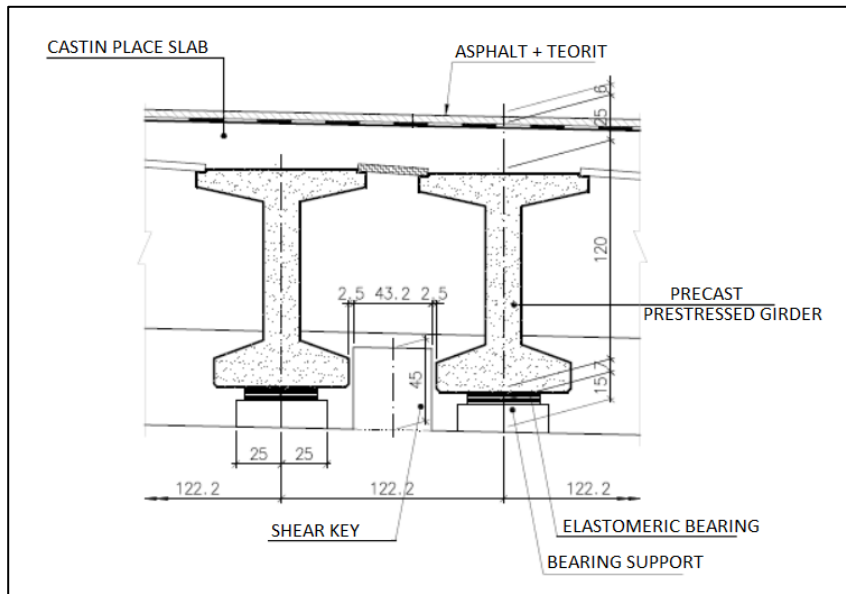


Figure 4.9 Detail of the Shear Key (Panayir Bridge) (in cm)

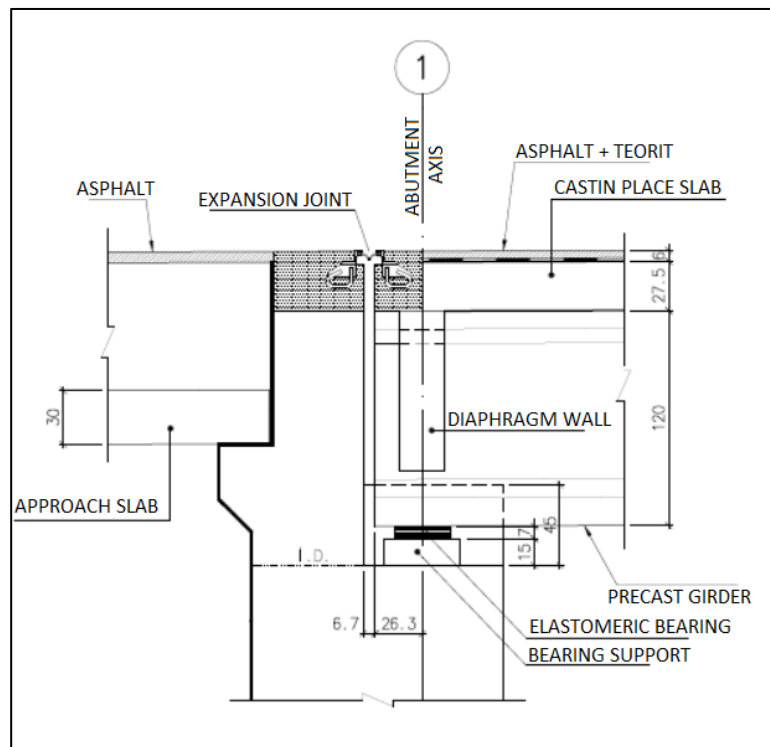


Figure 4.10 Superstructure Details on Abutment (Panayir Bridge) (in cm)

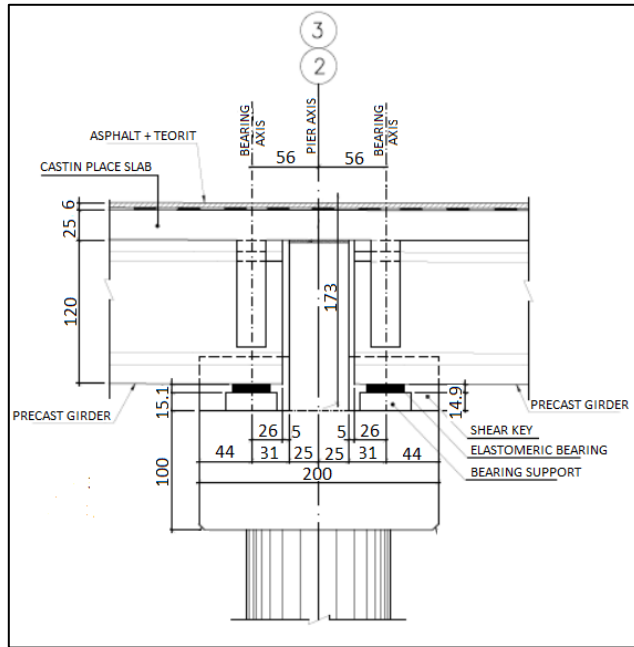


Figure 4.11 Superstructure Details on Pier (Panayir Bridge) (in cm)

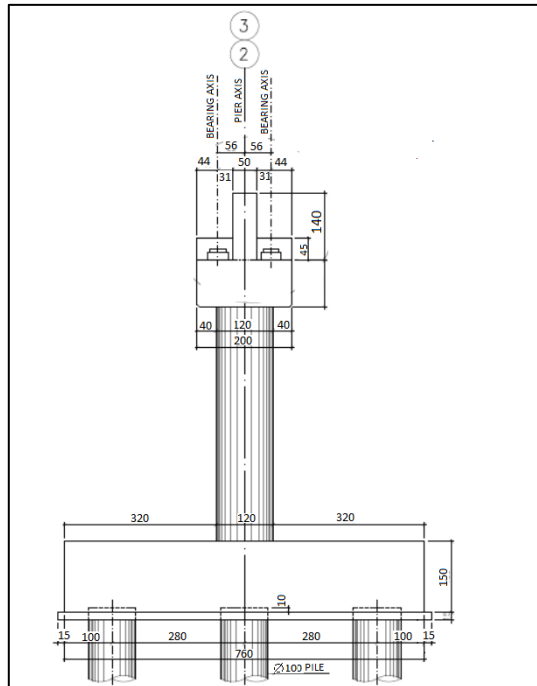


Figure 4.12 Pier Detail (Panayir Bridge) (in cm)

Maximum net column heights are 6.28 m on 2nd and 3rd axes. Central piers are composed of two oval shaped columns and capping beam with pile foundation where abutments are composed of capping beam resting on pile columns. Detail of a typical pier is shown on Figure 4.12 and cross section of the column is presented in Figure 4.13.

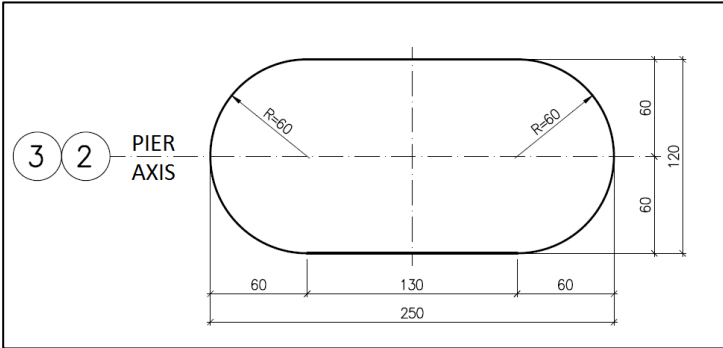


Figure 4.13 Cross Section of the Column (Panayir Bridge) (in cm)

4.1.2 Balikli Bridge

Balikli Bridge is located on the Bursa – Yalova State Highway between Km: 2+722.9 and Km: 2+770.1. Plan view of the bridge is given in Figure 4.14.

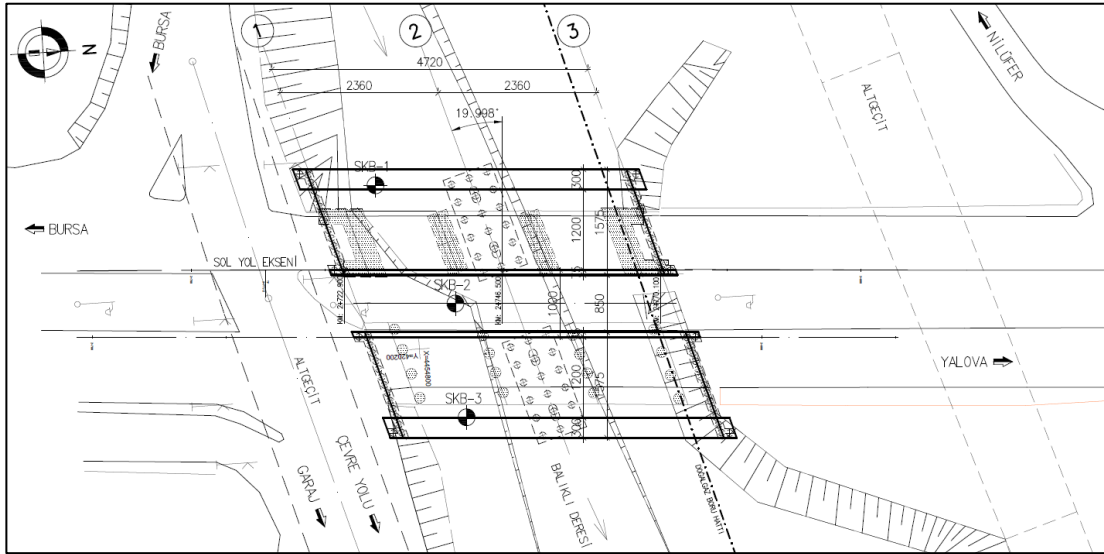


Figure 4.14 Plan View (Balikli Bridge) (in cm)

Total length of the bridge is 47.2 meters and the platform width is 12.00 meters. The angle of skew is given as 19.998° . In Figure 4.15 design level scheme is given where in Figure 4.16 elevation view is presented.

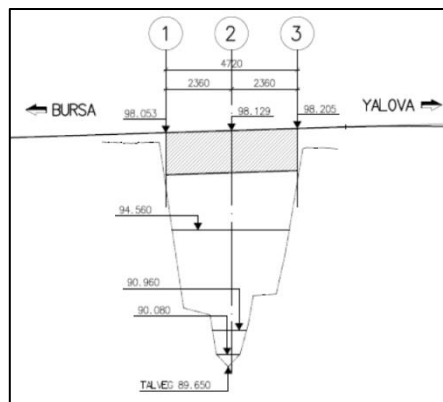


Figure 4.15 Scheme of Design Level (Balikli Bridge) (elevations in m, lengths in cm)

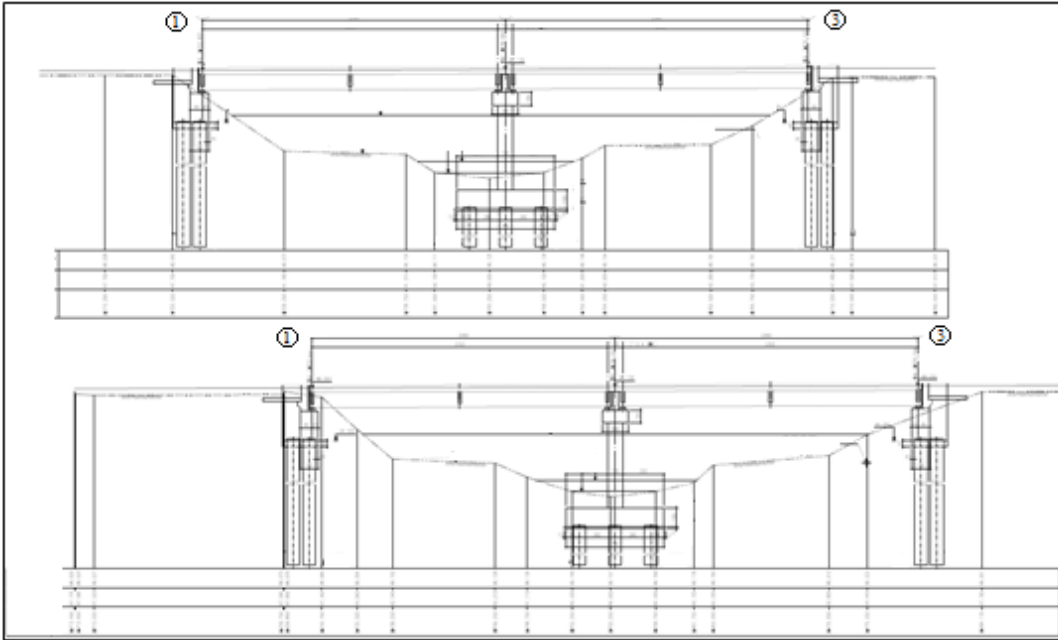


Figure 4.16 Elevation View (Balikli Bridge)

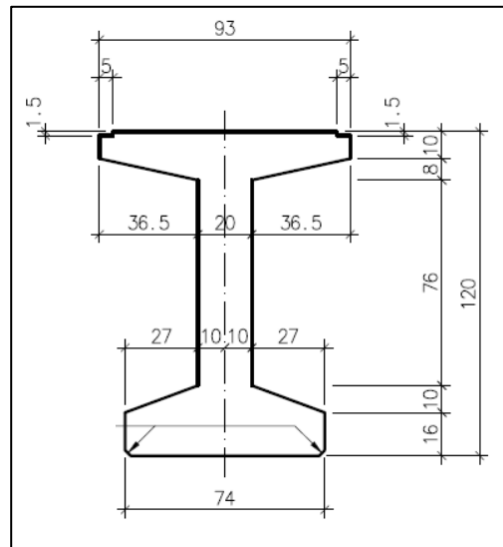


Figure 4.17 Beam Cross Section (Balikli Bridge) (in cm)

There are 10 pre-stressed pre-tensioned I girders with a height of 120 cm, supporting a 25 cm thick slab (Figure 4.17). Spacing between two adjacent girders is designed to be 1.629 meters. In Figure 4.18 vertical cross section of the girders is shown.

Totally there are 6 diaphragm walls -3 for each span- to consider live load distribution properly. Expansion joints leaving a gap of 6.7 cm are used in abutments for movements in longitudinal axes caused by earthquake, shrinkage and thermal effects to satisfy slab level continuity. Also shear keys are used to prevent collision between two adjacent girders.

Detail of the shear key is shown in Figure 4.19 where details of diaphragm walls and expansion joints are demonstrated in Figure 4.20 and 4.21.

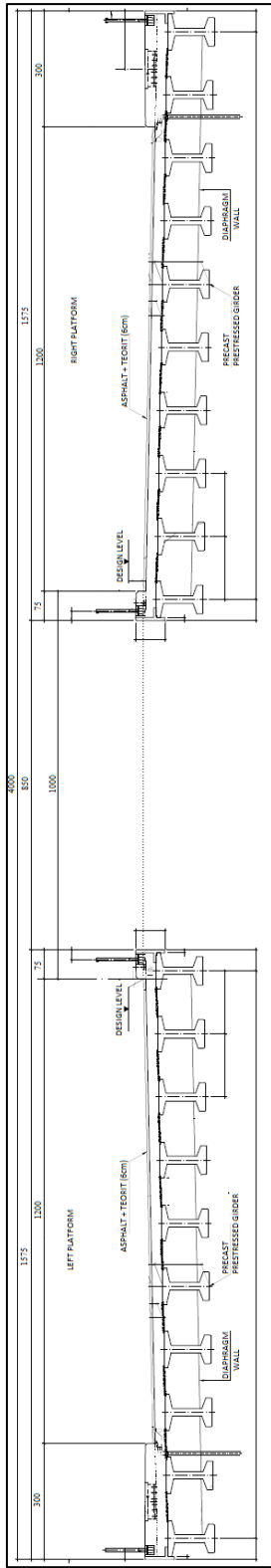


Figure 4.18 Vertical Cross Section of Superstructure (Balikli Bridge)

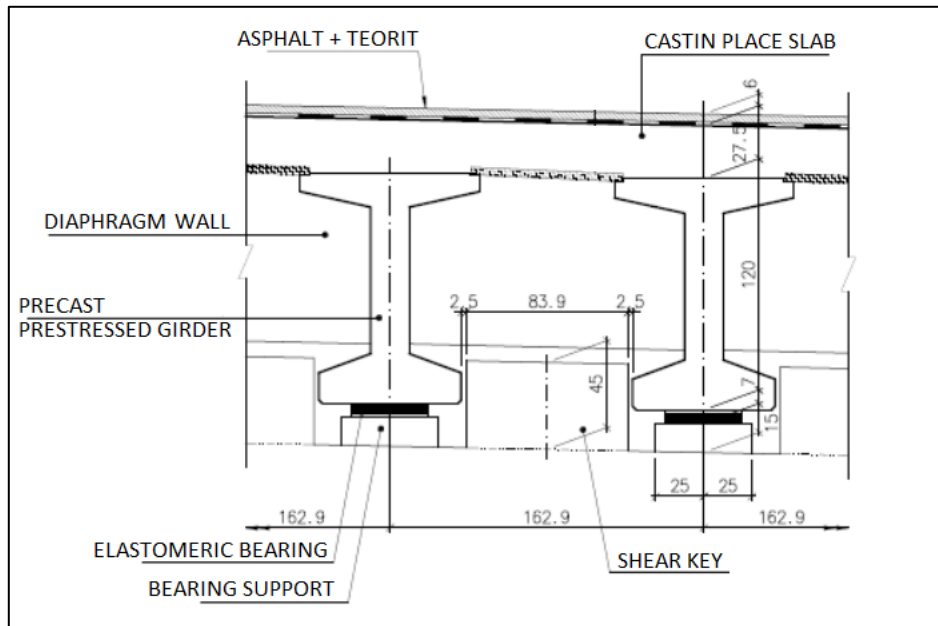


Figure 4.19 Detail of the Shear Key (Balikli Bridge) (in cm)

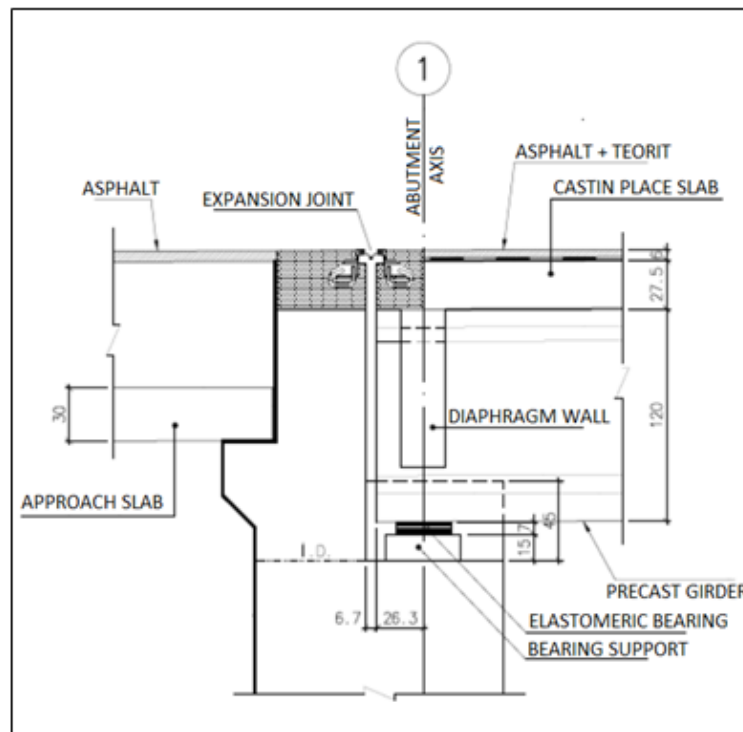


Figure 4.20 Superstructure Details on Abutment (Balikli Bridge) (in cm)

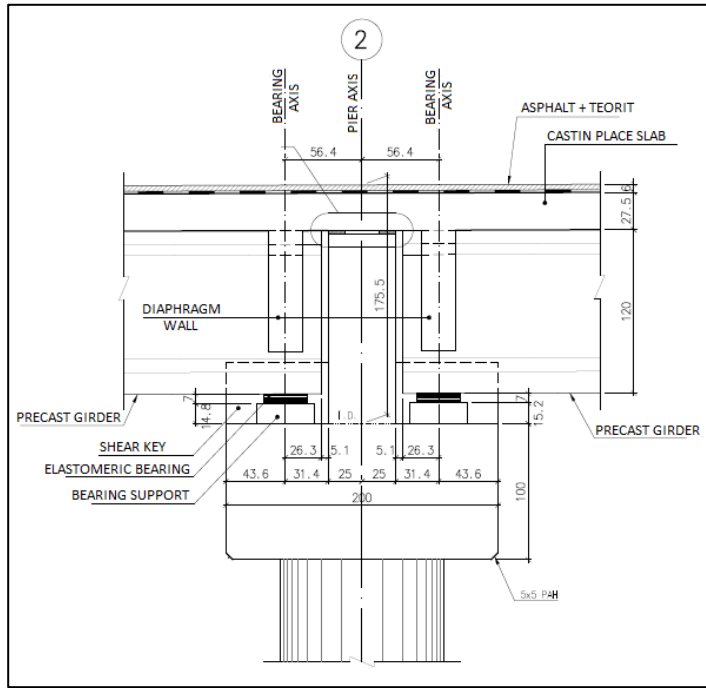


Figure 4.21 Superstructure Details on Pier (Balikli Bridge) (in cm)

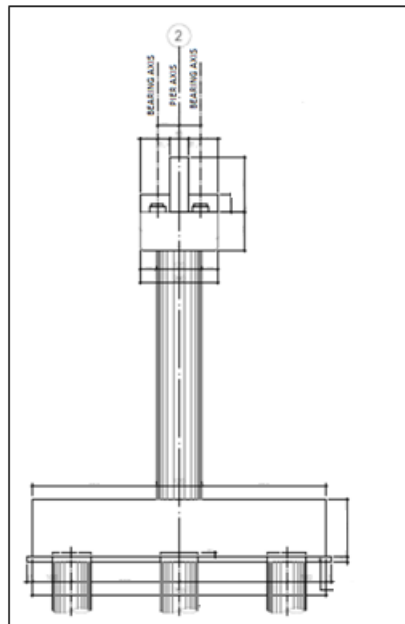


Figure 4.22 Pier Detail (Balikli Bridge)

Maximum net column height is 6.5m on 2nd axis. Central piers are composed of two oval shaped columns and capping beam with pile foundation where abutments are composed of capping beam resting on pile columns. Detail of a typical pier is shown on Figure 4.22 and cross section of the column is presented in Figure 4.23.

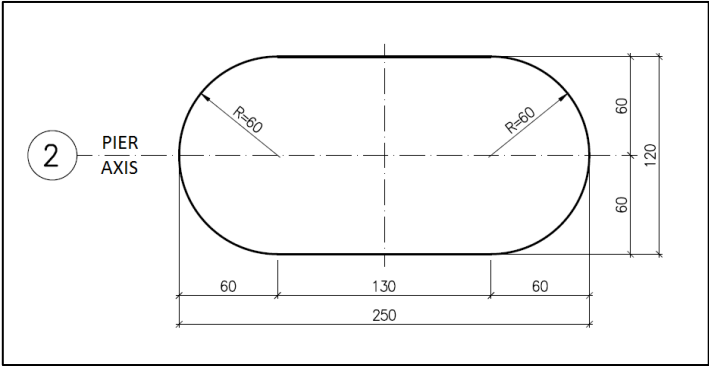


Figure 4.23 Cross Section of the Column (Balikli Bridge) (in cm)

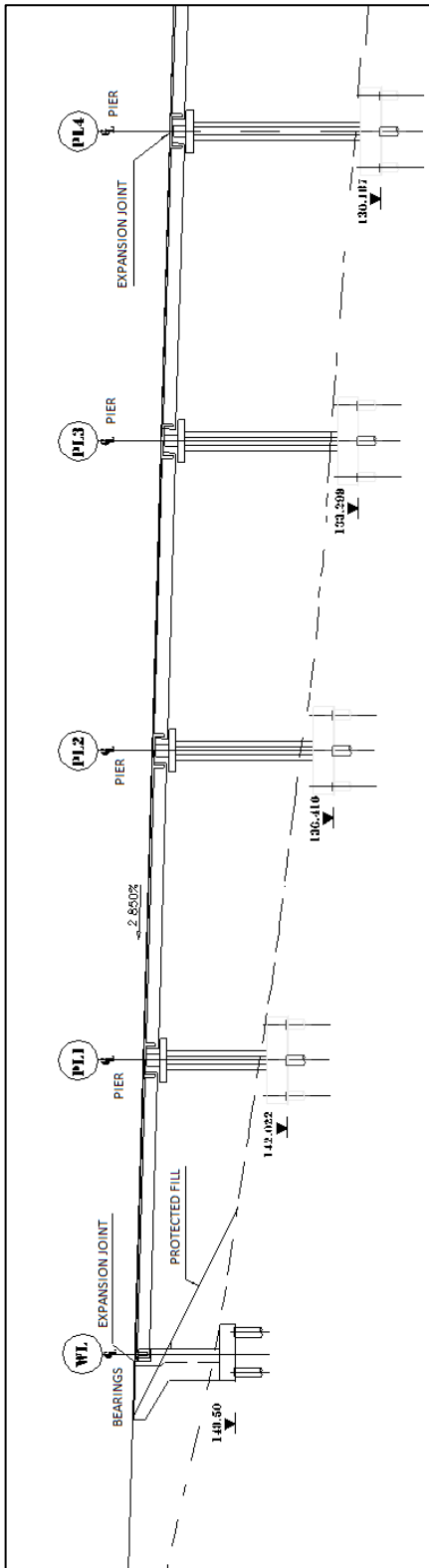
4.1.3 Demirtas Bridge

Demirtas Bridge is located on the İstanbul – Bursa – Balıkesir – İzmir Motorway between Km: 6+334 and Km: 7+422. The bridge has twenty-eight spans with 37.00 m span lengths between abutments and adjacent columns and 39.00 m span lengths between all interior columns. Elevation view of the bridge for three parts selected from the start, middle and end are shown in Figure 4.24.

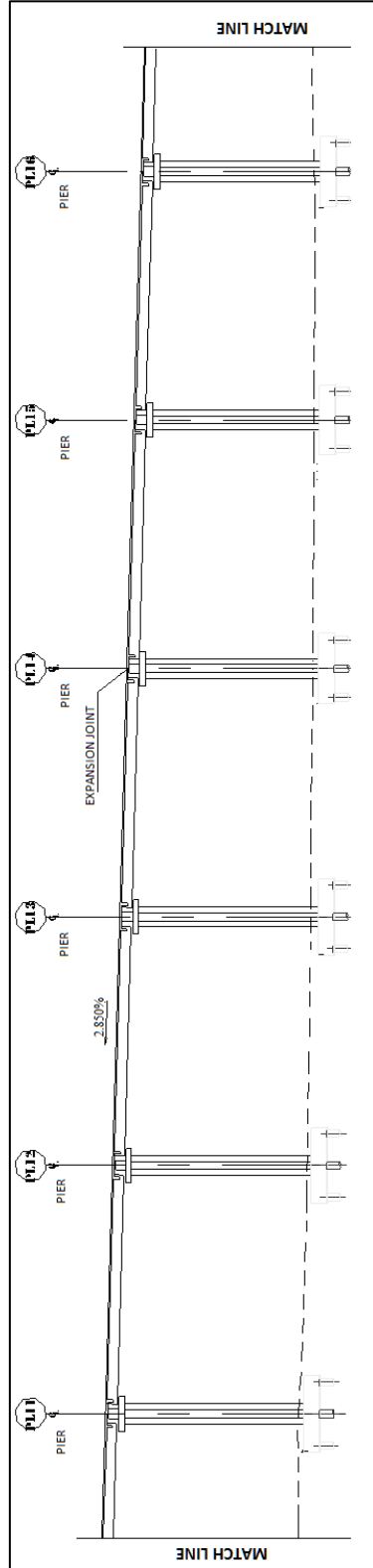
There are 12 pre-stressed pre-tensioned I girders (Figure 4.25) with a height of 160 cm (Figure 4.26), supporting a 20 cm thick slab. Total length of the bridge is 1088 meters and the platform width is 17.50 meters. There is no angle of skew. Spacing between two adjacent girders is designed to be 1.46 meters.

Totally there are 56 diaphragm walls -2 for each span- to consider live load distribution properly. Expansion joints leaving a gap of 10 cm are used in abutments for movements in longitudinal axes caused by earthquake, shrinkage and thermal effects to satisfy slab level continuity. Also shear keys are used to prevent collision between two adjacent girders.

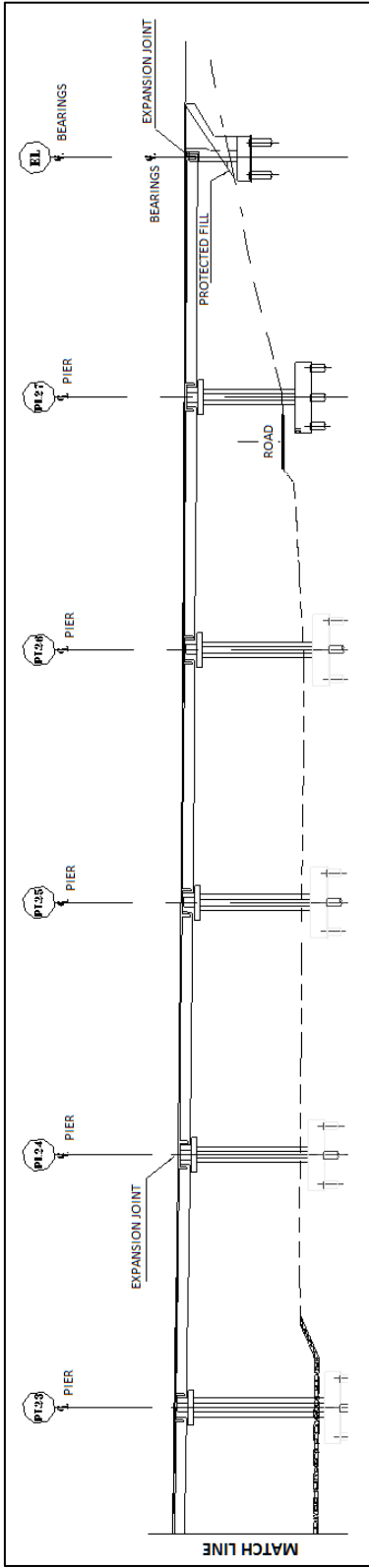
Detail of the shear key is shown in Figure 4.27 where details of diaphragm walls and expansion joints are demonstrated in Figure 4.28 and 4.29.



(a)



(b)



(c)

Figure 4.24 Elevation View (a) Start, (b) Middle and (c) End (Demirtas Bridge)

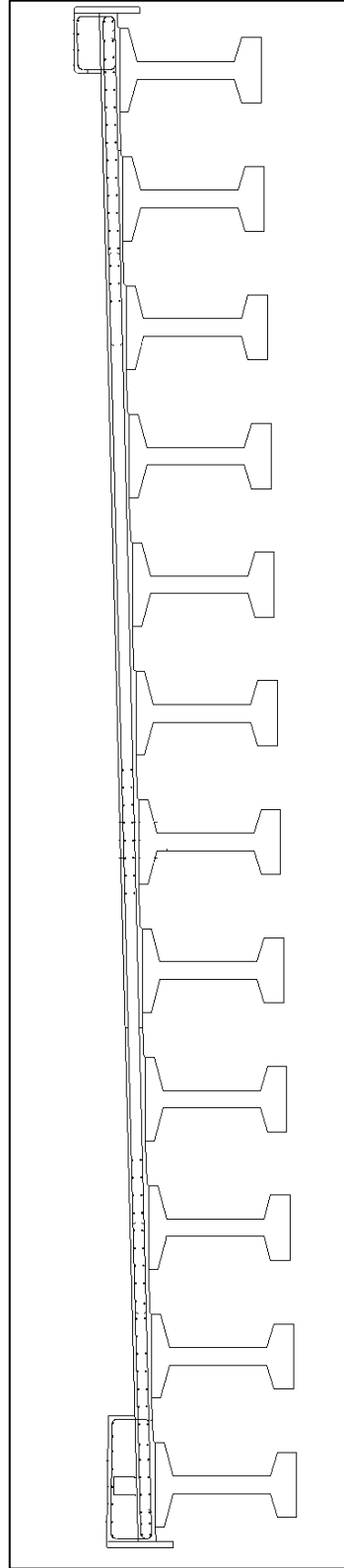


Figure 4.25 Vertical Cross Section of the Superstructure (Demirtas Bridge)

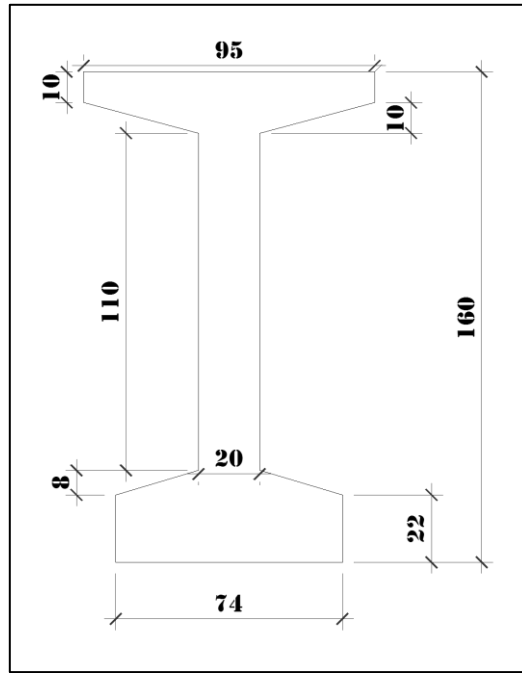


Figure 4.26 Cross Section of the Beam (Demirtas Bridge) (in cm)

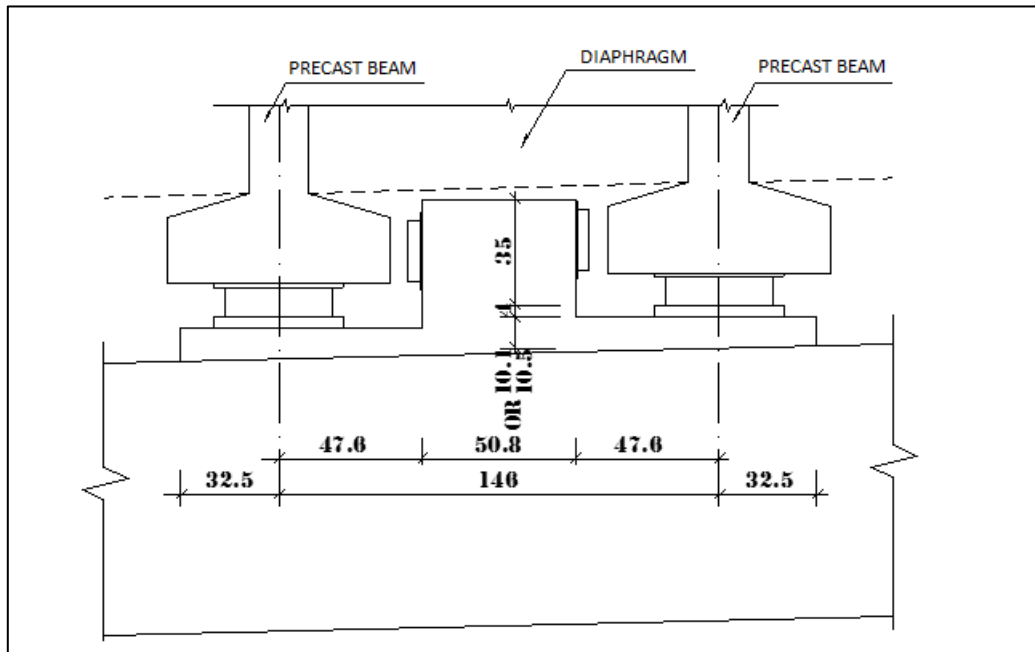


Figure 4.27 Detail of the Shear Key (Demirtas Bridge) (in cm)

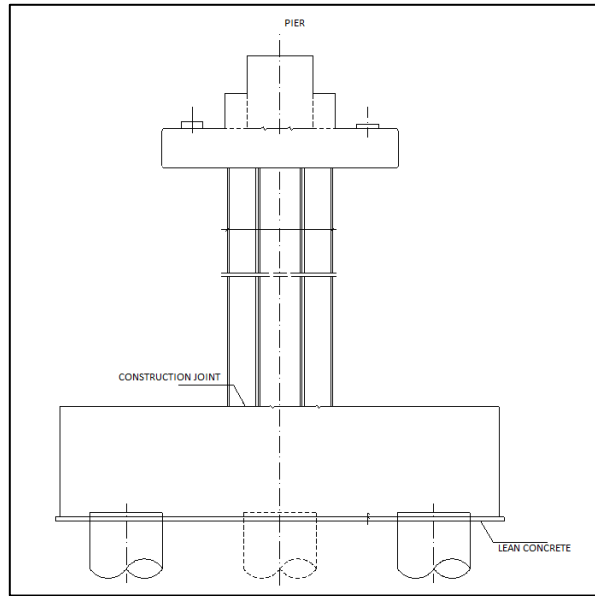


Figure 4.30 Pier Detail (Demirtas Bridge)

Maximum net column height is 29m on 2nd axis. Central piers are composed of I shaped columns and capping beam with pile foundation where abutments are composed of capping beam resting on pile columns. 120 cm diameter piles are used for the foundation of central piers. Detail of a typical pier is shown on Figure 4.30 and cross section of the column is presented in Figure 4.31.

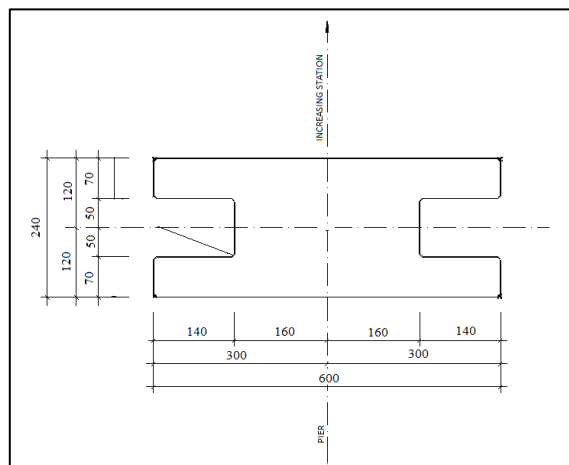


Figure 4.31 Cross Section of the Column (Demirtas Bridge) (in cm)

A summary of the necessary information for the analyses of these bridges is given in Table 4.1. Since Panayir and Balikli bridges have skew angles, results are evaluated accordingly. Fundamental period values are calculated with the help of eigenvalue analysis on the composed models.

Table 4.1 Information about the Bridges

Name of the Bridge	Latitude (°)	Longitude (°)	# of Spans	Superstructure	Length (m)	Skew Angle (°)	Longitudinal Fundamental Period (sec)	Transverse Fundamental Period(sec)
Demirtas (AASHTO 2010 Class D)	40.28 N	29.10 E	28	Pretensioned	1088	0	1.90	1.07
Panayir (AASHTO 2010 Class C)	40.24 N	29.06 E	3	Pretensioned	87	15	0.70	0.17
Balikli (AASHTO 2010 Class D)	40.22 N	29.06 E	2	Pretensioned	49	20	0.74	0.19

4.2 Computer Modelling

Demirtas, Panayir and Balikli bridges are modelled using LARSA 4D Structural and Earthquake Engineering Integrated Analysis and Design Software (version 7.07). Models are composed of three different parts which are namely the superstructure, substructure and supports. Girders, cap beams and the slab (deck) are the main components of the superstructure. Columns, foundation elements such as piles and pile caps are the main components of the substructure where shear keys and the

bearings are the main components of the supports. In Figure 4.32 several components of the bridge are shown on a sample model.

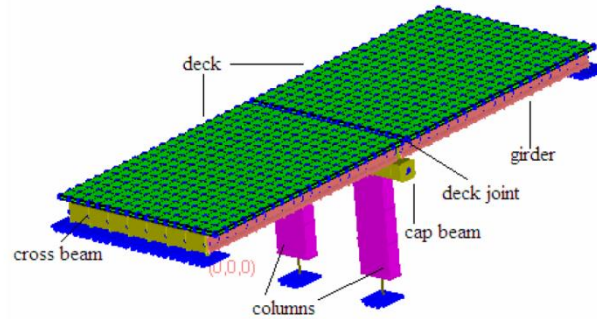


Figure 4.1: Bridge components

Figure 4.32 A Typical Bridge Model (Adopted from Sevgili, 2007)

Different types of models are used for the selected bridges as they differ in several characteristics. Demirtas Bridge has 28 spans in total which may be counted as a large number for modelling. Thus, only 5 columns in the middle of the bridge represented in Figure 4.33 are chosen to be modelled as they are considered to be the most critical ones. For the superstructure, a single beam element is used instead of using shell elements to represent the whole structure in order to save time during analyses. In this approximation, the stiffness and mass properties of the superstructure are assigned to a single beam element. According to a previous study (Domaniç, 2008), this approximation does not bring too much error when the dynamic response of the structure is considered. For the beams and columns, instead of creating an exact cross section, equivalent necessary characteristics are assigned to the beam elements. Fixed supports are assigned in the bottom of columns to represent the foundation. Rigid members are used between the lower element of column and the foundation. For the abutments, fixed supports are used with x-axis translational springs which allow bridge to move in longitudinal direction.

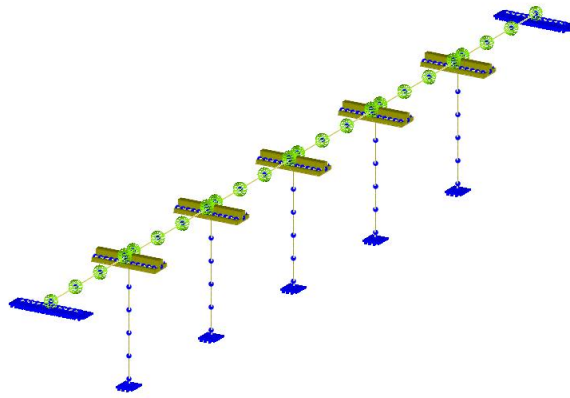
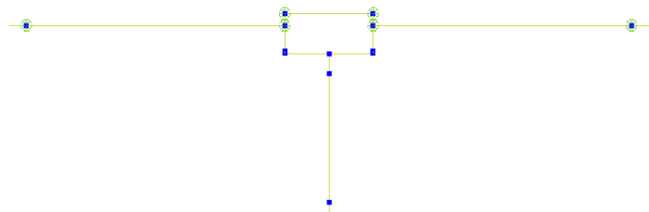
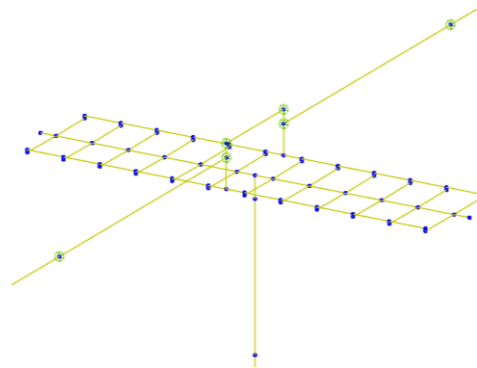


Figure 4.33 Model of Demirtas Bridge on LARSA 4D

Rigid members are used to satisfy the connection between slab-girder and girder-cap beam. Elastomeric bearings are represented with linear springs on the cap beam (Figure 4.34).



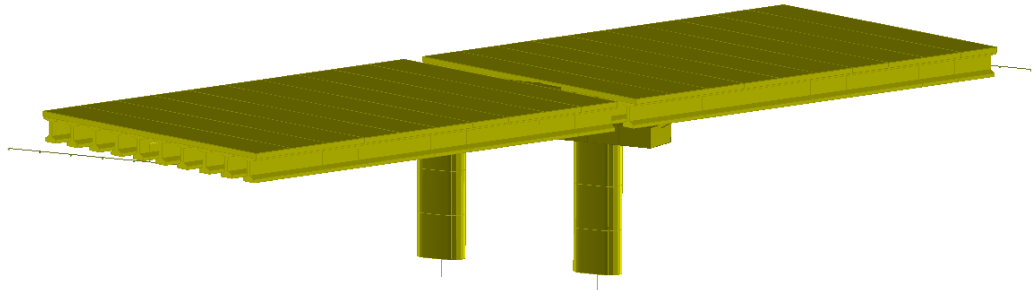
(a) Side view



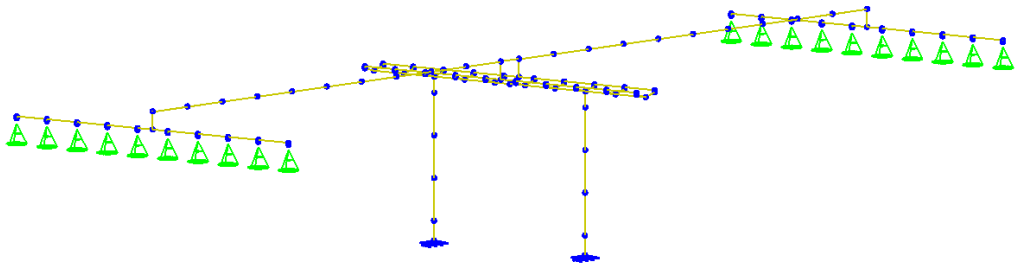
(b) Isometric view

Figure 4.34 Modelling of Superstructure and Supports at Piers (Demirtas Bridge)

Since Balikli bridge has only two spans, the whole structure is modelled on LARSA 4D (Figure 4.35). Slab is not modelled so the effects of the loads caused by the slab are ignored which does not have a significant impact on the results. On the other hand, the whole girder system is again represented by a single beam. Angle of skew of the bridge is taken into account for the modelling. Assignment of rigid members and springs in the model are similar to Demirtas bridge, so they will not be repeated in this section in detail (Figure 4.36).

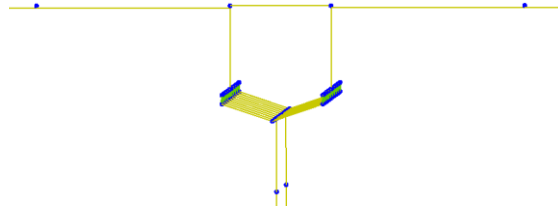


(a) Complete Rendering

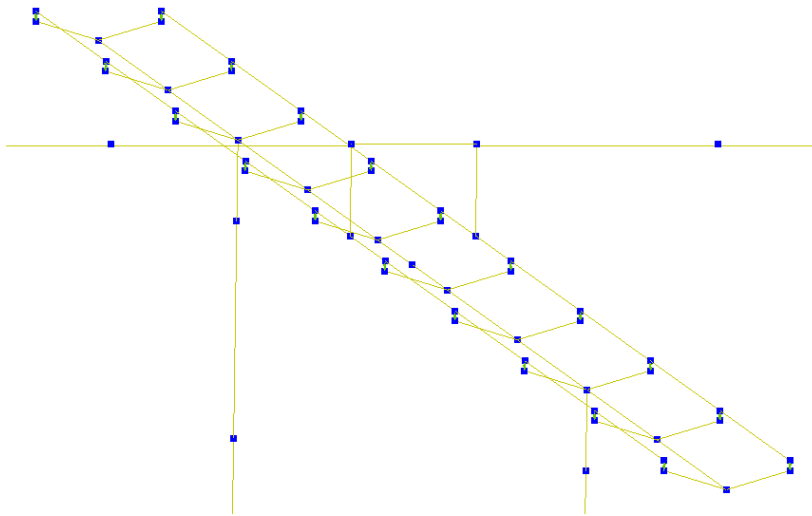


(b) Simple Rendering

Figure 4.35 Representation of Balikli Bridge on LARSA 4D



(a) Side View



(b) Isometric View

Figure 4.36 Modelling of Superstructure and Supports at Piers (Balikli Bridge)

For the modelling of Panayir bridge, similar procedures are applied with Demirtas and Balikli bridges (Figure 4.37). Since it is a relatively small bridge with 3 spans, again whole structure is modelled. Instead of using a single beam, all beams are modelled and the slab is modelled separately. They are linked to each other with the help of rigid elements as shown in Figure 4.38.

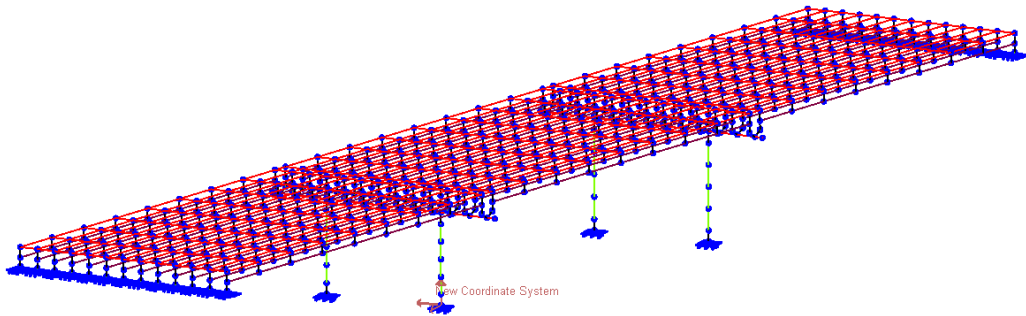
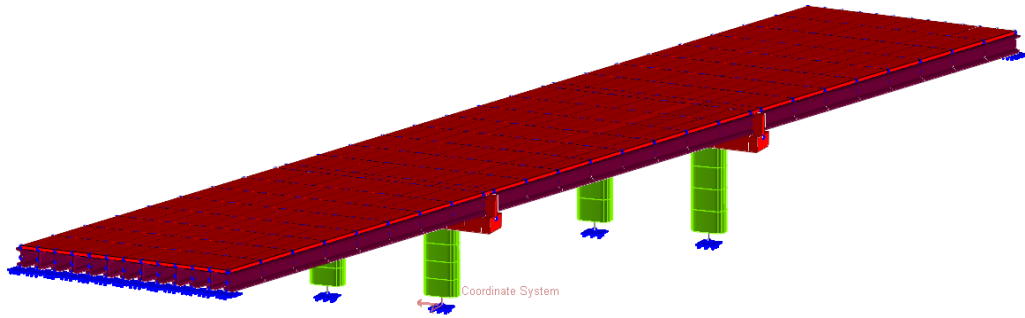
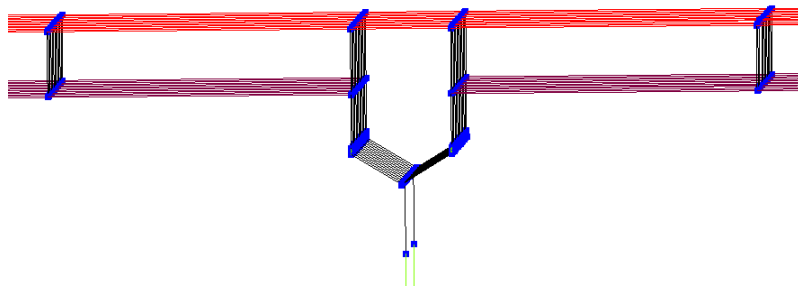
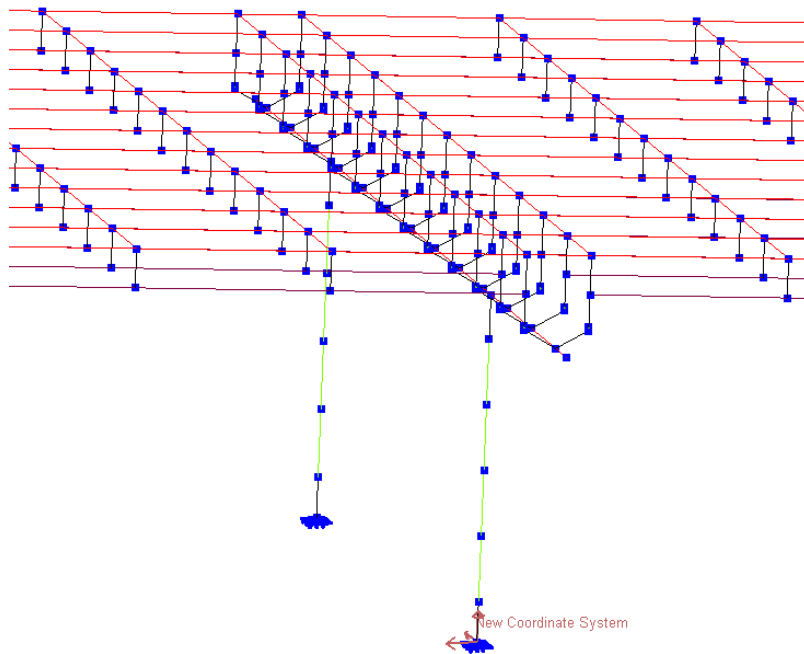


Figure 4.37 Representation of Panayir Bridge on LARSA 4D



(a) Side view



(b) Isometric view

Figure 4.38 Modelling of Superstructure and Supports at Piers (Panayir Bridge)

4.3 Dynamic Analysis of Bridges

In the dynamic analysis chapter of AASHTO (2010) which is used as a guide for the analysis in this thesis, it is stated that mass, stiffness and damping characteristics shall be modelled for structural components of a bridge in dynamic behaviour analysis. Relevant characteristics of the structure and excitation shall be included in dynamic models.

Relevant structural characteristics may be listed as;

- Mass distribution,
- Stiffness distribution,
- Damping characteristics.

Relevant characteristics of excitation may be listed as;

- Frequency of the forcing function,
- Application duration,
- Direction of application.

According to AASHTO (2010), bridges in Seismic Zone 1 (low probability of occurrence of earthquakes) regardless of their geometry and operational classes as well as bridges with single-span regardless of their seismic zone do not require seismic analysis. However, since the selected bridges are in the Seismic Zone 4 according to Table 4.2 and they do not have single-span, necessary seismic analyses shall be applied to observe their seismic demands.

Table 4.2 Seismic Zones in AASHTO 2010

Acceleration Coefficient, S_{D1}	Seismic Zone
$S_{D1} \leq 0.15$	1
$0.15 < S_{D1} \leq 0.30$	2
$0.30 < S_{D1} \leq 0.50$	3
$0.50 < S_{D1}$	4

Seismic zone, regularity, and operational classification are the factors that must be taken into account for the selection of the method of dynamic analysis. Operational classification is explained in detail in the previous chapters. Distribution of weight and stiffness along with the number of spans are the main components of regularity.

Bridges with less than seven spans and with no abrupt changes in weight, stiffness or geometry from span to span or support to support except the abutments can be called as “regular bridges”. Regularity can be assessed directly from Table 4.3. The bridges that do not satisfy the given requirements in this table shall be called as “irregular bridges”.

Table 4.3 Regular Bridge Requirements

Parameter	Value				
	2	3	4	5	6
Number of Spans	2	3	4	5	6
Maximum subtended angle for a curved bridge	90°	90°	90°	90°	90°
Maximum span length ratio from span to span	3	2	2	1.5	1.5
Maximum bent/pier stiffness ratio from span to span, excluding abutments	—	4	4	3	2

After deciding on regularity, seismic zone and operational classification of a bridge, requirements of minimum analysis can be selected with the help of Table 4.4 in which:

* = no seismic analysis required

UL = uniform load elastic method

SM = single-mode elastic method

MM = multimode elastic method

TH = time history method

Table 4.4 Minimum Analysis Requirements for Seismic Effects

Seismic Zone	Single-Span Bridges	Multispan Bridges					
		Other Bridges		Essential Bridges		Critical Bridges	
		regular	irregular	regular	irregular	regular	irregular
1	No seismic analysis required	*	*	*	*	*	*
2		SM/UL	SM	SM/UL	MM	MM	MM
3		SM/UL	MM	MM	MM	MM	TH
4		SM/UL	MM	MM	MM	TH	TH

As Demirtas bridge has 28 spans, it can be directly called as an irregular bridge which is in Seismic Zone 4. If it is chosen to be designed as a critical bridge, time history method is the minimum requirement. On the other hand, if it is chosen to be designed as an essential bridge, multimode elastic method is the minimum requirement. Balikli and Panayir bridges are regular bridges according to the given specifications. If they are chosen to be designed as critical bridges, minimum required method is time history method. If they are chosen to be designed as essential bridges, minimum required method is the multimode elastic method.

In this study, response spectrum analyses (multimode elastic method) are applied for all selected bridges where time history method is only applied for Demirtas bridge as it is considered to be a critical bridge. Balikli and Panayir bridges are chosen to be considered as essential bridges.

4.4 Response Spectrum Analysis (RSA) on LARSA 4D Software

Response Spectrum Analysis (RSA) is utilized to obtain the peak response of a multiple degree of freedom system (LARSA Dynamic Analysis Manual, version 7.07). Although the results obtained with the help of RSA are not exact, they are generally accepted as accurate enough for structural design applications. Response of a structure under shock loading conditions (seismic loading etc.) in terms of forces and deformations can be estimated utilizing RSA.

It would be more appropriate to describe RSA as a procedure for dynamic analysis which excludes response history rather than describing it directly as a dynamic analysis type. It is considered as a dynamic analysis procedure as it makes use of the vibration properties such as natural frequencies, mode shapes and modal damping ratios while it also uses the ground motional characteristics in the form of response spectrum.

An eigenvalue analysis with a given spectrum is required to obtain natural frequencies and mode shapes which will be used in RSA to calculate the peak displacement, force and stress responses in the structure. Natural frequencies and mode shapes can be calculated either prior to RSA in the same analysis or may have already been calculated before.

To combine the peak modal responses for determination of the peak total response, modal combination methods can be used. Since the peaks for modal responses are at various instants while the peak for the total response is at another instant, modal combination rules are used.

For the estimation of member forces and displacements, Complete Quadratic Combination (CQC) method, which combines the respective response quantities (force, moment, displacement etc.) in different modes, may be applied. According to (Wilson, 1981) member forces and displacements computed with the help of CQC method are generally sufficient and acceptable for most bridge models.

For the cases where CQC method is not used, alternative methods including the absolute sum (ABSSUM) and square-root-of-sum-of-squared (SRSS) modal combination rules may be applied. SRSS is the alternative to be applied for well-separated modes where ABSSUM should be used for closely spaced modes. Since CQC method eliminates the limitations of SRSS and as ABSSUM is usually considered to be too conservative, CQC is employed for the following response spectrum analyses.

For multimode spectral analysis method given in AASHTO (2010) number of modes must be selected in a manner that they should be greater than the three times of the number of spans of the model. In this study for each bridge model 30 modes of vibration are preferred to be analysed to satisfy the mass participation criteria.

After the construction of models on LARSA4D, a couple of load cases are defined which are mentioned before in detail (AASHTO, 2010);

Earthquake Load Component 1: Dead Load+ 100% EQ Longitudinal + 30% EQ Transverse

Earthquake Load Component 2: Dead Load+ 30% EQ Longitudinal + 100% EQ Transverse

With the definition of load cases, RSA are applied using the mean and mean-plus-one-standard-deviation site-specific response spectra presented previously and AASHTO design spectra (2007 and 2010). In Figure 4.39 the definition of the global axes for models can be seen.

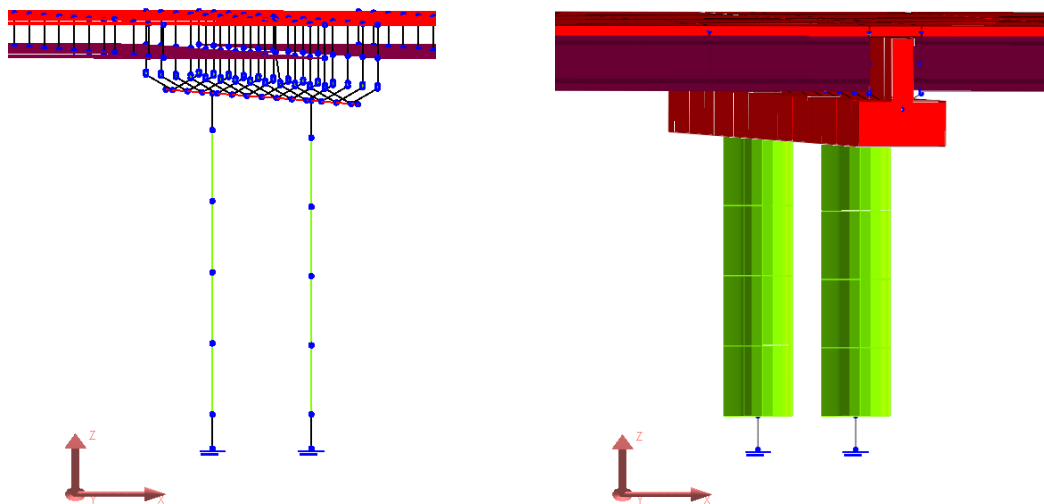


Figure 4.39 Definitions of Global Axes for Bridge Models (X-Axis in Longitudinal and Y-Axis in Transverse Direction)

4.5 Results of Response Spectrum Analyses

Results of RSA are given in terms of global (transverse and longitudinal) moment values. In the comparisons, the largest value of the moments in two directions is taken into account. When the results of the response spectrum analyses for Demirtas bridge are considered (Table 4.5), it is observed that the mean site-specific spectrum load case yields substantially smaller moment values for $3.5 < M_w < 4.5$ and $4.5 < M_w < 5.5$ bins compared to the corresponding AASHTO load cases (2007 and 2010). Moment values in $3.5 < M_w < 4.5$ bin are nearly four times smaller than the ones in AASHTO (2007 and 2010) whereas moment values in $4.5 < M_w < 5.5$ bin are nearly half of the values in AASHTO (2007 and 2010). For the $5.5 < M_w < 6.5$ bin, the maximum column moment obtained from the analyses seems closer to the results of AASHTO load cases (2007 and 2010). As expected, the results from site-specific spectra for $6.5 < M_w < 7.5$ bin overestimate those from the design spectra for this bridge which has a longer fundamental period than the other bridges. This is an important observation that could lead to a definition of special specifications for the design spectra in the long-period range for the near-field, large magnitude events.

For Balikli and Panayir bridges, the results of mean site-specific spectrum are smaller than the AASHTO cases (2007 and 2010) for the majority of the magnitude bins. One exception is the $6.5 < M_w < 7.5$ bin for the Panayir bridge where the results of mean site-specific spectrum are close to the AASHTO cases (2007 and 2010).

Although there is an increasing demand of column moments for increasing magnitude ranges for Demirtas bridge, it may be observed from Table 4.6 and Table 4.7 that the column moment values do not show a regular trend for Balikli and Panayir bridges. It may be a result of the fluctuations in mean site-specific spectral amplitudes for those sites as well as the angle of skew of bridges.

When the maximum column moment values and column tip displacements given in Table 4.8, Table 4.9 and Table 4.10 which are obtained from RSA are considered for each bridge, it is seen that they are consistent.

Finally, it must be noted that the differences between bridge responses to the mean site-specific spectrum for each case and design spectra can be attributed to different fundamental period values of each bridge.

Table 4.5 Maximum Column Moment Values for Different RSA Cases for Demirtas Bridge

Demirtas Bridge	Maximum Column Moment Values (kN.m)	
	Transverse	Longitudinal
Case		
MEAN $3.5 < M_w < 4.5$	114816	33045
MEAN + STD $3.5 < M_w < 4.5$	218236	61458
MEAN $4.5 < M_w < 5.5$	232910	60405
MEAN + STD $4.5 < M_w < 5.5$	400740	127848
MEAN $5.5 < M_w < 6.5$	509190	162458
MEAN + STD $5.5 < M_w < 6.5$	763176	271733
MEAN $6.5 < M_w < 7.5$	624024	239766
MEAN + STD $6.5 < M_w < 7.5$	875816	367385
AASHTO 2007	521279	214414
AASHTO 2010	559093	190423

Table 4.6 Maximum Column Moment Values for Different RSA Cases for Balikli Bridge

Balikli Bridge	Maximum Column Moment Values (kN.m)	
	Transverse	Longitudinal
Case		
MEAN $3.5 < M_w < 4.5$	8352	7332
MEAN + STD $3.5 < M_w < 4.5$	10900	9615
MEAN $4.5 < M_w < 5.5$	9656	6563
MEAN + STD $4.5 < M_w < 5.5$	14482	8749
MEAN $5.5 < M_w < 6.5$	13776	7116
MEAN + STD $5.5 < M_w < 6.5$	18744	9677
MEAN $6.5 < M_w < 7.5$	13411	6919
MEAN + STD $6.5 < M_w < 7.5$	17326	8946
AASHTO 2007	15409	8288
AASHTO 2010	15586	8079

Table 4.7 Maximum Column Moment Values for Different RSA Cases for Panayir Bridge

Panayir Bridge Case	Maximum Column Moment Values (kN.m)	
	Transverse	Longitudinal
MEAN $3.5 < M_w < 4.5$	15577	8159
MEAN + STD $3.5 < M_w < 4.5$	20758	10954
MEAN $4.5 < M_w < 5.5$	17523	9372
MEAN + STD $4.5 < M_w < 5.5$	22076	12631
MEAN $5.5 < M_w < 6.5$	15873	16817
MEAN + STD $5.5 < M_w < 6.5$	17294	25000
MEAN $6.5 < M_w < 7.5$	14090	20542
MEAN + STD $6.5 < M_w < 7.5$	20781	28441
AASHTO 2007	17070	19300
AASHTO 2010	16454	25170

Table 4.8 Maximum Column Tip Displacement Values for Different RSA Cases for Demirtas Bridge

Demirtas Bridge Case	Maximum Column Tip Displacement Values (m)	
	Longitudinal	Transverse
MEAN $3.5 < M_w < 4.5$	0.0678	0.0721
MEAN + STD $3.5 < M_w < 4.5$	0.1432	0.1384
MEAN $4.5 < M_w < 5.5$	0.1472	0.1482
MEAN + STD $4.5 < M_w < 5.5$	0.3222	0.2556
MEAN $5.5 < M_w < 6.5$	0.4149	0.3255
MEAN + STD $5.5 < M_w < 6.5$	0.6954	0.4881
MEAN $6.5 < M_w < 7.5$	0.6144	0.3992
MEAN + STD $6.5 < M_w < 7.5$	0.9424	0.5603
AASHTO 2007	0.5480	0.3332
AASHTO 2010	0.4862	0.3574

Table 4.9 Maximum Column Tip Displacement Values for Different RSA Cases for Balikli Bridge

Balikli Bridge	Maximum Column Tip Displacement Values (m)	
Case	Longitudinal	Transverse
MEAN $3.5 < M_w < 4.5$	0.0152	0.0080
MEAN + STD $3.5 < M_w < 4.5$	0.0199	0.0103
MEAN $4.5 < M_w < 5.5$	0.0195	0.0071
MEAN + STD $4.5 < M_w < 5.5$	0.0294	0.0091
MEAN $5.5 < M_w < 6.5$	0.0282	0.0070
MEAN + STD $5.5 < M_w < 6.5$	0.0383	0.0095
MEAN $6.5 < M_w < 7.5$	0.0275	0.0068
MEAN + STD $6.5 < M_w < 7.5$	0.0355	0.0088
AASHTO 2007	0.0314	0.0081
AASHTO 2010	0.0318	0.0081

Table 4.10 Maximum Column Tip Displacement Values for Different RSA Cases for Panayir Bridge

Panayir Bridge	Maximum Column Tip Displacement Values (m)	
Case	Longitudinal	Transverse
MEAN $3.5 < M_w < 4.5$	0.0127	0.0091
MEAN + STD $3.5 < M_w < 4.5$	0.0172	0.0122
MEAN $4.5 < M_w < 5.5$	0.0147	0.0103
MEAN + STD $4.5 < M_w < 5.5$	0.0227	0.0130
MEAN $5.5 < M_w < 6.5$	0.0306	0.0095
MEAN + STD $5.5 < M_w < 6.5$	0.0455	0.0105
MEAN $6.5 < M_w < 7.5$	0.0374	0.0086
MEAN + STD $6.5 < M_w < 7.5$	0.0518	0.0127
AASHTO 2007	0.0351	0.0102
AASHTO 2010	0.0458	0.0101

CHAPTER 5

FURTHER APPLICATIONS: LINEAR TIME HISTORY ANALYSES (LTHA) ON A SELECTED BRIDGE

5.1 Definition and Procedure

A time history analysis can be employed either in a linear or nonlinear fashion. Response of the structure to time-dependent loads can be computed with this method using excitation records.

According to AASHTO (2010), especially for critical (which are defined in previous chapters) and geometrically complex bridges or those that are close to earthquake faults, time history method must be applied with comprehensive care.

The seismic environment of the input time history selected to describe the proper earthquake load must include tectonic environment, earthquake magnitude, type of faulting, distance of seismic source to site, local site conditions and ground motion characteristics information. In addition, time history inputs developed from representative ground motions should be response spectrum-compatible. Time histories should be selected such that they involve similar earthquake magnitudes, site conditions and distances as the region of interest. This is because selected time histories have a strong influence on the response spectral content, the shape of spectra, strong shaking duration, and near-source ground-motion characteristics.

The procedures for response spectrum matching involves the methods in which time history modification is conducted in time domain (Lilhanand and Tseng, 1988; Abrahamson, 1992) and frequency domain (Gasparini and Vanmarcke ,1976; Silva

and Lee, 1987; Bolt and Gregor, 1993). Both methods alter the time series to obtain a proper match to the target response spectrum. However, during this process, the basic time domain character of time history records must be protected. For reducing variations in time domain characteristics, shape of the response spectrum obtained from original time history record should be similar to the target spectrum.

Following the response spectrum analyses presented in the previous chapter, linear time history analysis (LTHA) is applied on Demirtas bridge with LARSA 4D. The main reason behind preferring this bridge to analyse is the irregularity caused by the number of spans. Moreover, since it is significant for the transportation in Bursa region it can be defined as a critical bridge due to the regulations mentioned in the previous chapter. Thus, applying time history analyses on this bridge would be appropriate. LTHA is particularly chosen rather than Nonlinear Time History Analysis (NLTHA) to observe the structural response more clearly. Since there are several different variables in NLTHA which can influence the behaviour of the structure, it is not considered to be consistent to observe the effects of alternative spectra on the structural response.

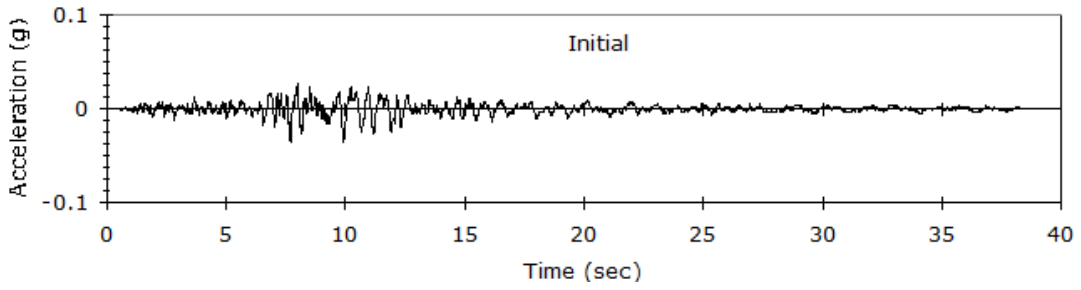
To provide input time history data to the software for analyses, spectral matching is applied on several ground motions selected according to the recommendations given in Tall Buildings Initiative (2010) developed by Pacific Earthquake Engineering Research Centre. Representative original ground motions with properties that are consistent with the tectonics of the region as well as the local site conditions are chosen as inputs. Ground motion records from 1986 Chalfant Valley ($M_w=6.2$), 1999 Duzce ($M_w=7.2$) and 1979 Imperial Valley ($M_w=6.5$) earthquakes are used for spectral matching applications. Detailed information on the records is presented in Table 5.1.

Table 5.1 Information on the Records Used in Spectral Matching

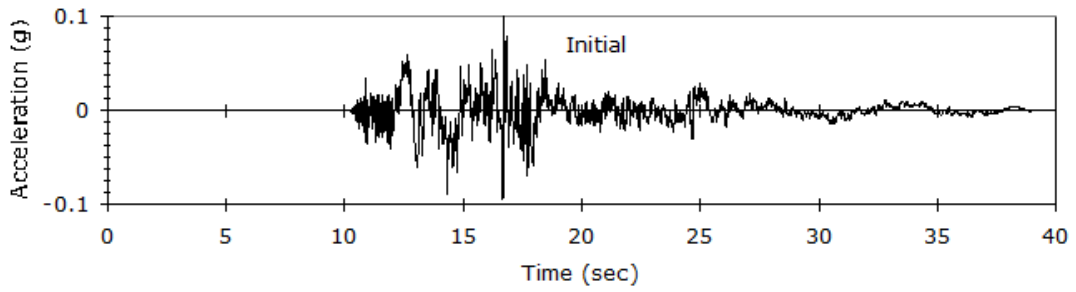
Record ID	Station Name	Earthquake Name and Date (M/D/Y)	M_w	Source Mechanism	V_{s30} (m/s)
DZC-DZC 1058E	Lamont station 1058	Duzce 11/12/99	7.2	Strike-slip	282
A-TIN000	Timemaha res. 000	Chalfant valley 07/21/86	6.2	Strike-slip	345
H-SUP135	Superstition mtn camera 135	Imperial valley 10/15/79	6.5	Thrust	362

EZ-FRISK (version 7.43), a software package for site-specific earthquake hazard analysis, is used for matching applications. Relative figures of the matches to the selected ground motions on response spectrum curves are presented in Appendix C while the original time history records are demonstrated in Figure 5.1.

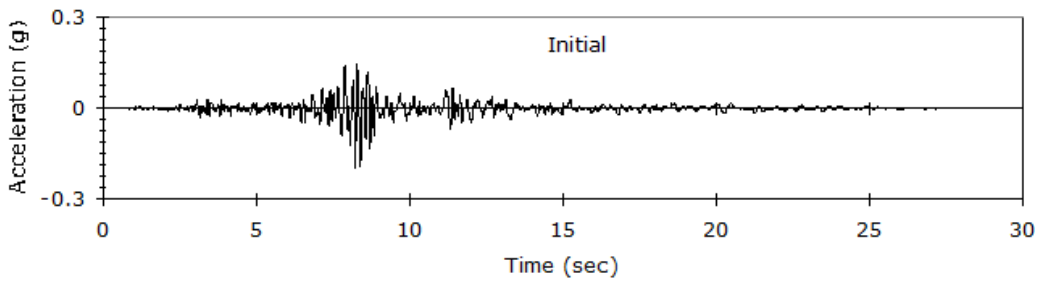
Non-stationary spectral matching algorithm (Abrahamson 1992; Abrahamson and Al Atik, 2010) is used to match the design spectra. For the selected cases, maximum number of iterations is kept constant at 30 while a tolerance of 0.01g is employed. Finally, all records are filtered between 0.25 Hz - 25Hz.



(a)



(b)



(c)

Figure 5.1 Ground Motion Records Used in Spectral Matching (a) A-TIN000, (b) DZC-DZC 1058e and (c) H-SUP135

5.2 Results of Time History Analyses

When the results of linear time history analyses on Demirtas bridge are considered, it is noted that since the AASHTO (2007) design spectra has a flat portion in the small periods, matched time history outputs have large peak ground acceleration values. As a result, the moments obtained for AASHTO (2007) case are much larger than the other cases. Maximum column moments from time history analyses via three records that are scaled to match each spectra of interest are presented in Table 5.2.

Maximum column moments seem to be consistent and in the same order of magnitude with the results of RSA. Moreover, when the LTHA results of different cases are compared, similar conclusions to those of Chapter 4 can be derived. It is observed that the moments increase with increasing M_w . AASHTO (2010) design spectra gives similar moment values for $5.5 < M_w < 6.5$ bin as in the case of RSA. However, the moment values for $3.5 < M_w < 4.5$ and $4.5 < M_w < 5.5$ bins are smaller than the design spectra while they are larger for $6.5 < M_w < 7.5$ bin when compared to the design spectra. When the column tip displacements given in Table 5.3 are considered, it is seen that they are consistent with the maximum column moment values. Also, it is noted that overall LTHA results are consistent with those of RSA.

Table 5.2 Maximum Column Moment Values for Different Linear Time History Analyses Cases for the Bridges Selected

	Maximum Column Moment Values (kN.m)	
	Transverse	Longitudinal
	(EQ given in X direction)	(EQ given in Y direction)
AASHTO (2010)	DZC-DZC 1058E	A-TIN000
	645923	-197633
	A-TIN000	HSUP-135
	-567445	-167708
	HSUP-135	DZC-DZC 1058E
	-667730	187621
AASHTO (2007)	DZC-DZC 1058E	A-TIN000
	-926911	353708
	A-TIN000	HSUP-135
	-933121	-371498
	HSUP-135	DZC-DZC 1058E
	-954570	-393680
MEAN		
3.5<M _w <4.5	DZC-DZC 1058E	A-TIN000
	182808	-41204
	A-TIN000	HSUP-135
	-141276	-46608
	HSUP-135	DZC-DZC 1058E
	161075	37381
4.5<M _w <5.5	DZC-DZC 1058E	A-TIN000
	288146	-56939
	A-TIN000	HSUP-135
	244730	-73783
	HSUP-135	DZC-DZC 1058E
	249441	-58965
5.5<M _w <6.5	DZC-DZC 1058E	A-TIN000
	-613454	-152101
	A-TIN000	HSUP-135
	590863	171686

	Maximum Column Moment Values (kN.m)	
	Transverse	Longitudinal
	(EQ given in X direction)	(EQ given in Y direction)
	HSUP-135	DZC-DZC 1058E
	-673289	180325
6.5<M _w <7.5	DZC-DZC 1058E	A-TIN000
	630433	251122
	A-TIN000	HSUP-135
	806877	245897
	HSUP-135	DZC-DZC 1058E
	697263	-222127
MEAN+STD		
3.5<M _w <4.5	DZC-DZC 1058E	A-TIN000
	-249455	72077
	A-TIN000	HSUP-135
	240736	-65273
	HSUP-135	DZC-DZC 1058E
	231729	70679
4.5<M _w <5.5	DZC-DZC 1058E	A-TIN000
	-445090	-119406
	A-TIN000	HSUP-135
	504042	95975
	HSUP-135	DZC-DZC 1058E
	428326	129442
5.5<M _w <6.5	DZC-DZC 1058E	A-TIN000
	-841155	255166
	A-TIN000	HSUP-135
	215017	264841
	HSUP-135	DZC-DZC 1058E
	-845764	116780
6.5<M _w <7.5	DZC-DZC 1058E	A-TIN000
	950079	328854
	A-TIN000	HSUP-135
	957262	361562
	HSUP-135	DZC-DZC 1058E
	947785	339437

Table 5.3 Maximum Column Tip Displacement Values for Different Linear Time History Analyses Cases for the Bridges Selected

	Maximum Column Tip Displacement Values (m)	
	Longitudinal	Transverse
	(EQ given in X direction)	(EQ given in Y direction)
AASHTO (2010)	DZC	ATIN
	0.5061	0.4084
AASHTO (2010)	ATIN	HSUP
	0.4309	0.3641
AASHTO (2010)	HSUP	DZC
	0.4890	0.4235
AASHTO (2007)	DZC	ATIN
	0.8846	0.6316
AASHTO (2007)	ATIN	HSUP
	0.8863	0.6138
AASHTO (2007)	HSUP	DZC
	0.9434	0.5986
MEAN		
3.5<M _w <4.5	DZC	ATIN
	0.0664	0.1173
	ATIN	HSUP
	0.0990	0.0891
	HSUP	DZC
	0.0722	0.0960
4.5<M _w <5.5	DZC	ATIN
	0.1353	0.1840
	ATIN	HSUP
	0.1794	0.1549
	HSUP	DZC
	0.1332	0.1557
5.5<M _w <6.5	DZC	ATIN
	0.3920	0.3918
	ATIN	HSUP
	0.4471	0.3763

	Maximum Column Tip Displacement Values (m)	
	Longitudinal	Transverse
	HSUP	DZC
	0.4621	0.4267
6.5<M _w <7.5	DZC	ATIN
	0.6259	0.3995
	ATIN	HSUP
	0.6244	0.5157
	HSUP	DZC
	0.5517	0.4386
MEAN + STD		
3.5<M _w <4.5	DZC	ATIN
	0.1649	0.1469
	ATIN	HSUP
	0.1550	0.1504
	HSUP	DZC
	0.1588	0.1531
4.5<M _w <5.5	DZC	ATIN
	0.2941	0.2830
	ATIN	HSUP
	0.2867	0.3169
	HSUP	DZC
	0.2944	0.2706
5.5<M _w <6.5	DZC	ATIN
	0.6513	0.5328
	ATIN	HSUP
	0.6809	0.1367
	HSUP	DZC
	0.2901	0.5392
6.5<M _w <7.5	DZC	ATIN
	0.8500	0.6118
	ATIN	HSUP
	0.9102	0.7150
	HSUP	DZC
	0.8390	0.6500

CHAPTER 6

CONCLUSIONS AND FUTURE WORK

In this study, normalized site-specific mean response spectra are obtained for two site classes and different M_w bins using the Turkish ground motion dataset. Mean site-specific spectra are compared against the corresponding design spectra in AASHTO (2007 and 2010). Next, RSA and LTHA are performed to observe bridge responses to differences in the spectrum shapes. Maximum column moment in the bridges is selected as the main parameter for comparison of different load cases.

Main findings and conclusions of this study are as follows:

- RSA and LTHA yield mostly consistent numerical results and similar conclusions: It is observed that mean site-specific response spectra for Site Classes C and D (AASHTO 2010) both give smaller maximum column moment values for the small to moderate M_w levels when compared to those of AASHTO (2007 and 2010). Hence, AASHTO (2007 and 2010) may be considered to overestimate the seismic demand for $3.5 < M_w < 4.5$, $4.5 < M_w < 5.5$ and $5.5 < M_w < 6.5$ bins for the cases explored in this thesis.
- However, for larger earthquakes ($6.5 < M_w < 7.5$), site-specific spectra are observed to have higher spectral amplitudes in the long period range than the design spectra given in AASHTO specifications. This observation could have two meanings: first one is the bias due to unequal number of records in different magnitude bins where much less number of records is available for large events. The second consequence is the fact that design spectra in AASHTO do not include magnitude levels as a direct parameter for

estimating the spectral amplitudes and thus could underestimate the spectral levels for large events. (Normalization of spectral amplitudes with respect to PGA values includes magnitude information in the design spectra only indirectly.)

- The combined site-specific spectra of Site C and D obtained by merging data from all magnitude bins together are observed to lie below the design spectra.
- Finally, for bridges with longer fundamental periods mean site-specific response spectra create larger deviations from the AASHTO load case in terms of moment values. Indeed, for bridges with smaller fundamental periods, results are closer to each other for each load case (each magnitude interval and site class combination) than those for bridges with higher fundamental periods. Thus, the conclusions presented herein are indeed dependent on the type and dynamic properties of the bridges studied.

Potential future studies related to this thesis can be summarized as follows:

- Earthquake data collection and classification practices are important for unbiased results. Number of earthquakes with larger magnitudes is naturally less than those from small and moderate size events. However, whenever possible, data from large earthquakes should be recorded. Strong motion networks in seismically-active areas (and thus, datasets) should be enlarged for similar future studies for complete and unbiased conclusions.
- Since design spectra is dependent directly on the site class, it is important to identify the site classes at strong motion stations of interest. In Turkey, still more than half of the strong motion stations do not have a site class pointer such as V_{S30} or SPT values. It is thus critical to assess the local site conditions at strong motion stations in the near future.
- Since the results depend on fundamental periods, other bridges with different periods and structural properties should be examined for extending the conclusions of this thesis.

- It must be noted that the analyses for each spectra are compared in terms of maximum column moments for both RSA and LTHA. Thus, the ground motion duration effects could not be assessed here directly. For further studies, a more direct measure of the duration effects could be assessed in LTHA.
- This thesis focused on bridge response and AASHTO. However, for more general conclusions, different seismic codes and alternative structure types should be studied.
- This study and similar studies are inherently region-specific. Thus, ground motion records from other tectonic regions and site conditions should also be assessed.
- A design spectrum is generally derived from probabilistic seismic hazard analyses. However, considering the deterministic mean site-specific response spectra for different site classes, source mechanisms and magnitude ranges (such as the ones in this thesis), a novel design spectrum can be generated/augmented for Turkey with the help of further detailed studies in the near future.

REFERENCES

1. AASHTO (2007). *LRFD Bridge Design Specifications*, Customary U.S. Units Washington DC.
2. AASHTO (2010). *LRFD Bridge Design Specifications*, Customary U.S. Units Washington DC.
3. AASHTO (2012). *LRFD Bridge Design Specifications*, Customary U.S. Units Washington DC.
4. Abrahamson N. A. (1992). *Non-stationary Spectral Matching Program*, Seismological Research Letters. Vol. 63, No.1. Seismological Society of America, El Cerrito.
5. Abrahamson N. A. and Al Atik L. (2010). *An Improved Method for Non-stationary Spectral Matching*, *Earthquake Spectra*, Vol. 26, pp. 601-617.
6. Akkar S., Çağnan Z., Yenier E., Erdoğan Ö., Sandikkaya M. A., Gülkan P. (2010). *The recently compiled Turkish strong motion database: preliminary investigation for seismological parameters*, *Journal of Seismology*, Vol. 14, pp 457-479.
7. Anderson A.W., Blume J.A., Degenkolb H.J., Hammill H.B., Knapik E.M., Marchand H.L., Powers H.C., Rinne J.E., Sedgwick, G.A. and Sjoberg, H.O. (1952). *Lateral Forces of Earthquake and Wind*, *Transactions of the ASCE*, Vol. 117, pp. 716–780.
8. Atkinson G. M. and Boore D. M. (1990). *Recent trends in ground motion and spectral response relations for North America*, *Earthquake Spectra*, Vol. 6, pp. 15–35.
9. Biot M. A. (1941). *A mechanical analyzer for the prediction of earthquake stresses*, *Bulletin of the Seismological Society of America*, Vol. 31, pp. 151–71.
10. Biot M. A. (1942). *Analytical and experimental methods in engineering seismology*, *Proceedings of the ASCE*, Vol. 68, pp. 49–69.

11. Blume J. A., Sharpe R. L., Dalal J. S. (1972). *Recommendations for shape of earthquake response spectra*, San Francisco, California.
12. Bolt B. A. and Gregor N. J. (1993). *Synthesized Strong Ground Motions for the Seismic Condition Assessment of the Eastern Portion of the San Francisco Bay Bridge*, Report UCB/EERC-93.12. Earthquake Engineering Research Center, University of California at Berkeley, Berkeley, CA.
13. Bommer J. J., Elnashai A. S., Weir A. G. (2000). *Compatible acceleration and displacement spectra for seismic design codes*, Proceedings of the 12th World Conference of Earthquake Engineering, Auckland, Paper no. 207.
14. CALTRANS (2014). *Seismic Design Criteria*, Version 1.7, California Department of Transportation, Sacramento, California.
15. Campbell K., and Bozorgnia Y. (2008). *NGA ground motion model for the geometric mean horizontal component of PGA, PGV, PGD and 5% damped linear elastic response spectra for periods ranging from 0.01 to 10 s*, Earthquake Spectra, Vol. 24, pp. 139 - 172.
16. Chai J. F., Teng T. J., Loh, C. H. (2004). *Determination of first mode ground period and site-dependent design response spectrum for Taiwan High Speed Rail*, Soil Dynamics and Earthquake Engineering, Vol. 24, pp.527-536.
17. Chiou B., and Youngs R., (2008). *An NGA model for the average horizontal component of peak ground motion and response spectra*, Earthquake Spectra, Vol. 24, pp. 173-216.
18. Chopra S., Choudhury P. (2011). *A study of response spectra for different geological conditions in Gujarat, India*, Soil Dynamics and Earthquake Engineering, Vol. 11, pp.1551-1564.
19. Crouse C. B. and McGuire J. W (1996). *Site response studies for purpose of revising NEHRP seismic provisions*, Earthquake Spectra, Vol.12, pp. 407–30.
20. Doğangün A. and Livaoğlu R. (2006). *A comparative study of the design spectra defined by Eurocode 8, UBC, IBC and Turkish Earthquake Code on R/C Sample Buildings*, Journal of Seismology, Vol. 10, pp. 335-351.

21. Domaniç K. A. (2008) *Effects of Vertical Excitation on Seismic Performance of Highway Bridges and Hold-Down Device Requirements*, Master Thesis, Department of Civil Engineering, METU, Ankara.
22. EZ-FRISK v7.43 Build 000, Copyright 2001-2009: Risk Engineering, Inc.
23. Gasparini D. and Vanmarcke E. H. (1976). *SIMQKE: A Program for Artificial Motion Generation*. Department of Civil Engineering, Massachusetts Institute of Technology, Cambridge, MA.
24. Hall W. J., Mohraz B, Newmark N. M. (1975). *Statistical analysis of earthquake response spectra*, Proceedings of third international conference on structure mechanics in reactor technology, London.
25. Hall W. J., Mohraz B, Newmark N. M. (1975). *Statistical studies of vertical and horizontal earthquake spectra*, Urbana, Illinois.
26. Hayashi S., Tsuchida H., Kurata E. (1971). *Average response spectra for various subsoil conditions*, Proceedings of third joint meeting, U.S. Japan panel on wind and seismic effects. UJNR, Tokyo.
27. Housner G. W. (1941). *An investigation of the effects of earthquakes on building*, California Institute of Technology, Pasadena, California.
28. Housner G. W. (1959). *Behavior of structures during earthquakes*, Proceedings of the ASCE, Vol. 85, pp. 109–29.
29. Hudson D. (1956). *Response spectrum techniques in engineering seismology*, *Proceedings of the World Conference on Earthquake Engineering*, Berkeley, California.
30. LARSA 4D v7.07 r16: LARSA, Inc., New York, USA.
31. Manceaux D. (2008). *New Seismic 1000 Year Return Period – Impact to Bridge Design Methodologies*, The Sixth National Conference on Bridges & Highways, Charleston, South Carolina.
32. Mohraz B. (1976). *A study of earthquake response spectra for different geological conditions*, Bulletin of the Seismological Society of America, Vol. 66, pp. 915–35.
33. Mohraz B., Hall W. J., Newmark N. M. (1972). *A study of vertical and horizontal earthquake spectra*, Urbana, Illinois.

34. Petersen M. D., Frankel A. D., Harmsen S. C., Mueller C. S., Haller K. M., Wheeler R. L., Wesson R. L., Zeng Y. B., Oliver S., Perkins D. M., Luco N. F. E. H., Wills C. J., and Rukstales K. S. (2008). *Documentation for the 2008 Update of the United States National Seismic Hazard Maps: U.S. Geological Survey*, Open-FileReport.
35. Sabetta F. and Pugliese A. (1996). *Estimation of response spectra and simulation of nonstationary earthquake ground motions*, Bulletin of the Seismological Society of America, Vol. 86, pp. 337–52.
36. Sandikkaya M. A. (2008). *Site Classification of Turkish National Strong-Motion Recording Sites*, Master Thesis, Department of Civil Engineering, METU, Ankara.
37. Sandikkaya M. A., Yilmaz M. T., Bakır S. B., Akkar S. (2008). *An Evaluation of Site Classification for National Strong-Motion Recording Stations in Turkey*, Geotechnical Earthquake Engineering and Soil Dynamics, ASCE.
38. Sandikkaya M. A., Yilmaz M. T., Bakır S. B., Yilmaz Ö. (2010). *Site Classification of Turkish National Strong-Motion Recording Sites*, Journal of Seismology, Vol. 14, pp. 543-563.
39. Seed H. B. and Idriss I. M. (1979). *Influence of soil conditions on ground motions during earthquakes*, Journal of the Soil Mechanics and Foundations Division, ASCE, Vol. 95:99–137.
40. Seed H. B., Ugas C., Lysmer J. (1976). *Site dependent spectra for earthquake-resistant design*, Bulletin of the Seismological Society of America, Vol. 66, pp. 221–43.
41. SeismoSignal v5.0.0: SeismoSoft.
42. Sevgili G. (2007). *Seismic Performance Of Multisimple-Span Skew Bridges Retrofitted With Link Slabs*, Master Thesis, Department of Civil Engineering, METU, Ankara.
43. Shannola and Wilson, Inc., (1974). *Soil behaviour under earthquake loading conditions in procedures for evaluation of vibratory ground motions of soil deposits for nuclear power plant sites prepared for United States Atomic Energy Commission*, Division of Reactor Safety Research.

44. Sigmund A. F. (2007). *Response Spectra As a Useful Design and Analysis Tool for Practicing Structural Engineers*, ISET Journal of Earthquake Technology, Vol. 44, pp. 25-37.
45. Silva W. and Lee K. (1987). *State-of-the-Art for Assessing Earthquake Hazards in the United State: Report 24 WES RASCAL Code for Synthesizing Earthquake Ground Motions*, Miscellaneous Paper 5-73-1. U. S. Army Engineer Waterways Experiment Station, Vicksburg, MS.
46. Singh J. P. (1985). *Earthquake ground motions: implications for designing structures and reconciling structural damage*, Earthquake Spectra, Vol. 1, pp. 239–70.
47. Su F., Anderson J. G., Zeng Y. (2006). *Characteristics of ground motion response spectra from recent large earthquakes and their comparison with IEEE standard 693*, Proceedings of 100th anniversary earthquake conference, commemorating the 1906 San Francisco Earthquake, San Francisco, California.
48. Tall Buildings Initiative (2010) *Guidelines for Performance-based Seismic Design of Tall Buildings*, Developed by Pacific Earthquake Engineering Research Center, Report No: 2010/05.
49. Tehranizadeh M. and Safi M. (2004). *Application of artificial intelligence for construction of design spectra*, Engineering Structures, Vol. 26, pp. 707-720.
50. Trifunac M. D. (2012). *Earthquake Response Spectra for performance based design - A critical review*, Soil Dynamics and Earthquake Engineering, Vol. 37, pp. 73-83.
51. TÜBİTAK (2009-2014) *KAMAG 1007 110G093 Ongoing project*.
52. *Turkish National Strong-Motion Observation Network*, <http://kyh.deprem.gov.tr/>
53. Wilson, E. L., Kiureghian A. D. and Bayo E. P. (1981). *A Replacement for the SRSS Method in Seismic Analysis*, International Journal of Earthquake Engineering and Structural Dynamics, Vol. 9, pp. 187–194.
54. Yılmaz T. (2008). *Seismic Response Of Multi-Span Highway Bridges With Two-Column Reinforced Concrete Bents Including Foundation and Column Flexibility*, Master Thesis, Department of Civil Engineering, METU, Ankara.

APPENDIX A

SELECTED STATIONS WITH MEAN SHEAR VELOCITY VALUES

Table A.1 V_{S30} Values for Selected Stations and Corresponding Site Classes for Different Building Codes (Sandikkaya, 2008)

Station Code	GWL (m)	$V_{S,30}$ (m/s)	N_{mean}	Site Class NEHRP V_s Criteria	Site Class NEHRP SPT Criteria	Site Class EC-8 V_s Criteria	Site Class EC-8 SPT Criteria	Site Class TSDC V_s Criteria	Site Class TSDC SPT Criteria
AI 001_IST	NA	595.2	100.0	C	C	B	B	Z3	-
AI 002_GBZ	NA	701.1	100.0	C	C	B	B	Z2	-
AI 003_IZN	4.8	251.2	12.3	D	E	C	D	Z3	Z3
AI 004_IZT	NA	826.1	100.0	B	C	A	B	Z2	-
AI 005_SKR	NA	412.0	55.9	C	C	B	B	Z3	Z1
AI 006_AKY	6.7	271.6	22.8	D	D	C	C	Z3	Z3
AI 007_GYN_BHM	12.4	471.7	39.3	C	D	B	C	Z3	-
AI 008_GYN_DH	9.5	347.7	21.0	D	D	C	C	Z3	Z3
AI 009_MDR	10.8	355.4	48.6	D	D	C	C	Z2	Z2
AI 010_BOL	2.7	293.6	29.5	D	D	C	C	Z3	Z1
AI 011_DZC	6.3	282.0	31.0	D	D	C	C	Z3	Z3
AI 012_MEN	3.7	364.7	21.1	C	D	B	C	Z3	Z3
AI 013_CER	4.5	347.9	41.0	D	D	C	C	Z2	-
AI 014_KBK	NA	702.6	100.0	C	C	B	B	Z3	-
AI 015_GRD	8.2	444.7	77.3	C	C	B	B	Z3	-
AI 016_BEY	19.5	339.6	51.9	D	C	C	B	Z2	Z2
AI 017_HAY	NA	418.8	100.0	C	C	B	B	Z3	-
AI 018_CMR	6.3	312.5	51.4	D	C	C	B	Z3	-
AI 019_MRS	2.4	366.4	25.5	C	D	B	C	Z2	Z2
AI 020_KRT	7.3	485.1	95.3	C	C	B	B	Z2	-
AI 021_CYH_PTT	3.1	223.0	16.5	D	D	C	C	Z4	Z2
AI 022_CYH_TIM	3.2	263.8	16.3	D	D	C	C	Z3	Z2
AI 023_MAT17	4.3	349.9	51.7	D	C	C	B	Z2	Z2
AI 024_MAT18	NA	430.4	100.0	C	C	B	B	Z3	-
AI 025_MAT06_MET	2.3	395.2	29.7	C	D	B	C	Z2	Z2

Station Code	GWL (m)	$V_{s,30}$ (m/s)	N_{mean}	Site Class NEHRP V_s Criteria	Site Class NEHRP SPT Criteria	Site Class EC-8 V_s Criteria	Site Class EC-8 SPT Criteria	Site Class TSDC V_s Criteria	Site Class TSDC SPT Criteria
AI_026_MAT06_MIM	10.7	309.6	42.9	D	D	C	C	Z3	Z2
AI_027_MAT01	3.2	209.6	28.1	D	D	C	C	Z3	Z2
AI_028_MAT03	13.5	469.5	76.3	C	C	B	B	Z2	-
AI_029_MAT02	NA	343.6	59.9	D	C	C	B	Z3	-
AI_030_MAT04	NA	338.3	42.8	D	D	C	C	Z2	Z2
AI_031_MAT05	NA	539.2	100.0	C	C	B	B	Z2	-
AI_032_MAT07	20.2	271.6	19.8	D	D	C	C	Z3	Z3
AI_033_MAT08	NA	688.0	100.0	C	C	B	B	Z2	-
AI_034_MAT09	NA	618.0	100.0	C	C	B	B	Z2	-
AI_035_MAT15	NA	420.9	97.2	C	C	B	B	Z2	-
AI_036_MAT16	13.5	598.9	93.0	C	C	B	B	Z2	-
AI_037_MAT13	NA	390.5	34.1	C	D	B	C	Z2	Z2
AI_038_MAT14	23.6	484.4	100.0	C	C	B	B	Z2	-
AI_039_AND	8.3	610.8	44.3	C	D	B	C	Z2	-
AI_040_ELB	5.3	314.9	33.9	D	D	C	C	Z3	Z2
AI_041_MAT11	10.2	345.5	58.6	D	C	C	B	Z3	Z1
AI_042_MAT12_MET	NA	316.7	36.8	D	D	C	C	Z3	Z1
AI_043_KMR	NA	466.2	77.1	C	C	B	B	Z2	-
AI_044_MAT10	NA	671.1	100.0	C	C	B	B	Z2	-
AI_045_GOL	2.3	468.7	40.8	C	D	B	C	Z3	-
AI_046_DSH	NA	654.4	100.0	C	C	B	B	Z2	-
AI_047_MLT	NA	480.8	62.5	C	C	B	B	Z3	-
AI_048_ELZ	NA	407.3	82.7	C	C	B	B	Z3	-
AI_049_BNG	6.5	528.7	96.8	C	C	B	B	Z2	-
AI_050_SLH_OE	5.4	484.8	44.4	C	D	B	C	Z2	Z2

Station Code	GWL (m)	V _{s,30} (m/s)	N _{mean}	Site Class NEHRP V _s Criteria	Site Class NEHRP SPT Criteria	Site Class EC-8 V _s Criteria	Site Class EC-8 SPT Criteria	Site Class TSDC V _s Criteria	Site Class TSDC SPT Criteria
AI_051_SLH_MET	6.5	462.7	55.3	C	C	B	B	Z2	Z1
AI_052_MUS	11.2	314.5	22.6	D	D	C	C	Z3	Z3
AI_053_MLZ	NA	311.2	31.0	D	D	C	C	Z3	Z1
AI_054_TAT	11.3	273.0	36.4	D	D	C	C	Z3	-
AI_055_VAN	NA	363.1	37.4	C	D	B	C	Z3	Z1
AI_056_MUR	7.3	292.6	16.7	D	D	C	C	Z3	Z2
AI_057_DBY	NA	270.7	22.7	D	D	C	C	Z3	Z2
AI_058_AGR	7.3	294.8	29.0	D	D	C	C	Z3	Z2
AI_059_HRS	NA	316.4	49.4	D	D	C	C	Z3	Z1
AI_060_KRS	6.7	269.7	21.5	D	D	C	C	Z3	Z3
AI_061_ARD	NA	431.7	70.6	C	C	B	B	Z2	-
AI_062_ERZ	NA	374.9	79.5	C	C	B	B	Z2	Z1
AI_063_TER_MET	16.3	319.6	23.1	D	D	C	C	Z3	Z2
AI_064_TER_PTT	10.5	349.8	56.3	D	C	C	B	Z2	Z1
AI_065_ERC	10.2	314.2	17.4	D	D	C	C	Z3	Z2
AI_066_ZAR	16.5	281.6	19.1	D	D	C	C	Z3	Z2
AI_067_REF_HK	8.1	433.1	26.5	C	D	B	C	Z2	Z3
AI_068_REF_KM	NA	413.1	57.8	C	C	B	B	Z2	Z2
AI_069_SSH	11.4	413.4	81.4	C	C	B	B	Z2	-
AI_070_RES	5.7	376.2	80.5	C	C	B	B	Z2	-
AI_071_TKT	6.3	323.8	54.3	D	C	C	B	Z2	Z1
AI_072_ERB	2.1	326.6	56.7	D	C	C	B	Z3	Z1
AI_073_AMS_MZFL	5.5	283.9	35.7	D	D	C	C	Z3	Z2
AI_074_AMS_BAY	11.4	443.3	84.4	C	C	B	B	Z3	-
AI_075_MRZ	NA	368.4	40.9	C	D	B	C	Z3	Z2

Station Code	GWL (m)	V _{s,30} (m/s)	N _{mean}	Site Class NEHRP V _s Criteria	Site Class NEHRP SPT Criteria	Site Class EC-8 V _s Criteria	Site Class EC-8 SPT Criteria	Site Class TSDC V _s Criteria	Site Class TSDC SPT Criteria
AI_076_OSM_BEL	4.3	314.9	43.9	D	D	C	C	Z3	Z2
AI_077_OSM_EHK	2.5	254.6	14.9	D	E	C	D	Z3	Z2
AI_078_KRG	NA	687.8	100.0	C	C	B	B	Z1	-
AI_079_TOS	NA	361.8	76.2	C	C	B	B	Z2	-
AI_080_YLV	3.4	261.2	30.0	D	D	C	C	Z3	-
AI_081_IZN_KY	0	196.7	3.3	D	E	C	D	Z4	Z3
AI_082_CEK	NA	283.3	33.0	D	D	C	C	Z3	Z1
AI_083_ERG	5.5	325.2	28.8	D	D	C	C	Z3	Z3
AI_084_TKR_MET	2.1	471.9	97.5	C	C	B	B	Z3	-
AI_085_TKR_HK	NA	408.7	100.0	C	C	B	B	Z3	-
AI_086_SRK	5.5	225.0	20.2	D	D	C	C	Z4	Z3
AI_087_GLI	NA	285.9	81.8	D	C	C	B	Z3	Z1
AI_088_CNK	1.2	191.8	18.6	D	D	C	C	Z4	Z3
AI_089_KRB	NA	683.2	95.9	C	C	B	B	Z2	-
AI_090_BGA	NA	303.7	47.9	D	D	C	C	Z3	Z2
AI_091_GNN	1.7	397.2	83.9	C	C	B	B	Z3	-
AI_092_EDN_SO	23.5	330.0	50.1	D	C	C	B	Z2	Z2
AI_093_EDN_KGI	NA	520.1	100.0	C	C	B	B	Z3	-
AI_094_YNC	NA	324.1	49.8	D	D	C	C	Z3	Z1
AI_095_EZN	NA	403.2	82.6	C	C	B	B	Z2	Z1
AI_096_EDR	10.5	223.3	37.4	D	D	C	C	Z4	Z2
AI_097_AYV	NA	386.6	43.2	C	D	B	C	Z3	-
AI_098_DKL	2.3	193.2	10.7	D	E	C	C	Z3	Z4
AI_099_KNK	NA	558.0	68.2	C	C	B	B	Z2	-
AI_100_AKS	4.5	291.7	18.8	D	D	C	C	Z3	Z2

Station Code	GWL (m)	$V_{s,30}$ (m/s)	N_{mean}	Site Class NEHRP V_s Criteria	Site Class NEHRP SPT Criteria	Site Class EC-8 V_s Criteria	Site Class EC-8 SPT Criteria	Site Class TSDC V_s Criteria	Site Class TSDC SPT Criteria
AI_101_GOR	NA	629.4	100.0	C	C	B	B	Z2	-
AI_102_DMR	NA	335.8	92.7	D	C	C	B	Z3	-
AI_103_SMV	3.6	259.0	19.4	D	D	C	C	Z3	Z2
AI_104_GDZ	NA	343.2	65.9	D	C	C	B	Z3	-
AI_105_USK	NA	285.5	24.8	D	D	C	C	Z3	Z2
AI_106_BLD	NA	345.4	84.2	D	C	C	B	Z3	-
AI_107_DNZ_MET	NA	345.9	33.1	D	D	C	C	Z2	Z2
AI_108_DNZ_BAY	5.5	355.9	91.7	D	C	C	B	Z3	-
AI_109_ALA	NA	358.1	42.1	D	D	C	C	Z3	Z2
AI_110_SAL	10.7	272.9	29.4	D	D	C	C	Z3	Z2
AI_111_ODM	NA	286.3	25.6	D	D	C	C	Z3	Z2
AI_112_MNS	NA	340.3	46.8	D	D	C	C	Z2	Z2
AI_113_FOC	9.6	327.7	43.5	D	D	C	C	Z3	Z2
AI_114_GZL_MET	NA	770.7	100.0	B	C	B	B	Z2	-
AI_115_BRN_BAY	3.5	195.5	7.4	D	E	C	D	Z4	Z3
AI_116_BRN_EU	7	270.0	33.8	D	D	C	C	Z3	Z2
AI_117_KUS_MET	NA	369.3	100.0	C	C	B	B	Z3	-
AI_118_KUS_HSL	1.3	273.5	13.8	D	E	C	D	Z3	Z3
AI_119_AYD_HH	NA	310.9	44.4	D	D	C	C	Z2	Z1
AI_120_AYD_DSI	NA	271.4	38.5	D	D	C	C	Z3	Z2
AI_121_BDR	NA	746.9	100.0	C	C	B	B	Z2	-
AI_122_MLS	19	323.5	30.9	D	D	C	C	Z3	Z2
AI_123_YTG	NA	695.9	100.0	C	C	B	B	Z2	-
AI_124_YER	NA	813.4	100.0	B	C	A	B	Z2	-
AI_125_MAR	12.3	392.5	52.8	C	C	B	B	Z3	Z1

Station Code	GWL (m)	$V_{s,30}$ (m/s)	N_{mean}	Site Class NEHRP V_s Criteria	Site Class NEHRP SPT Criteria	Site Class EC-8 V_s Criteria	Site Class EC-8 SPT Criteria	Site Class TSDC V_s Criteria	Site Class TSDC SPT Criteria
AI_126_KOY	NA	371.9	25.2	C	D	B	C	Z2	Z2
AI_127_FTH	0.7	248.2	19.5	D	D	C	C	Z3	Z2
AI_128_CAM	NA	344.1	100.0	D	C	C	B	Z3	-
AI_129_FNK	0.5	299.4	27.0	D	D	C	C	Z3	Z2
AI_130_BCK_KGI	NA	713.7	100.0	C	C	B	B	Z3	-
AI_131_BCK_OM	NA	693.8	100.0	C	C	B	B	Z1	-
AI_132_TFN	NA	366.9	71.5	C	C	B	B	Z2	Z1
AI_133_BRD1	16.5	334.6	48.9	D	D	C	C	Z2	Z1
AI_134_BRD2	11.8	294.1	36.4	D	D	C	C	Z3	Z2
AI_135_SNK	NA	445.1	50.3	C	C	B	B	Z2	Z2
AI_136_CRD	25.5	395.1	63.9	C	C	B	B	Z3	Z1
AI_137_DIN	2.3	198.1	15.9	D	D	C	C	Z4	Z2
AI_138_SDL	17.2	357.4	46.4	D	D	C	C	Z2	Z2
AI_139_AFY	5.1	225.6	17.3	D	D	C	C	Z3	Z3
AI_140_STG	4.3	407.4	35.1	C	D	B	C	Z3	-
AI_141_KUT_BAY	2.8	266.6	6.9	D	E	C	D	Z3	Z3
AI_142_KUT_SS	3.2	242.5	10.2	D	E	C	D	Z4	Z3
AI_143_EMT	NA	303.6	19.0	D	D	C	C	Z3	Z2
AI_144_DUR_MET	NA	560.7	100.0	C	C	B	B	Z2	-
AI_145_DUR_KGI	NA	495.9	100.0	C	C	B	B	Z3	-
AI_146_BLK	NA	662.0	100.0	C	C	B	B	Z2	-
AI_147_BGC	3.4	299.9	31.5	D	D	C	C	Z3	Z1
AI_148_SNG	3.7	237.7	19.5	D	D	C	C	Z3	Z3
AI_149_BND_MET	NA	321.0	38.2	D	D	C	C	Z2	Z1
AI_150_BND_TDM	NA	416.7	75.2	C	C	B	B	Z2	Z1

Station Code	GWL (m)	$V_{s,30}$ (m/s)	N_{mean}	Site Class NEHRP V_s Criteria	Site Class NEHRP SPT Criteria	Site Class EC-8 V_s Criteria	Site Class EC-8 SPT Criteria	Site Class TSDC V_s Criteria	Site Class TSDC SPT Criteria
AI_151_MKP	NA	264.9	47.7	D	D	C	C	Z3	Z2
AI_152_BYT02	3.2	249.1	21.2	D	D	C	C	Z3	Z3
AI_153_ING	4.5	252.0	27.4	D	D	C	C	Z3	Z2

APPENDIX B

AASHTO (2010) SITE CLASSIFICATION FOR SELECTED STATIONS

Table B.1 Site Classification of the Selected Sites According to AASHTO (2010)

No.	Station Code NSMP	Station Code GDDA (new)	V _{S30} (m/s)	Site Class AASHTO 2010 (Vs Criteria)
21	AI_021_CYH_PTT	104	223.00	D
22	AI_022_CYH_TIM	105	263.80	D
20	AI_020_KRT	110	485.10	C
45	AI_045_GOL	202	468.70	C
139	AI_139_AFY	301	225.60	D
137	AI_137_DIN	302	198.10	D
138	AI_138_SDL	308	357.40	D
58	AI_058_AGR	401	294.80	D
57	AI_057_DBY	402	270.70	D
73	AI_073_AMS_MZFL	501	283.90	D
74	AI_074_AMS_BAY	502	443.30	C
75	AI_075_MRZ	504	368.40	C
16	AI_016_BEY	601	339.60	D
17	AI_017_HAY	602	418.80	C
129	AI_129_FNK	703	299.40	D
119	AI_119_AYD_HH	901	310.90	D
120	AI_120_AYD_DSI	902	271.40	D
117	AI_117_KUS_MET	905	369.30	C
118	AI_118_KUS_HSL	906	273.50	D
146	AI_146_BLK	1001	662.00	C
97	AI_097_AYV	1005	386.60	C
149	AI_149_BND_MET	1006	321.00	D
150	AI_150_BND_TDM	1007	416.70	C
147	AI_147_BGC	1008	299.90	D
144	AI_144_DUR_MET	1009	560.70	C

No.	Station Code NSMP	Station Code GDDA (new)	V_{s30} (m/s)	Site Class AASHTO 2010 (Vs Criteria)
145	AI_145_DUR_KGI	1010	495.90	C
92	AI_092_EDN_SO	1011	330.00	D
93	AI_093_EDN_KGI	1012	520.10	C
96	AI_096_EDR	1013	223.30	D
91	AI_091_GNN	1014	397.20	C
148	AI_148_SNG	1015	237.70	D
49	AI_049_BNG	1201	528.70	C
50	AI_050_SLH_OE	1208	484.80	C
51	AI_051_SLH_MET	1209	462.70	C
54	AI_054_TAT	1301	273.00	D
10	AI_010_BOL	1401	293.60	D
15	AI_015_GRD	1402	444.70	C
7	AI_007_GYN_BHM	1403	471.70	C
8	AI_008_GYN_DH	1404	347.70	D
12	AI_012_MEN	1405	364.70	D
9	AI_009_MDR	1406	355.40	D
133	AI_133_BRD1	1501	334.60	D
134	AI_134_BRD2	1502	294.10	D
130	AI_130_BCK_KGI	1503	713.70	C
131	AI_131_BCK_OM	1504	693.80	C
132	AI_132_TFN	1505	366.90	C
152	AI_152_BYT02	1601	249.10	D
153	AI_153_ING	1610	252.00	D
3	AI_003_IZN	1611	251.20	D
81	AI_081_IZN_KY	1612	196.70	D
151	AI_151_MKP	1614	264.90	D
88	AI_088_CNK	1701	191.80	D
90	AI_090_BGA	1703	303.70	D
95	AI_095_EZN	1704	403.20	C
87	AI_087_GL1	1705	285.90	D
89	AI_089_KRB	1706	683.20	C
94	AI_094_YNC	1707	324.10	D
13	AI_013_CER	1801	347.90	D
78	AI_078_KRG	1901	687.80	C
76	AI_076_OSM_BEL	1902	314.90	D

No.	Station Code NSMP	Station Code GDDA (new)	V _{S30} (m/s)	Site Class AASHTO 2010 (Vs Criteria)
77	AI_077_OSM_EHK	1903	254.60	D
107	AI_107_DNZ_MET	2001	345.90	D
108	AI_108_DNZ_BAY	2002	355.90	D
106	AI_106_BLD	2003	345.40	D
128	AI_128_CAM	2004	344.10	D
136	AI_136_CRD	2005	395.10	C
48	AI_048_ELZ	2301	407.30	C
65	AI_065_ERC	2401	314.20	D
67	AI_067_REF_HK	2403	433.10	C
68	AI_068_REF_KM	2404	413.10	C
63	AI_063_TER_MET	2405	319.60	D
64	AI_064_TER_PTT	2406	349.80	D
62	AI_062_ERZ	2501	374.90	C
59	AI_059_HRS	2503	316.40	D
140	AI_140_STG	2609	407.40	C
35	AI_035_MAT15	2701	420.90	C
36	AI_036_MAT16	2702	598.90	C
28	AI_028_MAT03	3101	469.50	C
29	AI_029_MAT02	3103	343.60	D
33	AI_033_MAT08	3104	688.00	C
34	AI_034_MAT09	3105	618.00	C
25	AI_025_MAT06_MET	3106	395.20	C
26	AI_026_MAT06_MIM	3107	309.60	D
31	AI_031_MAT05	3108	539.20	C
32	AI_032_MAT07	3109	271.60	D
27	AI_027_MAT01	3110	209.60	D
30	AI_030_MAT04	3111	338.30	D
135	AI_135_SNK	3201	445.10	C
19	AI_019_MRS	3301	366.40	C
1	AI_001_IST	3401	595.20	C
82	AI_082_CEK	3403	283.30	D
115	AI_115_BRN_BAY	3501	195.50	D
116	AI_116_BRN_EU	3502	270.00	D
98	AI_098_DKL	3503	193.20	D
113	AI_113_FOC	3504	327.70	D

No.	Station Code NSMP	Station Code GDDA (new)	V_{s30} (m/s)	Site Class AASHTO 2010 (Vs Criteria)
114	AI_114_GZL_MET	3506	770.70	B
99	AI_099_KNK	3508	558.00	C
111	AI_111_ODM	3509	286.30	D
60	AI_060_KRS	3601	269.70	D
79	AI_079_TOS	3701	361.80	D
4	AI_004_IZT	4101	826.10	B
2	AI_002_GBZ	4106	701.10	C
141	AI_141_KUT_BAY	4301	266.60	D
142	AI_142_KUT_SS	4302	242.50	D
143	AI_143_EMT	4303	303.60	D
104	AI_104_GDZ	4304	343.20	D
103	AI_103_SMV	4305	259.00	D
47	AI_047_MLT	4401	480.80	C
46	AI_046_DSH	4403	654.40	C
112	AI_112_MNS	4501	340.30	D
100	AI_100_AKS	4502	291.70	D
109	AI_109_ALA	4503	358.10	D
102	AI_102_DMR	4504	335.80	D
101	AI_101_GOR	4505	629.40	C
110	AI_110_SAL	4506	272.90	D
41	AI_041_MAT11	4601	345.50	D
42	AI_042_MAT12_MET	4602	316.70	D
43	AI_043_KMR	4603	466.20	C
39	AI_039_AND	4604	610.80	C
40	AI_040_ELB	4605	314.90	D
38	AI_038_MAT14	4606	484.40	C
44	AI_044_MAT10	4607	671.10	C
37	AI_037_MAT13	4608	390.50	C
121	AI_121_BDR	4802	746.90	C
127	AI_127_FTH	4803	248.20	D
126	AI_126_KOY	4804	371.90	C
125	AI_125_MAR	4805	392.50	C
122	AI_122_MLS	4806	323.50	D
123	AI_123_YTG	4807	695.90	C
124	AI_124_YER	4808	813.40	B

No.	Station Code NSMP	Station Code GDDA (new)	V_{S30} (m/s)	Site Class AASHTO 2010 (Vs Criteria)
52	AI_052_MUS	4901	314.50	D
53	AI_053_MLZ	4902	311.20	D
18	AI_018_CMR	5101	312.50	D
5	AI_005_SKR	5401	412.00	C
6	AI_006_AKY	5402	271.60	D
69	AI_069_SSH	5801	413.40	C
66	AI_066_ZAR	5802	281.60	D
84	AI_084_TKR_MET	5901	471.90	C
85	AI_085_TKR_HK	5902	408.70	C
83	AI_083_ERG	5903	325.20	D
86	AI_086_SRK	5904	225.00	D
71	AI_071_TKT	6001	323.80	D
72	AI_072_ERB	6003	326.60	D
70	AI_070_RES	6004	376.20	C
105	AI_105_USK	6401	285.50	D
55	AI_055_VAN	6501	363.10	D
56	AI_056_MUR	6502	292.60	D
61	AI_061_ARD	7501	431.70	C
80	AI_080_YLV	7705	261.20	D
14	AI_014_KBK	7801	702.60	C
23	AI_023_MAT17	8001	349.90	D
24	AI_024_MAT18	8002	430.40	C
11	AI_011_DZC-DZC 1058E	8101	282.00	D

APPENDIX C

EZ-FRISK ANALYSES

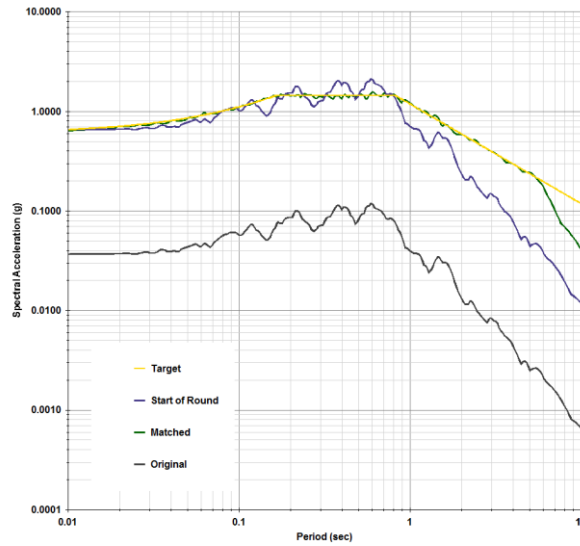


Figure C.1 Spectral Matching for AASHTO 2010 Using A-TIN000

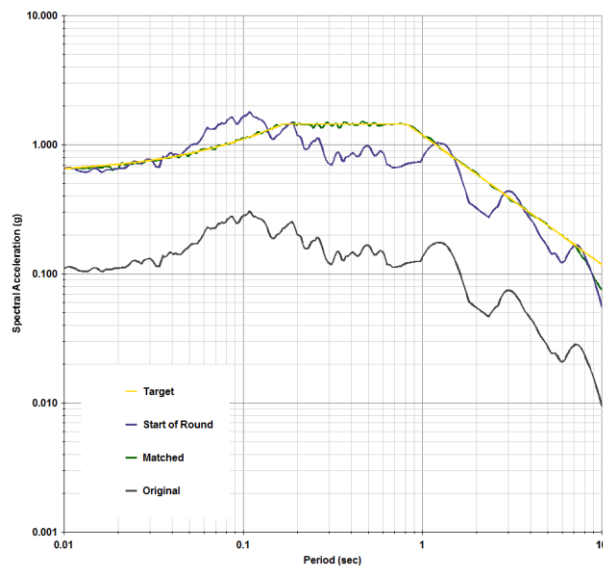


Figure C.2 Spectral Matching for AASHTO 2010 Using DZC-DZC 1058E

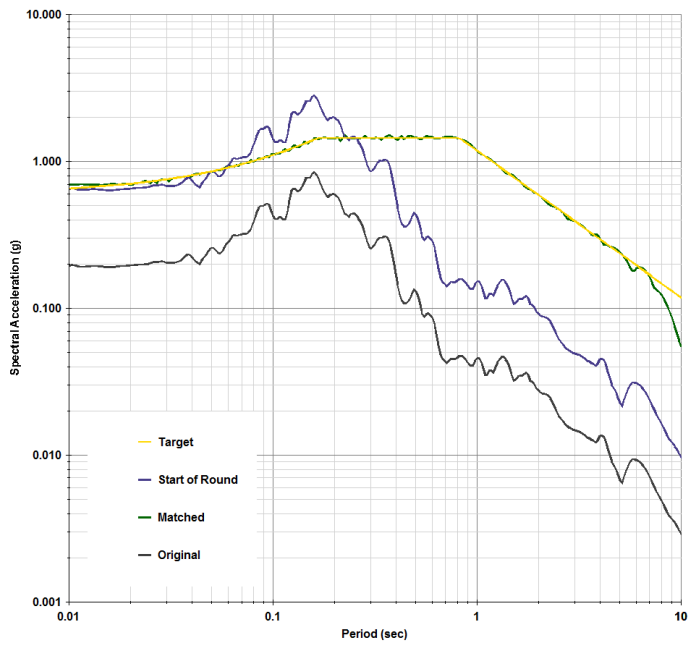


Figure C.3 Spectral Matching for AASHTO 2010 Using HSUP-135

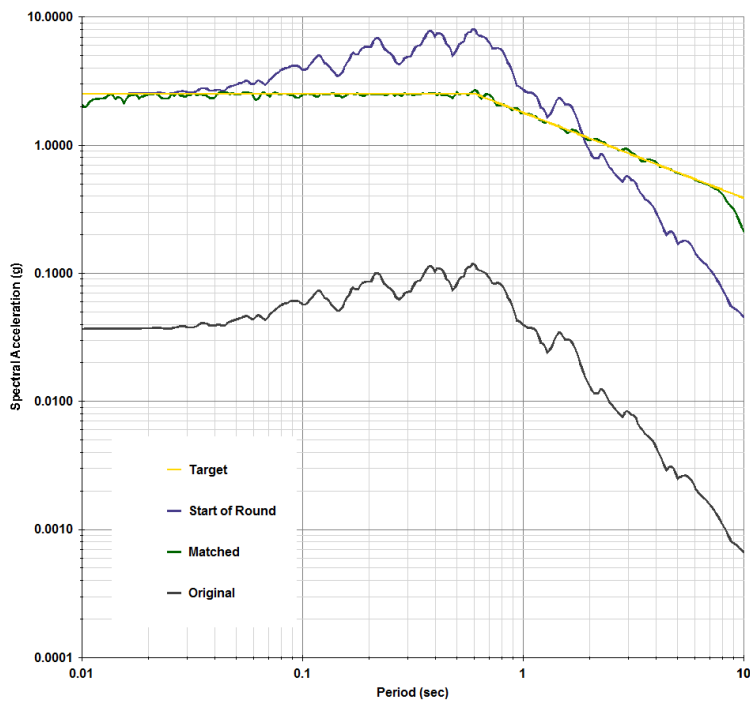


Figure C.4 Spectral Matching for AASHTO 2007 Using A-TIN000

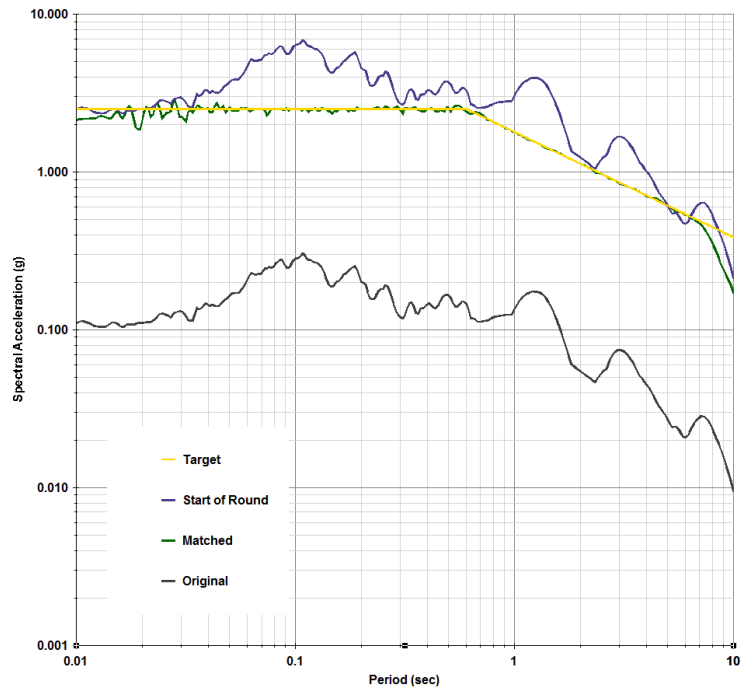


Figure C.5 Spectral Matching for AASHTO 2007 Using DZC-DZC 1058E

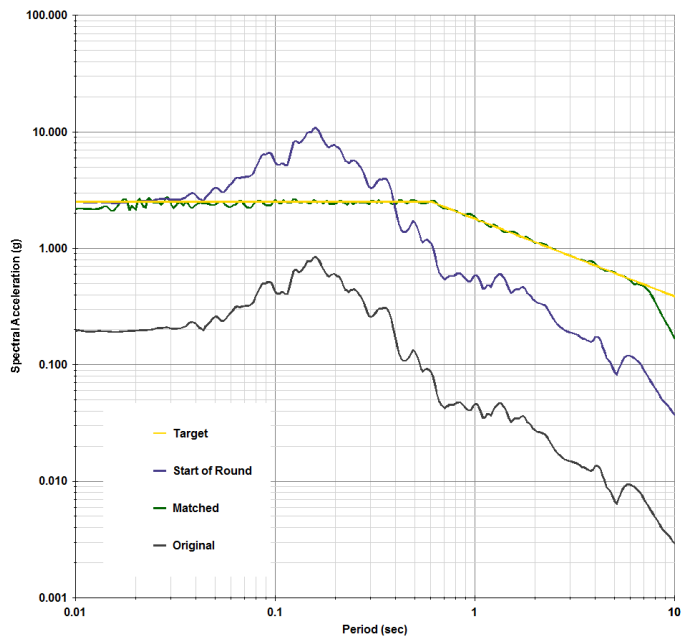


Figure C.6 Spectral Matching for AASHTO 2007 Using HSUP-135

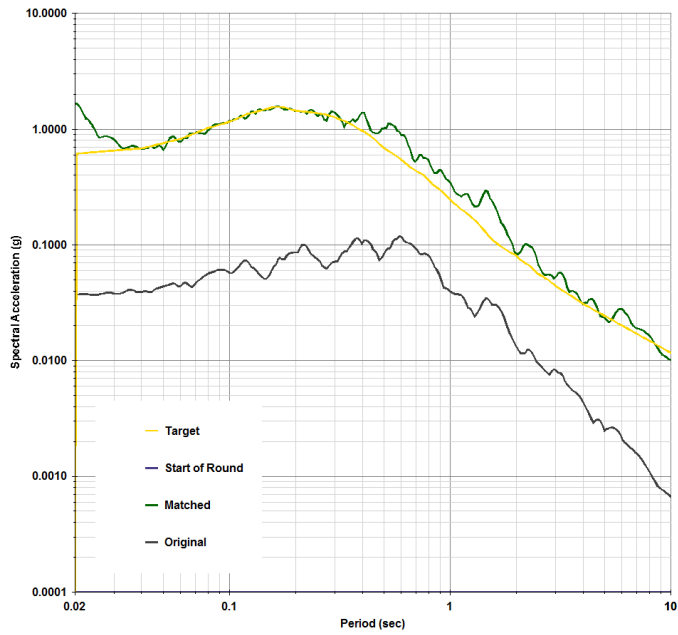


Figure C.7 Spectral Matching for $3.5 < M_w < 4.5$ Using A-TIN000 (mean)

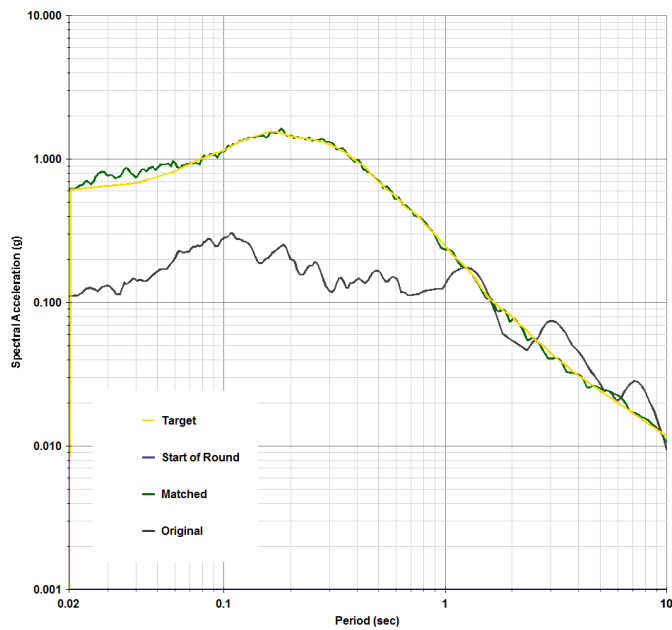


Figure C.8 Spectral Matching for $3.5 < M_w < 4.5$ Using DZC-DZC 1058E (mean)

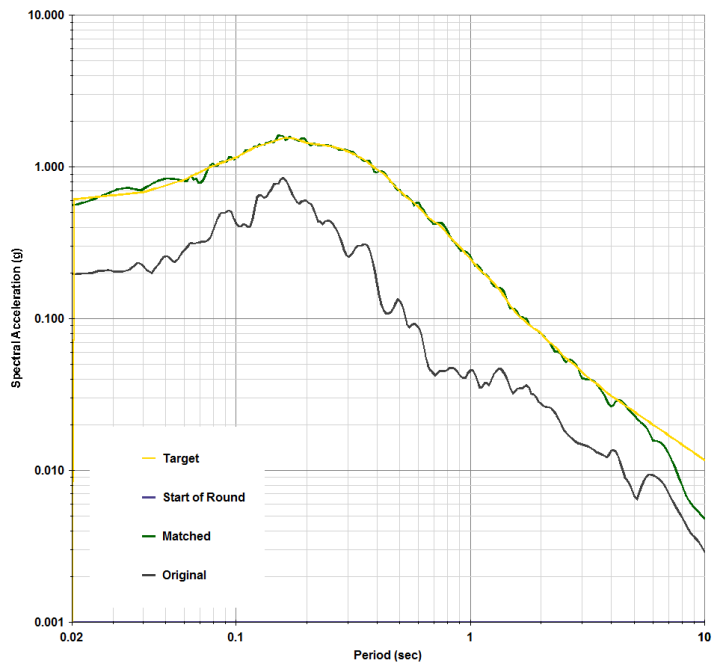


Figure C.9 Spectral Matching for $3.5 < M_w < 4.5$ Using HSUP-135 (mean)

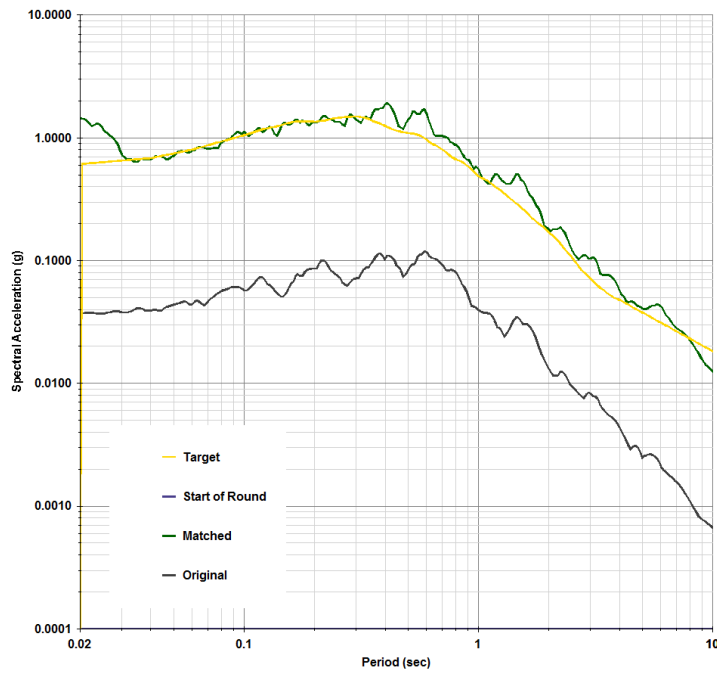


Figure C.10 Spectral Matching for $4.5 < M_w < 5.5$ Using A-TIN000 (mean)

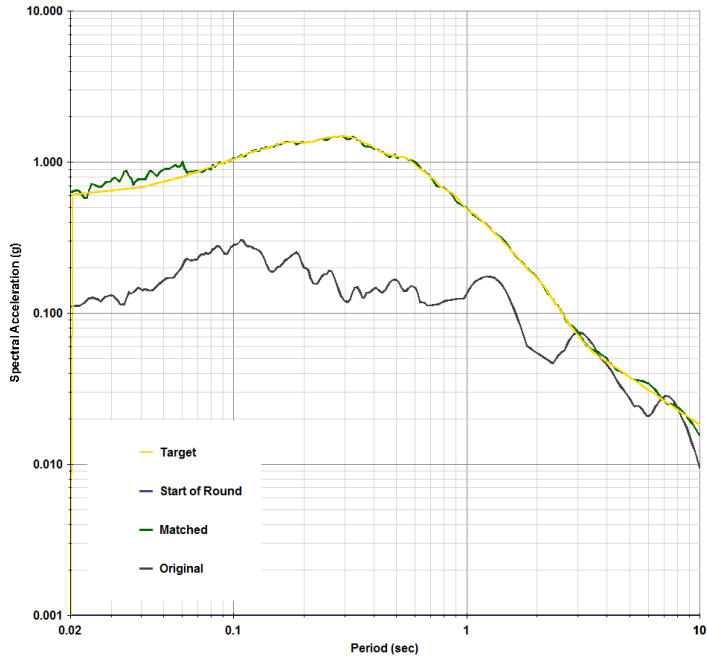


Figure C.11 Spectral Matching for $4.5 < M_w < 5.5$ Using DZC-DZC 1058E (mean)

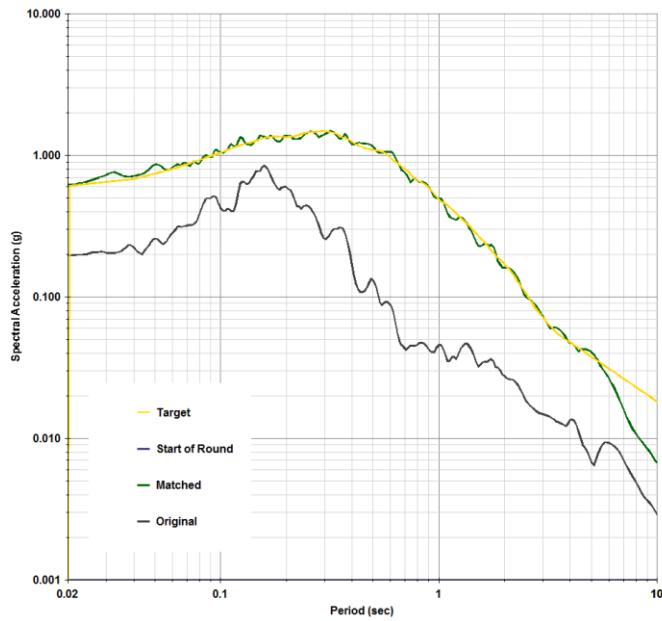


Figure C.12 Spectral Matching for $4.5 < M_w < 5.5$ Using HSUP-135 (mean)

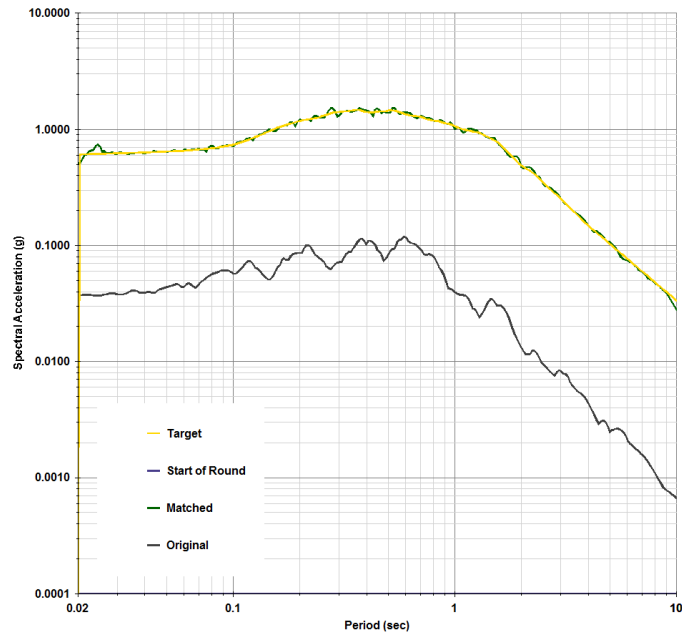


Figure C.13 Spectral Matching for $5.5 < M_w < 6.5$ Using A-TIN000 (mean)

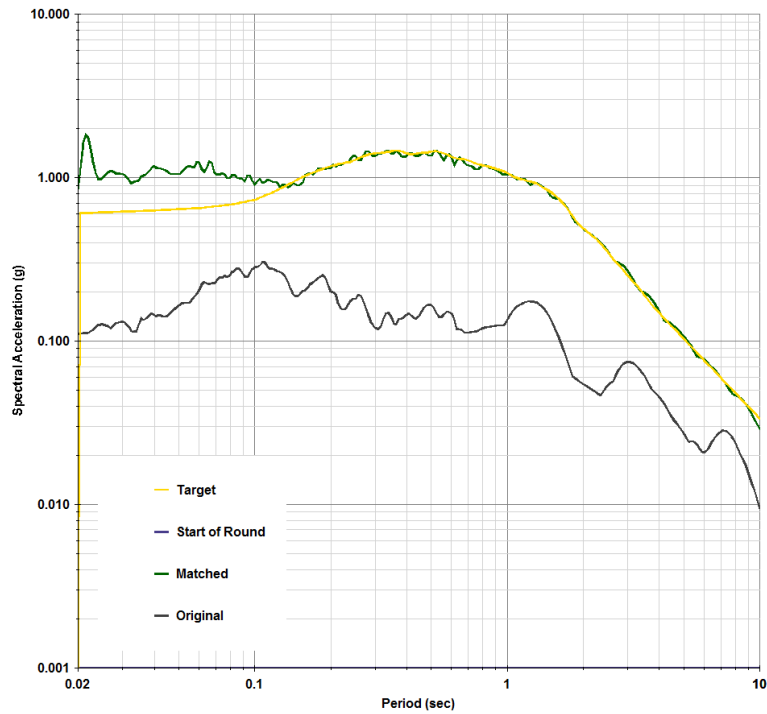


Figure C.14 Spectral Matching for $5.5 < M_w < 6.5$ Using DZC-DZC 1058E (mean)

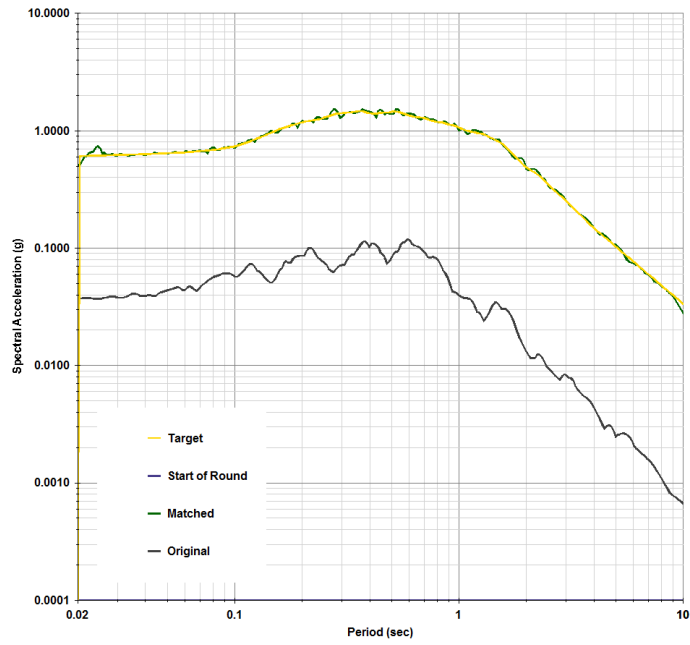


Figure C.15 Spectral Matching for $5.5 < M_w < 6.5$ Using HSUP-135 (mean)

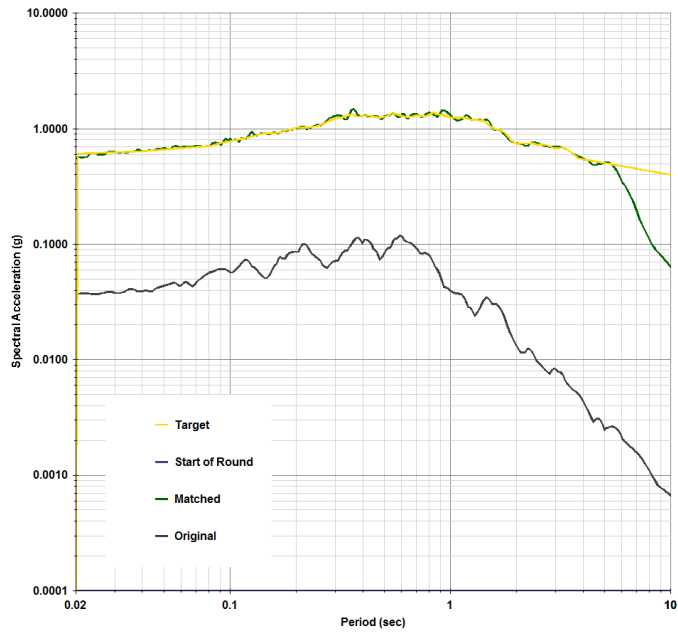


Figure C.16 Spectral Matching for $6.5 < M_w < 7.5$ Using A-TIN000 (mean)

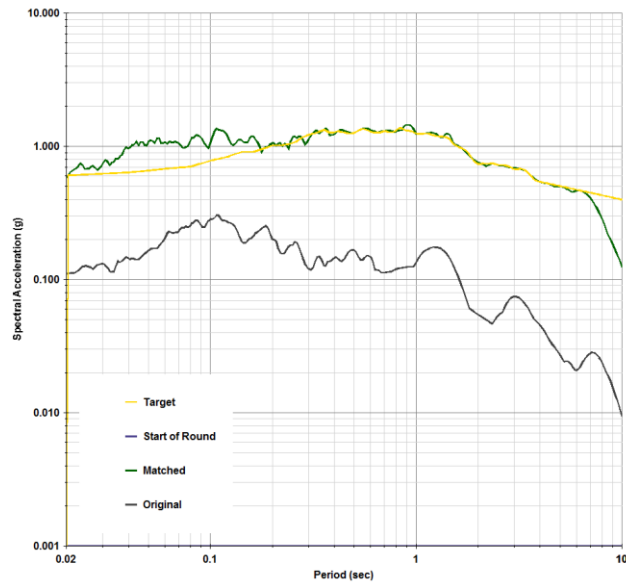


Figure C.17 Spectral Matching for $6.5 < M_w < 7.5$ Using DZC-DZC 1058E (mean)

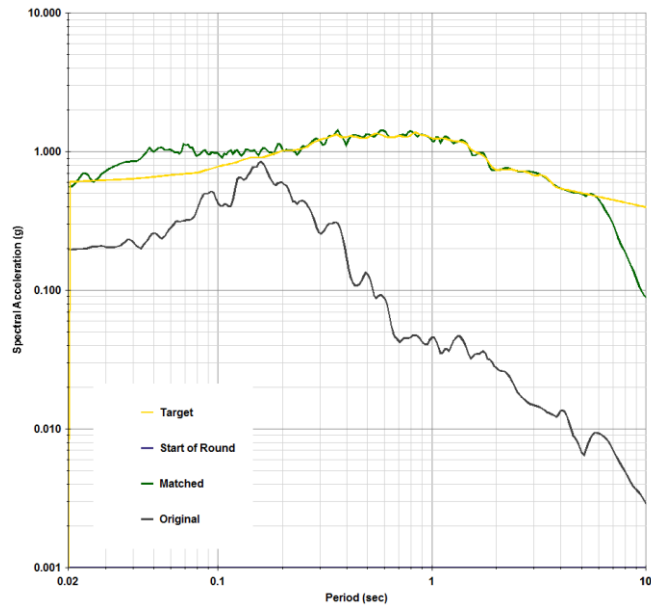


Figure C.18 Spectral Matching for $6.5 < M_w < 7.5$ Using HSUP-135 (mean)

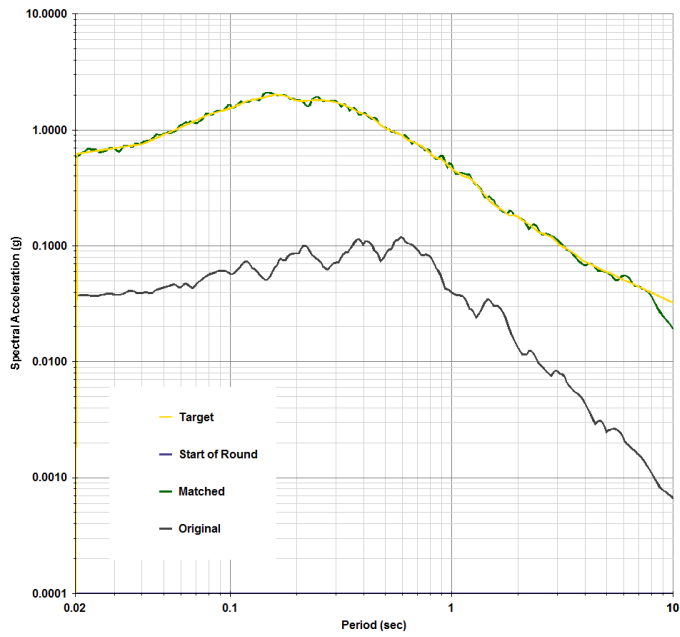


Figure C.19 Spectral Matching for $3.5 < M_w < 4.5$ Using A-TIN000 (mean+std)

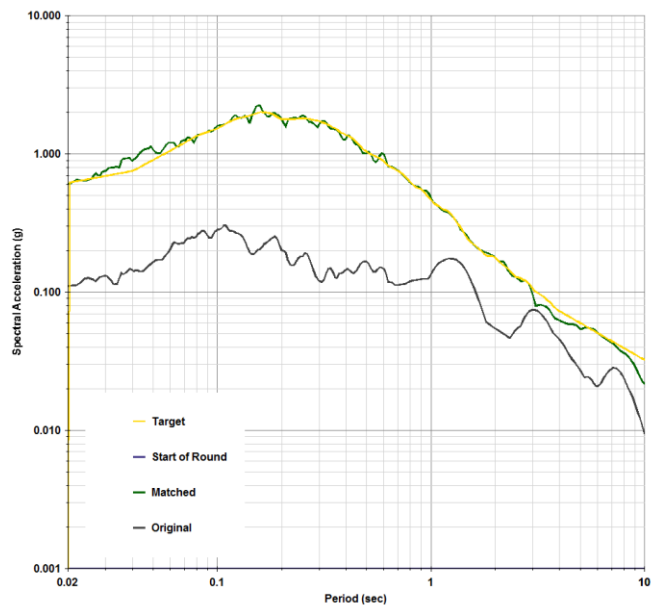


Figure C.20 Spectral Matching for $3.5 < M_w < 4.5$ Using DZC-DZC 1058E (mean+std)

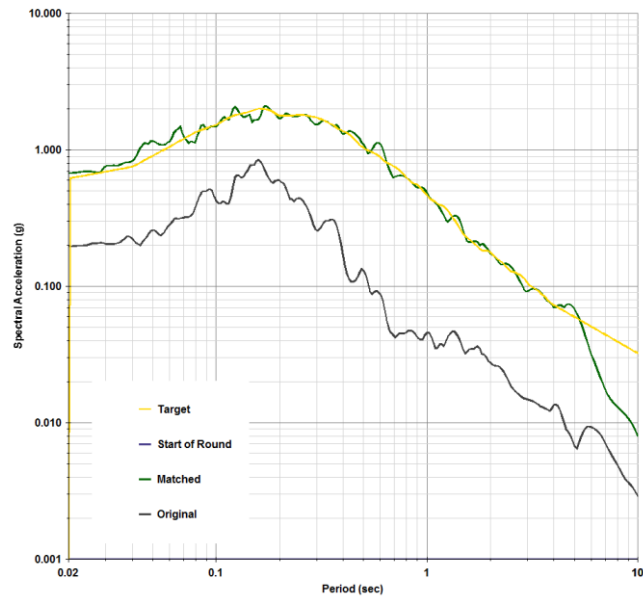


Figure C.21 Spectral Matching for $3.5 < M_w < 4.5$ Using HSUP-135 (mean+std)

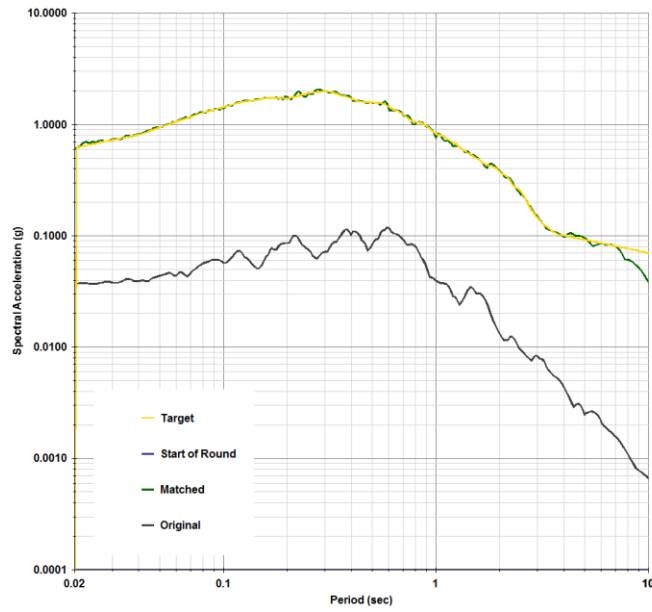


Figure C.22 Spectral Matching for $4.5 < M_w < 5.5$ Using A-TIN000 (mean+std)

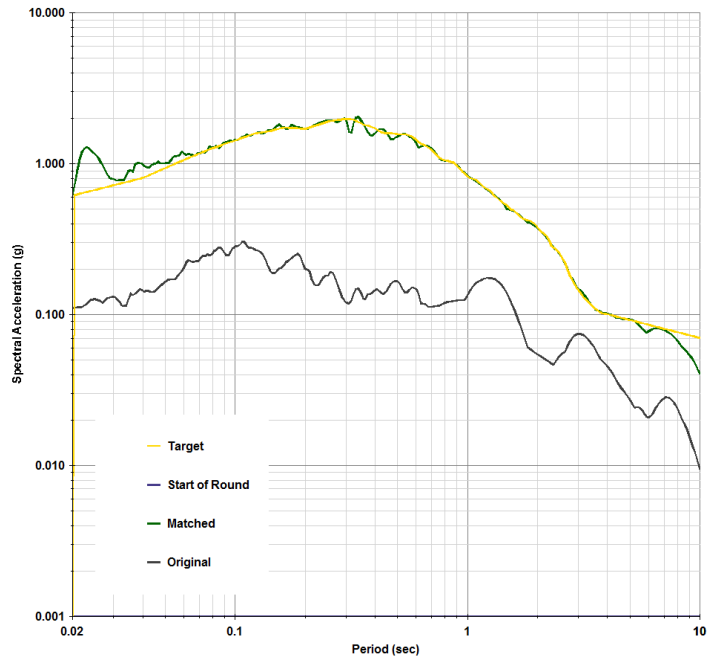


Figure C.23 Spectral Matching for $4.5 < M_w < 5.5$ Using DZC-DZC 1058E (mean+std)

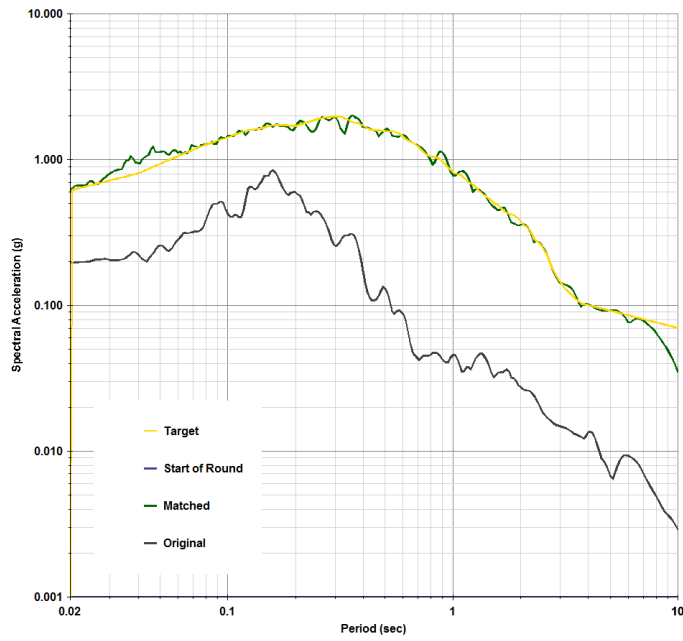


Figure C.24 Spectral Matching for $4.5 < M_w < 5.5$ Using HSUP-135 (mean+std)

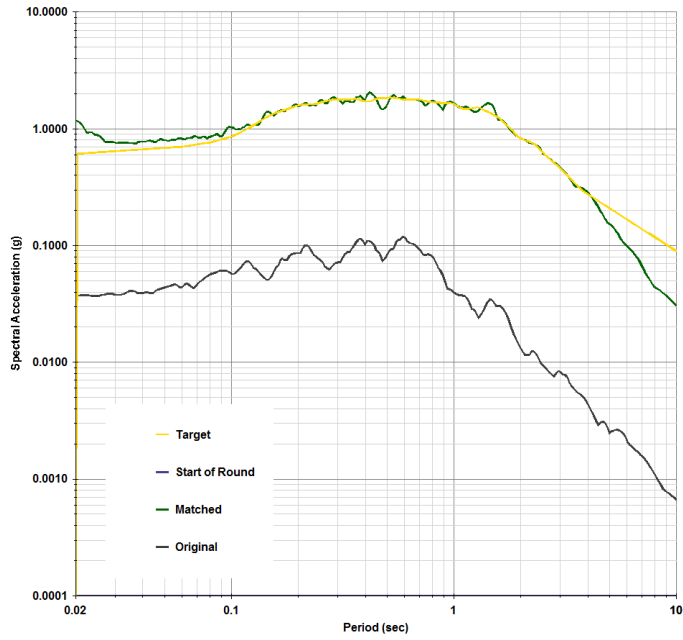


Figure C.25 Spectral Matching for $5.5 < M_w < 6.5$ Using A-TIN000 (mean+std)

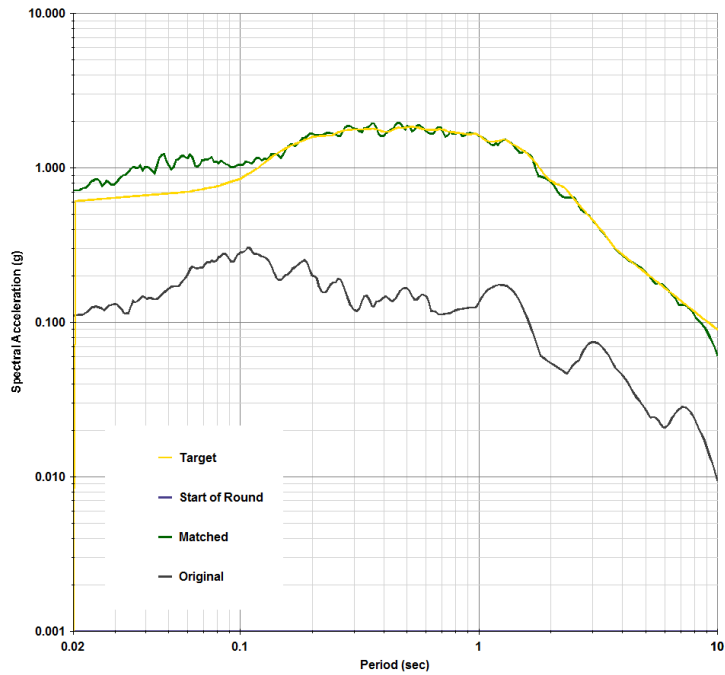


Figure C.26 Spectral Matching for $5.5 < M_w < 6.5$ Using DZC-DZC 1058E (mean+std)

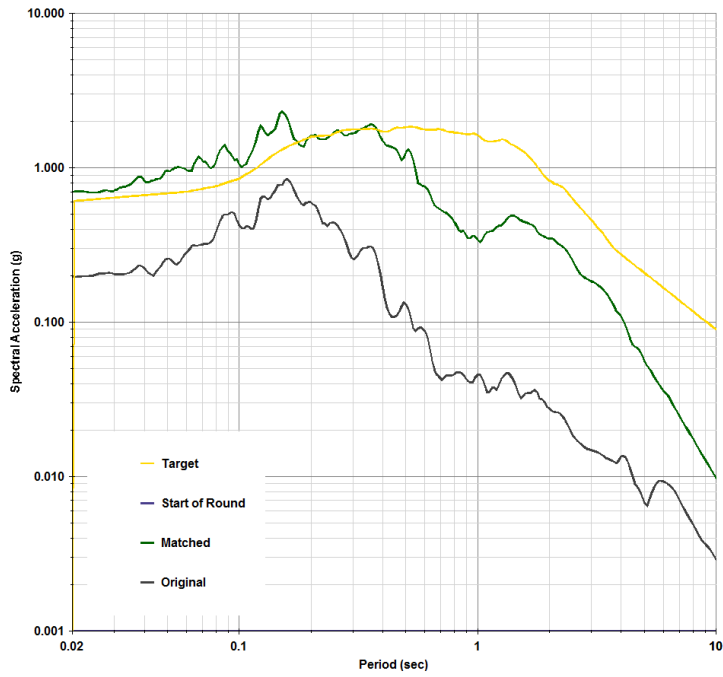


Figure C.27 Spectral Matching for $5.5 < M_w < 6.5$ Using HSUP-135 (mean+std)

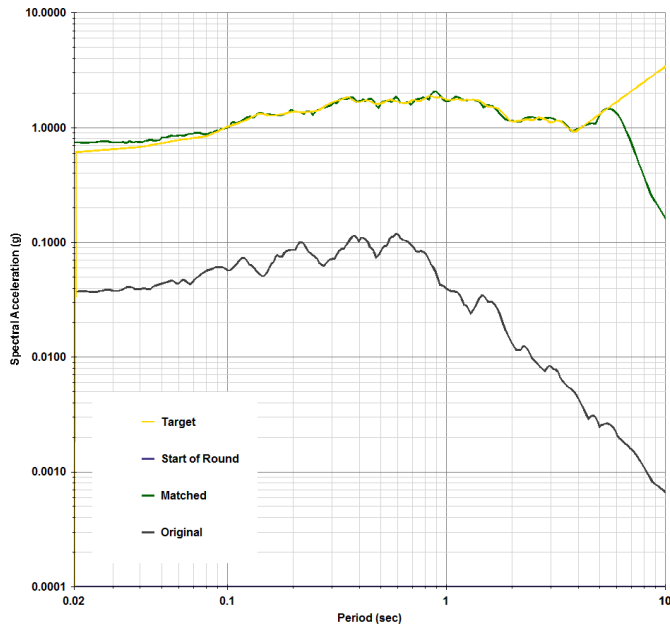


Figure C.28 Spectral Matching for $6.5 < M_w < 7.5$ Using A-TIN000 (mean+std)

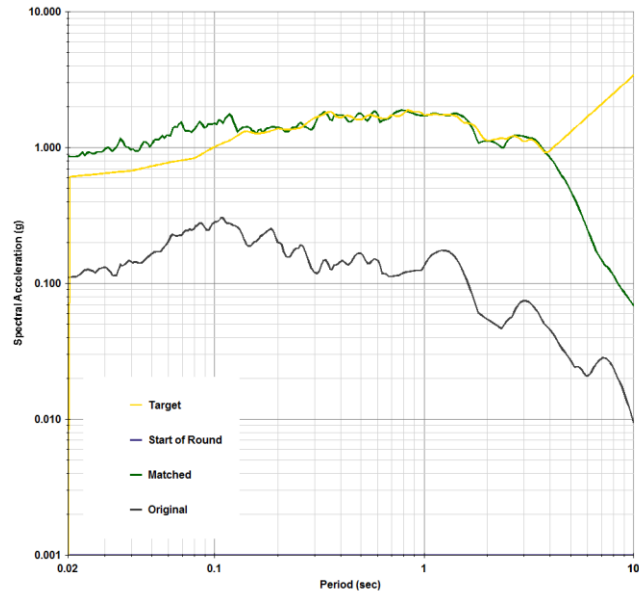


Figure C.29 Spectral Matching for $6.5 < M_w < 7.5$ Using DZC-DZC 1058E (mean+std)

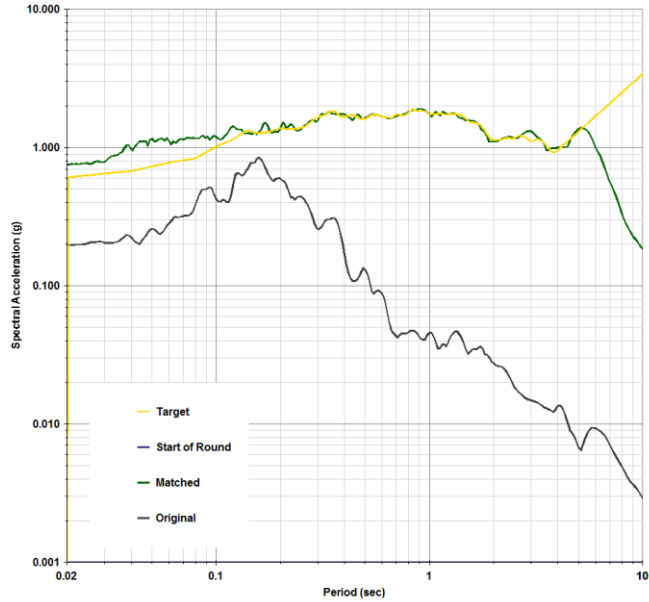


Figure C.30 Spectral Matching for $6.5 < M_w < 7.5$ Using HSUP-135 (mean+std)